Technical University of Munich
TUM School of Medicine and Health

Developing Bone Morphogenetic Protein 2 Transcript-activated Implants

Omnia Fayed

Complete reprint of the dissertation approved by the TUM School of Medicine and Health of the Technical University of Munich for the award of the Doktorin der Naturwissenschaften (Dr. rer. nat).

Chair: Prof. Dr. Dieter Saur

Examiners:

1. apl. Prof. Dr. Christian Plank
2. Prof. Dr. Andreas Bausch

The dissertation was submitted to the Technical University of Munich on 29th of January 2024 and accepted by the TUM School of Medicine and Health on 3rd of July 2024.

DECLARATION

The results gained in this thesis was previously published in the following publication:

Fayed, O.; van Griensven, M.; Tahmasebi Birgani, Z.; Plank, C.; Balmayor, E. R. Transcript-activated Coatings on Titanium Mediate Cellular Osteogenesis for Enhanced Osteointegration. *Molecular Pharmaceutics* **2021**, 18(3): 1121-1137.

doi: 10.1021/acs.molpharmaceut.0c01042.

PMID: 33492959

Contents

Figures

Tables

Acknowledgments

First and foremost, I am grateful to God the Almighty, whose mercy and grace have carried me through every moment of my life.

This dissertation is dedicated to my father Prof. Dr Mahmoud Fayed (may he rest in peace, I hope he is proud of me), my mother Prof. Dr Shahinaz Hussein (she is the shining star in my life), My brother Ahmed, and My best friend Samar Ali.

I would like to express gratitude to my thesis supervisor Prof. Dr Christian Plank for his invaluable feedback and support throughout the duration of this thesis work. I truly appreciate his patience, wisdom, and scientific guidance, which was always available to me when needed, whilst encouraging me to think and explore freely through this challenging and exciting journey. I would like to acknowledge his efforts in revising our published paper and this thesis - including the German summary section. Yet, words cannot describe my gratitude for his kindness, understanding and support during the difficult times along this journey.

I am most thankful for Prof. Dr. Martijn van Griensven for allowing me access to the laboratory facilities of the experimental trauma surgery department in the faculty of medicine, Technical University of Munich - which he was the head of at the time. His generous support has been foundational for this thesis experimental work. Moreover, he gave me many helpful pointers in scientific writing and presenting which I am most grateful for and following to this day.

I would like to thank my second advisor Prof. Dr. Andreas Bausch for kindly providing his knowledge, expertise, and unique perspectives to enrich our work.

I'm extremely grateful to my mentor Prof. Dr. Elizabeth Rosado Balmayor. Her invaluable support carried our work through to the finish line. She helped me hone my laboratory skills, optimize the experimental work, and aid me select the materials used. Additionally, she has been my scientific writing guru, whom I learned so much from. I thank her for her wonderful work revising this thesis and her remarkable role in getting our work published. I especially thank her for her patience and understanding during the difficult times.

I would like to thank both the Egyptian ministry of higher education and the German Academic Exchange Service (DAAD) for their joined programme German-Egyptian Research Long-term Scholarship (GERLS) that afforded me this amazing opportunity to pursue my postgraduate education in Germany. I thank them deeply for their financial and moral support.

My deepest thanks go to Ethris company and all its staff for allowing me to use the facilities to complete our work. They provided a lot of the materials and know-how we used, to conclude our research. All while offering a friendly and helpful scientific atmosphere to work in.

I deeply thank the staff and the fellow students in the experimental trauma surgery laboratory (Experimentelle Unfallchirurgie), medical faculty, technical university of Munich, especially Sandra Schneider and Anna Capri for supporting my work and teaching me many laboratory techniques.

My sincere gratitude to Prof. Dr Percy A. Knolle head of Institute of Molecular Immunology (IMI) in the medical faculty, Technical University of Munich, and all the friendly staff and fellow students in this department for supporting this work and my scientific progress in our monthly meetings. I am especially grateful to Wen Zhang for helping me learn many laboratory protocols, and Sara Al-Ageel, Abdallah, Abdul Moeed, and Soliman for their moral support and scientific brainstorming.

I would like to thank Dr. Jan Lang from the Orthopaedics department in the medical faculty, technical university of Munich, for helping me design and fabricate the inserts cutting guide used in our thesis work.

Finally, I would like to thank all my friends whose encouragement and care carried me through this journey: Loay Al-Alfy, Mohamed Al-Waziry, Ahmed Gamal, Ahmed Allam, Ahmed Yousef, Mahmoud Khaled, Islam Hosny, Karim Al-Gammal, Manal Elmasry, Carlos Diaz Cano, and Carlos Peniche Silva.

Omnia Fayed

Summary

Osteointegration is one of the crucial factors in implant success. Bone morphogenetic protein 2 (BMP2) biomolecule has been used in combination with various biodegradable natural and synthetic materials to enhance bone healing. Transcript therapy using chemically modified mRNA (cmRNA) is an emerging safer alternative for local protein delivery and gene therapy. We aimed to utilize transcript technology to create BMP2 transcript-activated coatings for Titanium (Ti) implants through screening different strategies of transcript incorporation, focusing on the effect of coating method and composition on transfection efficiency, kinetics, cell viability, and osteogenic activity in vitro.

METHODS: Ti discs were prepared to receive transcript-activated coating using physical adsorption and physical entrapment methods. The physical adsorption method (MetLuc-Ti group) was done through drying different concentrations of Metridia Luciferase reporter (MetLuc) cmRNA lipoplexes solutions on Ti discs. Physical entrapment Ti coating was done using either synthetic (we selected polylactide i.e., PDLLA) or natural (we selected fibrin) carrier polymers. Transcript-activated PDLLA coating (MetLuc-PDLLA group): the selected cmRNA concentration from the physical adsorption method (MetLuc-Ti) was further coated with different concentrations of PDLLA (3, 2, 1, 0.5, and 0.25 mg/well). Fibrin coating (MetLuc-FT or MetLuc-F groups): was done on clean Ti using Tissucol® fibrin glue kit. Ti discs were coated with fibrinogen mixed with MetLuc lipoplexes then thrombin with different concentrations was added and mixed (final coating volume ratios were 1, 0.5, 0.25, and 0 thrombin to fibrinogen). The fibrin-coated Ti discs were freeze-dried. Evaluation of transfection efficiency and kinetics, dose-dependence, cell viability, and cell proliferation were done using NIH3T3 cell line in vitro. Finally, BMP2 transcript-activated coatings were prepared according to the best previously optimized methods and transcript-release from the coating was evaluated. The BMP2

transcript-activated coating was evaluated in vitro using the C2C12 cell line for BMP2 protein expression using ELISA, osteogenic differentiation using alkaline phosphatase activity assay (ALP), and mineralization using alizarine red staining.

RESULTS AND CONCLUSION: The results demonstrated the ability of the developed coating strategies to transfect cells with MetLuc reporter, MetLuc-Ti samples showed the lowest transfection efficiency and kinetics/time followed by MetLuc-PDLLA samples showing a significant improvement with the least PDLLA coating concentrations (0.5 and 0.25 mg/well). Finally, fibrin coated Ti group (MetLuc-FT) showed the best MetLuc expression and kinetics of the 3 groups with fibrinogen-coated samples (MetLuc-F) taking the lead. The viability of the cells seeded on the different coated Ti groups had no significant differences indicating similar cell viability independent of the Ti coating type. As for cell proliferation, significant differences were notable in the early time points (days 1 and 3) indicating the superiority of both fibrin and fibrinogen coated Ti samples; however, this effect decreased in the later time points. By the end of the optimization phase, fibrinogen coated group had the best results with MetLuc reporter, thus we utilized it in the next phase for BMP2 transcript activated Ti (BMP2-F group). For the sake of comparison, we added transcript-activated fibrin group (BMP2-FT group). A transcript release study was done comparing both fibrin and fibrinogen coated groups. The results showed a burst of release from the fibrinogen coating in the 2 hrs. timepoint followed by a drop, then it peaked again on the 3rd day. On the one hand, fibrin showed minimal release in the beginning until it peaked on the 4th day. A detectable BMP2 protein expression along with increased alkaline phosphatase activity, and mineralized matrix deposition were detected only with fibrinogen coated Ti (BMP2-F group) with cmRNA concentrations of 500 and 250 ng/well. On the other hand, BMP2-FT group yielded negative results. Such findings presented BMP2 transcript-activated fibrinogen as a promising osteogenic implant-coating material.

Zusammenfassung

Die Osteointegration ist einer der entscheidenden Faktoren für den Erfolg von Implantaten. Das Biomolekül Bone Morphogenetic Protein 2 (BMP2) wurde in Kombination mit verschiedenen biologisch abbaubaren natürlichen und synthetischen Materialien zur Verbesserung der Knochenheilung eingesetzt. Die Transkript Therapie unter Verwendung chemisch modifizierter mRNA (cmRNA) ist eine aufkommende, sicherere Alternative für die lokale Proteinverabreichung und Gentherapie. Unser Ziel war es, die Transkript Technologie zu nutzen, um BMP2-transkriptaktivierte Beschichtungen für Titanimplantate zu schaffen, indem wir verschiedene Strategien der Transkript Inkorporation untersuchten und uns dabei auf die Auswirkungen der Beschichtungsmethode und -zusammensetzung auf die Transfektionseffizienz, Kinetik, Zelllebensfähigkeit und osteogene Aktivität in vitro fokussierten.

METHODEN: Ti-Scheiben wurden für die Aufnahme von Transkript aktivierten Beschichtungen mittels physikalischer Adsorptions- und physikalischer Einschlussmethoden vorbereitet. Die physikalische Adsorptionsmethode (MetLuc-Ti-Gruppe) erfolgte durch Trocknen verschiedener Konzentrationen von Metridia Luciferase Reporter (MetLuc) cmRNA Lipoplexlösungen auf Ti-Scheiben. Für die physikalische Beschichtung von Ti wurden entweder synthetische (wir wählten Polylactid, d.h. PDLLA) oder natürliche (wir wählten Fibrin) Trägerpolymere verwendet. Transkript-aktivierte PDLLA-Beschichtung (MetLuc-PDLLA-Gruppe): Die ausgewählte cmRNA-Konzentration aus der physikalischen Adsorptionsmethode (MetLuc-Ti) wurde zusätzlich mit verschiedenen Konzentrationen von PDLLA (3, 2, 1, 0,5 und 0,25 mg/Well) beschichtet. Fibrinbeschichtung (MetLuc-FT- oder MetLuc-F-Gruppen): wurde auf sauberem Ti mit dem Tissucol® Fibrinkleber-Kit durchgeführt. Die Ti-Scheiben wurden mit Fibrinogen beschichtet, das mit MetLuc-Lipoplexen

gemischt war, dann wurde Thrombin in verschiedenen Konzentrationen zugegeben und gemischt (das endgültige Beschichtungsvolumenverhältnis betrug 1, 0,5, 0,25 und 0 Thrombin zu Fibrinogen). Die mit Fibrin beschichteten Ti-Scheiben wurden gefriergetrocknet. Die Bewertung der Transfektionseffizienz und -kinetik, der Dosisabhängigkeit, der Zelllebensfähigkeit und der Zellproliferation erfolgte mit der NIH3T3-Zelllinie in vitro. Schließlich wurden BMP2-Transkript-aktivierte Beschichtungen nach den besten zuvor optimierten Methoden hergestellt und die Transkript-Freisetzung aus der Beschichtung bewertet. Die BMP2-Transkript-aktivierte Beschichtung wurde in vitro mit der C2C12-Zelllinie hinsichtlich der BMP2-Proteinexpression mittels ELISA, der osteogenen Differenzierung mittels alkalischem Phosphatase-Aktivitätstest (ALP) und der Mineralisierung mittels Alizarinrot-Färbung untersucht.

ERGEBNISSE UND SCHLUSSFOLGERUNGEN: Die Ergebnisse zeigten die Fähigkeit der entwickelten Beschichtungsstrategien, Zellen mit MetLuc-Reporter zu transfizieren. Die MetLuc-Ti-Proben zeigten die geringste Transfektionseffizienz und Kinetik/Zeit, gefolgt von den MetLuc-PDLLA-Proben, die eine signifikante Verbesserung mit den geringsten PDLLA-Beschichtungskonzentrationen (0,5 und 0,25 mg/Well) aufwiesen. Schließlich zeigte die mit Fibrin beschichtete Ti-Gruppe (MetLuc-FT) die beste MetLuc-Expression und -Kinetik der drei Gruppen, wobei die mit Fibrinogen beschichteten Proben (MetLuc-F) die Führung übernahmen. Die Lebensfähigkeit, der auf die verschiedenen beschichteten Ti-Gruppen ausgesäten Zellen wies, keine signifikanten Unterschiede auf, was auf eine ähnliche Lebensfähigkeit der Zellen unabhängig von der Art der Ti-Beschichtung hindeutet. Was die Zellproliferation anbelangt, so waren zu den ersten Zeitpunkten (Tag 1 und 3) signifikante Unterschiede festzustellen, was auf die Überlegenheit sowohl der fibrin- als auch der fibrinogenbeschichteten Ti-Proben hinweist; dieser Effekt nahm jedoch zu den späteren Zeitpunkten ab. Am Ende der Optimierungsphase hatte die mit Fibrinogen beschichtete

Gruppe die besten Ergebnisse mit dem MetLuc-Reporter, weshalb wir sie in der nächsten Phase für BMP2-Transkript-aktiviertes Ti (BMP2-F-Gruppe) einsetzten. Zum Vergleich fügten wir eine Transkript-aktivierte Fibrin-Gruppe (BMP2-FT-Gruppe) hinzu. Es wurde eine Studie zur Transkriptfreisetzung durchgeführt, bei der sowohl die mit Fibrin als auch die mit Fibrinogen beschichteten Gruppen verglichen wurden. Die Ergebnisse zeigten einen Ausbruch der Freisetzung aus der Fibrinogenbeschichtung nach 2 Stunden, gefolgt von einem Rückgang, der am dritten Tag seinen Höhepunkt erreichte. Bei Fibrin hingegen war die Freisetzung anfangs minimal, bis sie am 4. Tag ihren Höhepunkt erreichte. Eine nachweisbare BMP2-Proteinexpression zusammen mit einer erhöhten alkalischen Phosphataseaktivität und einer mineralisierten Matrixablagerung wurde nur bei fibrinogenbeschichtetem Ti (BMP2-F-Gruppe) mit cmRNA-Konzentrationen von 500 und 250 ng/Well festgestellt. Die BMP2-FT-Gruppe hingegen lieferte negative Ergebnisse. Diese Ergebnisse zeigen, dass BMP2-Transkript-aktiviertes Fibrinogen ein vielversprechendes osteogenes Implantatbeschichtungsmaterial ist.

Chapter 1: Introduction

1.1. Osteointegration of titanium implants

For decades, biocompatible titanium (Ti) and its alloys have been successfully used to restore lost hard tissue in both dentistry and orthopaedics [1,2]. Ti implants' biocompatible nature allows organized bone healing around its surface, forming a direct structural and functional connection, referred to as osteointegration [3]. Similar to fracture healing, osseointegration of Ti implants consists of four main stages: haemostasis, inflammation, proliferation, and finally remodelling [4].

Haemostasis starts immediately at the osteotomy site due to tissue and blood vessel damage caused by the implantation procedure. Proteins such as albumin, fibronectin, and fibrinogen begin to adsorb on the implant's surface, which will later facilitate cell adhesion and migration. Especially fibrinogen, which has the unique ability to adsorb to almost any surface and forms the blood clot by converting to fibrin in the presence of thrombin and other clotting factors. The fibrin clot, along with aggregated platelets form an organized thrombus. Besides achieving haemostasis, the organized thrombus is responsible for the release of important growth factors, and the activation of both complement and kinin pathways, paving the way for the inflammatory phase [4].

The implant's primary stability is derived from the mechanical friction between its surface and the bone at the osteotomy site. During the inflammatory phase, the implant starts to lose its primary stability due to the activation of polymorphonuclear leukocytes (PNL), monocytes, macrophages, and towards the end, osteoclasts. Such process is necessary for clearing up any bacterial contamination and bone and tissue debris [5]. Additionally, macrophages are responsible for the activation of fibroblasts and angiogenesis, which mark the start of the proliferative phase [5].

By the 3rd or 4th day after implantation, fibroblasts start producing the extracellular matrix required for healing. The low oxygen concentration at the wound site leads to the activation of macrophages and endothelial cells to release hypoxia-inducible factor (HIF) and vascular endothelial growth factor (VEGF) that activates perivascular mesenchymal stem cells (MSCs) to form new blood vessels to increase blood supply and form a solid foundation for the bone healing. By day seven, osteoclasts start to resorb bone around the implant makings space for bone healing releasing bone morphogenetic proteins (BMPs), transforming growth factor β (TGFβ), and Platelet-derived growth factor (PDGF) from the resorbed bone matrix. The released BMPs initiate bone formation via activation of MSCs that migrate to the bone trabeculae and the implant surface and differentiate into osteoblasts that start woven bone deposition, which marks the end of the proliferative phase [5]. This bone formation restores the lost primary stability from previous stages and initiates osteointegration via the mechanical interlocking achieved between the bone and the implant surface [5]. Figure 1 illustrates the main phases of osteointegration.

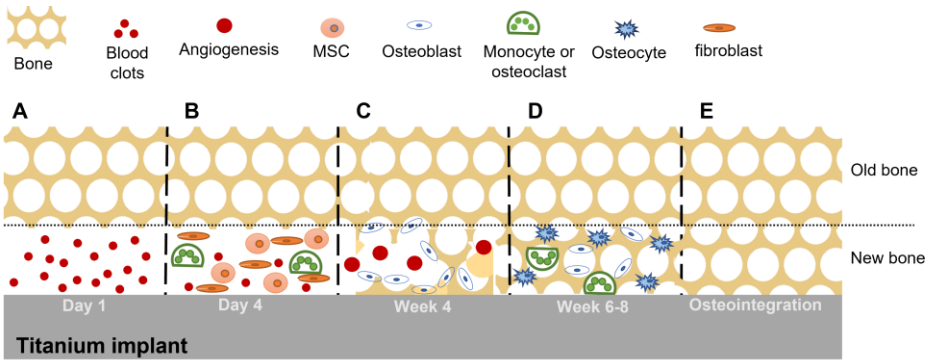

Figure 1: Schematic illustration showing implant osteointegration timeline starting with clot formation (A), cell recruitment e.g., MSCs and monocytes (B), cell differentiation leading to angio-osteogenesis (C), bone remodelling (D), and finally mature bone formation and complete osteointegration of the implant (E).

The quality of osteointegration is a particularly important determining factor for implants' success and longevity. It acts as an indicator of the implant's overall health, including its ability to provide support under functional load, and to support the surrounding soft tissue (i.e., an indicator of optimal implant function and aesthetics) [6,7]. These reasons have ignited the interest in understanding and promoting osteointegration of titanium implants which in turn may lead to faster healing and long-term clinical success [8].

Implants' osteointegration depends on factors related to both the bone and to the implant surface. The factors related to bone are for example, systemic factors, growth factors, and the bone lining cells, as well as the functional load the bone is subjected to [5]. Meanwhile, the factors related to the implant surface includes its topography and composition [5]. All the mentioned factors are illustrated in Figure 2 [5]. Studies in the past focused on modifying the implant related factors in a way that makes the implant more osteoconductive [9]. However, in recent years, implant modifications have included bioactive elements (e.g., bioactive materials and biomolecules) that elicit the required biological response instead of just being biocompatible [10–13].

The most used biomolecule to induce bone formation is bone morphogenetic protein 2 (BMP2), which has been used stand-alone or in tandem with various natural and synthetic implant coating materials [14,15]. Although BMP2 clinical use for few bone-related indications is FDA approved, many complications have been documented related to its use, such as ectopic bone formation, bone resorption, and hematoma [14]. Hence, the introduction of gene therapy and gene-activated matrices [16], and most recently transcript therapy (mRNA-therapy) as it provided a safer alternative to both gene therapy and local protein delivery [17–21].

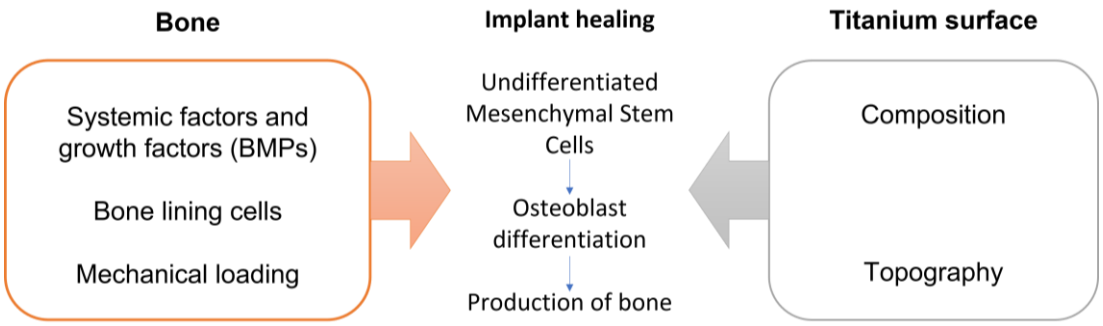

Figure 2: Diagram showing factors affecting the osteointegration process related to the implant and the bone tissue [5]

1.2. Titanium surface modification for bone regeneration

Among the parameters influencing implants' success, the implant-bone interface plays a key role in improving the longevity and function of the implant treatment. Implant surfaces have been developed to provide a faster and improved osseointegration using several surface modifications involving topography and composition alterations, as well as combinations of both [22–25]. Figure 3 is an illustration showing different ways implant surfaces could be modified for a better outcome.

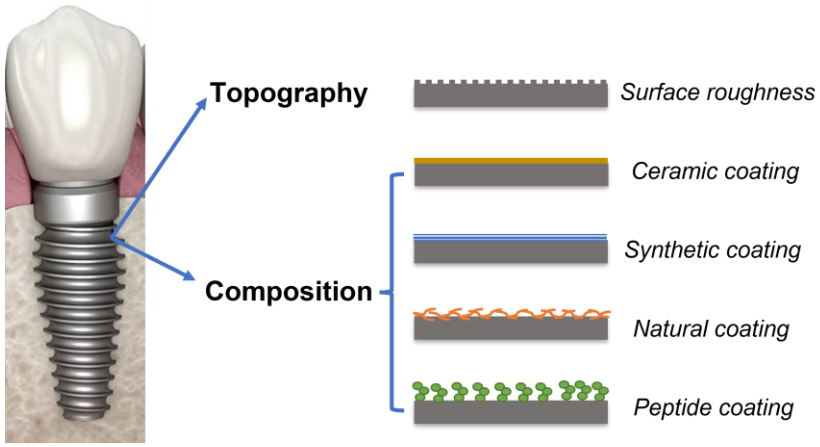

Figure 3: Illustration showing different modifications of titanium implant surface [26].

1.2.1. Ti surface topography modifications

Developments in altering surface topography on macro, micro, and nano scales have aimed to optimize the implant surface to the expected function. For example, highly polished surfaces were found to help the attachment of epithelial cells, which is needed for proper soft tissue seal at the cervical portion of the implant as well as on the attached dental abutments [27–29]. In contrast, roughened implant surfaces were found to support osteogenic differentiation and osteoblast attachment to the surface [5,26,30–33]. Thus, altering the surface topography of Ti implants' interface with the bone has been adopted as a standard process in the fabrication of Ti implants [34,35].

Many methods such as sand blasting, acid-etching, porous sintering, and plasma-spraying to name a few, have been used to alter the implant topography [36–41]. The most used procedures are sand blasting and acid etching [40]. Several strong acids such as hydrofluoric, nitric, and sulfuric acids have been used alone or in tandem to increase the surface roughness of the Ti surface [42–45]. A study using hydrofluoric acid (HF) to etch titanium oxide-grit-blasted surfaces was found to increase osteogenic markers (Runx2 and alkaline phosphatase) significantly both in vitro and in vivo compared to controls [46]. In another in vitro study using HF, the positive effects of acid etching such as cell adhesion and increased wettability were correlated to etching time; the investigators in that study have found that with increasing the etching time and consequently the Ti surface roughness improved both cell adhesion and wettability to a certain point. Interestingly, this improvement was lost when etching time was increased [44]. Another in vitro study compared sulfuric acid etched Ti discs with polished and sandblasted ones in terms of the proliferation and collagen production of osteoblast-like MC3T3-E1 cells found no significant differences in the results concluding that acid etching was a safe and effective method to alter Ti topography without affecting its biocompatibility [42]. However, the ultimate implant topography has not

been found up till the moment of writing this thesis; yet it is undeniable that altering the surface topography of metallic implants could have a positive effect on the implant's osteointegration [26].

1.2.2. Ti surface composition modifications (coating)

Both chemical and physical methods have been utilized for changing the implants' surface composition. The chemical methods depends on utilising covalent or ionic bonding to functionalize the Ti implant surface to improve osteoconductivity and/or initiate osteogenesis [47]. Meanwhile, the physical methods depend on physical coating and weaker surface interaction such as electrostatic forces, and hydrophobic interactions [47]. Although the chemical methods are more reliable and controllable, the physical methods are simpler and allow the modification of the Ti surfaces without affecting the integrity and/or composition of the used coating material [48]. Therefore, in our research we focused on physical modifications.

Creating an osteogenic Ti implant surface through altering surface composition has been heavily studied using various organic and inorganic materials [5,10,11,48–52]. Inorganic implant coatings such as calcium phosphates, hydroxyapatites, and bioactive glass have been heavily tested with varying degrees of success as they mimic the bone inorganic phase, thus encouraging cell adhesion and differentiation, leading to osteointegration in vitro and in vivo [53,54]. However, a recent systematic review that analysed the data of inorganic implant coatings studies focusing on tricalcium phosphates and hydroxyapatite, has concluded that the improved bone formation around coated implants lacked statistical significance in most studies [54]. The same review highlighted that there was almost no difference, between coated implants versus roughened ones in the short-term studies in large animals [54]. On the other hand, using organic or mixed organic-inorganic implant coatings was found to elicit a favourable biological response, as they mimic the natural bone environment and can induce

osteogenesis [55–57]. Hence, the focus of this research is on the organic implant coatings, which include synthetic and natural polymers as well as bioactive molecules (e.g., peptides).

1.2.2.1. Synthetic polymers

Biocompatibility, biodegradability, and mechanical stability are the most important parameters when selecting a synthetic polymer coating for Ti implants. Many synthetic polymers have been investigated such as polyglycolic acid (PGA), poly-β-hydroxybutyrate (PHB), poly (lactic acid-co-glycolic acid) (PLGA), poly-ε-caprolactone (PCL), as well as poly lactide (PLA) and many more [58]. PLA is among the most established biodegradable synthetic polymer coatings for metallic implants [59–65]. Its high mechanical stability provides a good platform for local controlled release of pharmaceutical agents (e.g., antibiotics and analgesics) and/or bioactive molecules [59–65]. Therefore, special attention is dedicated to PLA in the next few paragraphs.

Poly lactides (PLAs)

Poly lactide is a biocompatible, aliphatic polyester with the backbone formula of $(C_3H_4O_2)_n$ or $[–C(CH_3)HC(=O)O–]_n$, as shown in Figure 4. It was discovered in the 1700s by a Swedish chemist named Scheele. It is renewable, available, and easy to prepare, making it ideal for many biomedical applications [66]. PLA range from crystalline to amorphous in structure, and typically have 2 forms: poly L-lactide (PLLA) and poly D-lactide (PDLA), which could be mixed forming poly D, L-lactide (PDLLA), which is an amorphous co-polymer with no melting point [66]. PDLA is used for more industrial applications, while PLLA gained more interest in the biomedical field as it could be metabolized by the cells, thus decreasing the risk of adverse effects of its use [67]. PLLA hydrolyses, then is either integrated into the Krebs cycle, or turned into glycogen in the liver, and eventually excreted as water and carbon dioxide via the lungs [68,69]. Despite PLLA advantages, PDLLA degrades faster due to its amorphous nature [70–72], a quality that makes it advantageous as an implant coating

material. Faster degradation can lead to the delivery of therapeutic and/or bioactive agents to the implant-bone interface early in the healing process when it is crucial for preventing infections [62,63,73] and/or jumpstarting the healing process [61,69,74] leading to faster osseointegration and better treatment outcome.

As an example of infection prevention, Vester et al., used PDLLA loaded with Gentamicin antibiotic as a Ti implant coating aiming to study the drug release and efficacy both in vitro and in vivo in rat tibia [63]. The release results showed a similar pattern in both in vitro and in vivo conditions, characterized by an initial burst followed by slower release. The coating was found to decrease the bacterial adhesion on the Ti surface, have no adverse effects on osteoblasts, and cause no bacterial resistance [63]. In an earlier study by Lucke et al., it was found that PDLLA-Gentamicin coated Ti significantly reduced post-operative osteomyelitis in rat tibia model indicating the efficacy of the PDLLA as a local drug delivery coating that can prevent post-operative peri-implant infections in vivo [62].

Local growth factor delivery has been also studied using PDLLA Ti coatings as a sustained delivery carrier. An in vivo study was done to assess the treatment of rat cranial critical-size defect with Ti membranes coated with PDLLA containing TGFβ1, and insulin-like growth factor I (IGFI), with and without the supplementation with clindamycin antibiotic [75]. The results, after 4 weeks, showed complete closure of the critical-size defect of the groups treated with PDLLA-TGFβ1-IGFI with and without clindamycin in contrast to the respective controls. Nevertheless, no significant differences were found in the amount of bone formation among all groups and controls [75]. PDLLA was also used to locally deliver BMP2 from an intramedullary implant in a rat fracture tibia model [76]. In that study, fracture healing was examined both mechanically and histomorphologically at 2 time points (28- and

42-days after implantation). The results showed accelerated bone healing in the group treated with PDLLA-BMP2 coated Ti implants, evident by the increased torsional stability at both time points in comparison to the controls. The histomorphological analysis also confirmed the bone healing by showing increased callus mineralization, decrease cartilage, and advanced remodelling for PDLLA-BMP2 coated Ti compared to controls [76]. These findings show the benefit of using PDLLA as carrier for drugs and/or biomolecules.

Another biomolecule incorporated into PDLLA coating to be locally delivered to the implant's adjacent bone, is plasmid DNA. Kolk et al. developed and optimized gene-activated PDLLA coated Ti containing copolymer-protected gene vector (COPROG) with plasmid DNA encoding BMP2 [61]. The coating induced osteogenic differentiation of MSCs implanted on the surface of the coated Ti in vitro [61]. Later, the optimized coating was tested in vivo by the same author in a rat mandibular critical-size defect model [77]. The μCT and histological findings of this study showed partial bridging after 14 days, and complete healing after 112 days, for the defects treated with the coated implants with DNA/implant dose ≤ 2.5 mg in contrast to untreated controls [77]. However, the first in vivo study using that proposed system was done by Schwabe et al., to assess the biomechanical stability, histomorphology, and safety of the intramedullary PDLLA-COPROG-BMP2 coated Ti in a rat tibial fracture model [74]. The results showed significantly higher mechanical stability of the coated group versus the control, the transfection effect remained local with no biodistribution to distant organs detected, which highlighted the safety of the system [74]. Furthering their work, an additional study was done using the same coating by Haidari et al., to deliver not only BMP2 gene vectors but also active anti-infective agents aiming to induce bone formation and reduce peri-implant infections with promising results in vitro [78]. All these studies and more are convincing evidence that PDLLA was used successfully in vitro and in vivo as drugs- and/or biomolecules controlled-release coating for Ti implants.

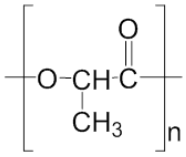

Figure 4: PDLLA polymer chemical formula

1.2.2.2. Natural polymers

Natural polymers gained a lot of attention due to their inherent low toxicity, availability, renewability, and low cost. They are naturally complex, making them harder to manufacture with high reproducibility in contrast to the synthetic options. However, this same complexity offers an advantageous role in their clinical use. They naturally facilitate cell adhesion, induce certain signalling pathways and modify bone remodelling [26]. Many natural polymers such as collagens, silk fibroin, gelatines, fibrin(ogen), and others have been researched extensively as osteogenic coating materials for metallic implants, either alone or as carriers for drugs or biomolecules to enhance osteointegration [79–82].

For example, Ti functionalized with collagen-I was able to integrate with the bone in an osteopenic rat model [79]. Sartori et al. compared collagen-I coating with acid-etched Ti screw-implant in an osteopenic rat femoral condyle, and they evaluated osteointegration mechanically, micrographically, and histologically at 4- and 12-weeks' time points [79]. They have found significantly higher mechanical stability and bone-to-implant contact of the collagen-I coated implants in contrast to acid-etched implants [79]. Another example is Ti implants coated with immobilized silk fibroin were found to facilitate cell adhesion and spreading leading to better mineralization and eventually osteointegration [83]. Also, natural polymers like gelatine were used to coat Ti implants to increase cells' reactivity to the Ti surface [81]. Still, among these polymers, fibrin(ogen) has gained the most attention when it comes to

tissue engineering applications due to its natural advantage as the primary healing scaffold in the body [84].

Fibrin

Fibrin (FT) is the body's primary framework for healing, which is formed when its precursor fibrinogen polymerizes. Fibrinogen (F) is a soluble, 340 kDa glycoprotein synthesized in the liver and found in the blood's plasma [85]. It consists of 2 sets of Aα, Bβ, and γ chains illustrated in Figure 5, which, in the presence of thrombin (T), Ca^{2+}, and other clotting factors, cleave inducing polymerization into protofibrils that are later crosslinked by factor VIII to increase the resultant fibrin's tensile strength and resistance to fibrinolysis [85]. It is well established that fibrinogen and fibrin provide support for cell adhesion, migration, and differentiation, as well as support extracellular matrix and cell-cell interactions, as part of their natural function [86].

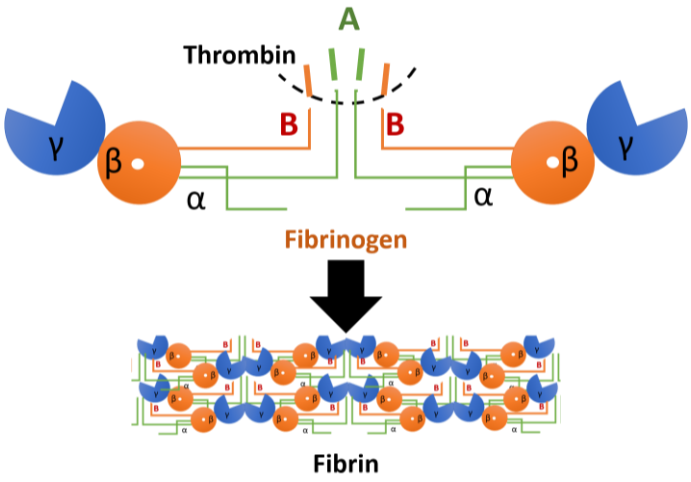

Figure 5: Illustration showing the composition of fibrinogen (top) which in the presence of thrombin and other clotting factors turns into polymerized fibrin (bottom).

Fibrin has been heavily studied as a tissue engineering scaffold as well as a drug delivery vehicle. It was used as a vehicle material for multiple osteoinductive biomolecules and growth factors. Fibrin hydrogels loaded with BMP2/BMP7 were studied as a bone substitute material for non-load-bearing

defects both in vivo and in vitro [87]. The results of that study showed an increase in alkaline phosphatase activity in pluripotent cells and bone regeneration in a rat calvarial model [87]. It was also utilized by Schillinger et al., using an injectable fibrin glue kit (TISSUCOL) as a carrier for the previously mentioned COPROG DNA construct encoding BMP2 to induce osteogenesis [88]. They co-lyophilized the fibrinogen component of the fibrin kit with COPROG BMP2, then thrombin, along with a mixture of primary keratinocytes and chondrocytes, were added upon rehydration. The results showed upregulation of alkaline phosphatase expression, and an increase in extracellular matrix production compared to controls in vitro [88]. Another osteogenic biomolecule that was loaded successfully in fibrin was messenger RNA coding for BMP2 (BMP2 mRNA). Balmayor et al., used fibrin gel loaded with BMP2 mRNA to stimulate osteogenic differentiation of MSCs in vitro, and compared it to BMP2 mRNA-loaded macro-micro-biphasic calcium phosphate [17]. The results showed a significantly slower release of the mRNA from fibrin gel. Nevertheless, both groups showed BMP2 secretion and expression of osteogenic markers from MSCs cultured on them, which demonstrated the efficacy of both biomaterials in inducing osteogenic differentiation in vitro [17].

Fibrin was used not only for non-load bearing defects, but also in combination with load-bearing implants. Van der Stok et al. utilized a selective laser melted porous titanium implant filled with fibrin gel loaded with BMP2 growth factor to treat a critical-sized segmental defect in a rat femur model [82]. They evaluated bone regeneration, bone quality, and the implants' mechanical stability via in- and ex-vivo μCT, histology, and torsion testing. The results showed full bone regeneration of the critical-sized defect of the Ti-Fibrin-BMP2 group after 8 weeks. After 12 weeks, the bone reshaped with open medullary spaces of the Ti-Fibrin-BMP2 group compared to controls. Similarly, the torsional mechanical stability of the implants exceeded twice the initial stability. Finally, the histological results showed the ingrowth of bone in the implants' pores of the same group. Such findings emphasized the

efficacy of combining fibrin as a carrier for BMP2 with metallic implants for better and faster bone regeneration for critical-sized defects [82].

Fibrinogen

While fibrin is widely used for bone regeneration, fibrinogen, on its own, is quite underestimated, despite its favourable interaction with different cells and tissues [89,90]. However, because of its nature, fibrinogen has been used in several tissue engineering applications. Donaldson et al., compared coated pieces of coverslip glass with fibrinogen versus fibronectin to evaluate cell attachment and migration on them when implanted under the skin of newt [91]. They concluded that both coatings allowed for epithelial cell attachment and migration highlighting the potential beneficial role of fibrinogen coating in wound healing [91].

Moreover, fibrinogen was used as an adsorbed coating in combination with other materials to modulate cell response and enhance the production of osteogenic factors. Oliveira et al. used fibrinogen adsorbed on chitosan substrate to study the response of primary human monocytes in vitro [92]. They found that fibrinogen-coated substrates induced BMP2 production from monocytes among other pro-osteogenic effects highlighting the significant role of adsorbed fibrinogen on bone regeneration around implanted materials [92].

Additionally, fibrinogen adsorption was studied by Boukari et al., on two different dental implants after incubation in fibrinogen solution, one sandblasted and the other covered with a calcium phosphate coating [93]. They examined the implants' surface via an electron microscope, and atomic force microscope to confirm and measure the detachment force of the adsorbed fibrinogen [93]. The experimental data showed successful adsorption on both materials with higher detachment force on the

sandblasted Ti surface after 1000 milliseconds interaction time, which in favour of the fibrinogen adsorption on the Ti surface [93].

Fibrinogen was also used in the fabrication of semi-synthetic polymer scaffolds as a carrier for osteogenic biomolecules. Ben-David et al. used PEGylated fibrinogen hydrogel loaded with BMP2 for the treatment of critical size maxillofacial bone defect in a rat model [94]. The μCT and histological findings showed better bone formation in the groups treated with PEGylated fibrinogen with BMP2 compared to respective controls in as little as 6 weeks after surgery [94]. Another study used chitosan-lactide-fibrinogen hydrogel loaded with BMP2 to induce bone formation both in vitro and in vivo [95]. The material showed a slow-release pattern after an initial burst of BMP2 and showed no toxicity to the cells seeded on it in vitro. While the loaded hydrogels used to treat rat's critical size segmental bone defects showed μCT and histological findings that confirmed the ability of the material to accelerate osteogenesis compared to controls after only 4 weeks [95].

Lately, liquid fibrinogen has been investigated as an alternative for leucocytes and platelet-rich-fibrin (L-PRF) which is well investigated in promoting healing after surgery [96]. It is a liquid concentrate rich in leukocytes, platelets, and fibrinogen obtained via blood centrifugation. Different growth factors are released from the liquid fibrinogen including TGFβ and BMP2 among other beneficial growth factors for soft and hard tissue healing, making it a great candidate for clinical use to promote healing [97]. Andrade et al. collected liquid fibrinogen from healthy donors and dipped five different commercially available Ti implants in the liquid for 60 minutes [98]. The implants were later fixed and examined by scanning electron microscopy (SEM) showing fibrin mesh covering of all implants used. However, the resulting fibrin layer varied significantly in terms of uniformity, and density depending on the commercially available implants' brand. These findings necessitate further investigation to evaluate

the clinical significance of fibrinogen use on the osteointegration of implants [98]. Yet, until the moment of writing this research, there are no studies investigating the fibrinogen as a standalone candidate for sustained release Ti implant coating which was a great motivator for us to investigate the exciting potential of this natural material.

1.2.2.3. Biomolecules

A range of bioactive peptides have been used to modify the surface of Ti implants to improve cell-response, and adhesion, and/or induce osteogenesis. For example, biomolecules such as fibronectin [5,91,99] and its related sequences (e.g., RGDs and PHSRN) [100–102] have been used to improve cell attachment and recruitment on the implant surface [103], also other biomolecules containing heparin-binding motifs were found to promote osteoblastic adhesion [104].

Additionally, various growth factors have been used to modify the Ti surface to induce osteogenesis around implants such as platelet-derived growth factor [105], insulin-like growth factor [106], and most importantly TGF-β family which contain bone morphogenetic proteins (BMPs) [103,105–107] that are known to play an important role in osteogenic differentiation. It was argued that BMPs are more favourable for bone healing around implants than commonly used RGDs as they are cell-specific whereas RGDs are not [103,108,109].

BMPs were first identified for causing bone formation in ectopic sites [103]. Many of the BMP family have been investigated for implant surface modification such as BMP2, BMP4, and BMP7 which are naturally expressed in bone. They play an important role in Runx2 regulation via several pathways which in turn regulates osteoblastic differentiation [110,111]. The most used growth factor in literature is BMP2 which plays a significant role in bone healing, and it will be discussed in more detail in the next section 1.3 of this thesis.

Ti surface modification with peptides could be achieved via chemical or physical methods. While some biomolecules such as RGDs could be immobilized chemically, with relative ease, to the surface of the implant, it is not the case for growth factors, as chemical immobilization could affect the biological activity of the molecules [103,112]. Thus, for growth factors immobilization, the focus would be on the physical methods of biomolecule incorporation. There are 2 main methods to immobilize biomolecules physically onto the implant surface; 1- physical adsorption (via weak bonds like van der Waals or electrostatic forces, hydrogen bonds, and hydrophobic interactions), 2- physical entrapment within biodegradable material (barrier material) [48].

Coating via physical adsorption depends on many factors such as surface chemistry, topography, hydrophobicity, and the electrostatic interaction between the surface and the used biomolecules [113,114]. It is a weak functionalization method, in which the particles adsorb and desorb from the surface in an uncontrolled manner (usually leads to fast release), which can increase the probability of excessive-dose side effects [15,115]. However, physical adsorption remains a simple and mild method that does not disrupt the structure of the used peptides.

On the other hand, the physical entrapment approach retains the mildness of the physical adsorption method, whilst allowing for controlled release, which can overcome the possible disadvantages of physical adsorption [48]. Many biodegradable synthetic and natural polymers have been investigated for the physical entrapment approach [84,116,117] as discussed in the previous sections (1.2.2.1 and 1.2.2.2 of this thesis).

1.3. Bone Morphogenetic Protein 2

Bone Morphogenetic Protein-2 (BMP2) is a member of the Transforming growth factor beta (TGF-β) superfamily of proteins. It is a multi-functional growth factor that is known for its ability to initiate

ectopic bone formation in adult animals [118]. In a study done by Stoeger et al., ectopic bone in rat muscle was induced via BMP2 carried in collagen-I sponges [119]. The resulting ectopic bone was found to have similar molecular gene expression to embryonic cartilage and bone, which emphasizes BMP2's importance in bone formation and development via both endochondral and intramembranous ossification pathways [119].

Its role in bone healing was demonstrated in a study by Tsuji et al., in which mice lacking the ability to produce BMP2 showed multiple spontaneous fractures in their limps that fail to resolve over time, indicating that the pathway of fracture healing was blocked despite the presence of other osteogenic factors in the BMP2-deficient bones [120]. Moreover, changes in BMP2 activity are noticed with old age, osteoporosis, osteoarthritis, and reduced fracture healing, thus highlighting its importance for bone health, maintenance, and regeneration [118].

BMP2 has two main receptor signalling pathways, canonical (Smad), and non-canonical (TAK1/MAPK) [121]. Both pathways start after BMP2 binds with the cells' BMP type II receptor. The bound receptor then recruits the BMP type I receptor to form a complex which mediates type I receptor phosphorylation. The canonical (Smad) pathway is mediated by receptor-regulated R-Smad (Smad1/5/8) phosphorylation and R-Smad/Co-Smad (Smad4) complex formation. After the R-Smad/ Co-Smad complex is formed, it transfers to the nucleus where it regulates target gene expression (such as Runx2 and Osterix1) by cooperating with other transcription factors [121]. This pathway plays an important role in osteoblast differentiation from many cell types [122]. Figure 6 illustrates the previously explained BMP2 canonical signalling pathway.

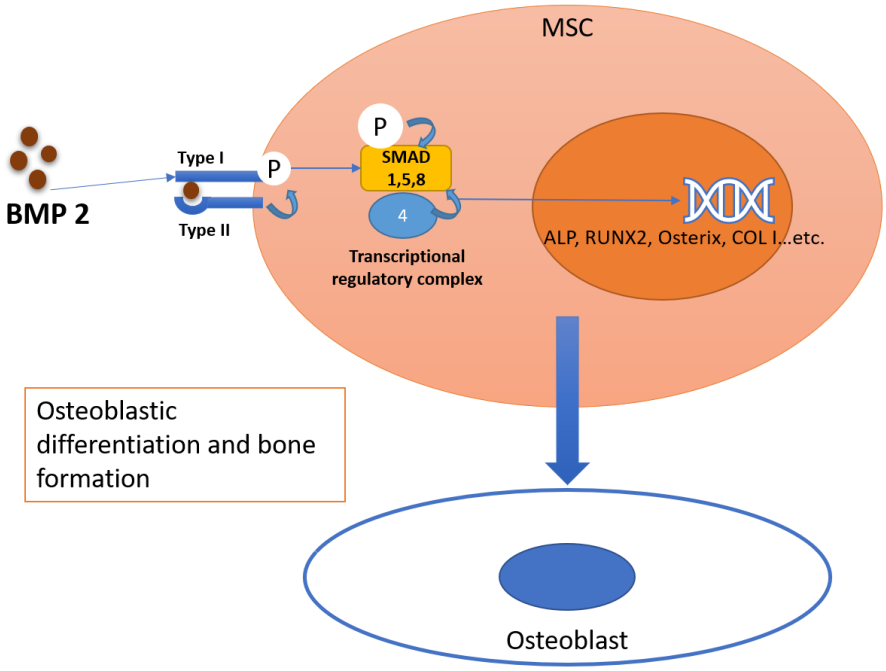

Figure 6: Diagram of one of the BMP2 signalling pathways for osteogenic differentiation. BMP2 signal transduction pathways. After BMP2 binding, the BMP type II receptor recruits the type I receptor to form a complex and mediates type I receptor phosphorylation. There are at least two signalling pathways involved in BMP receptor-mediated signal transduction: Smad and TAK1/MAPK. The canonical Smad pathway is mediated by receptor-regulated R-Smad (Smad1/5/8) phosphorylation and R-Smad/Co-Smad (Smad4) complex formation. After the R-Smad/ Co-Smad complex is formed, it transfers to the nucleus where it regulates target gene expression by cooperating with other transcription factors.[121,123]

1.3.1. Local protein administration

BMP2 has become one of the most used biomolecule for bone regeneration around Ti implants, either on its own or in combination with other biomaterials [14]. It has shown great results in bone healing in critical size defects in vivo when used in combination with porous Ti implants filled with BMP2 and fibrin [82]. Hunziker et al. incorporated BMP2 in calcium phosphate coating that released it gradually in the implants surrounding when the coating underwent osteoclast-mediated resorption [124]. The implants were tested in the maxillae of miniature pigs in contrast to implants with adsorbed BMP2, implants with incorporated and adsorbed BMP2, and implants with no BMP2 as controls. The implants were

retrieved 1, 2, and 3 weeks after implantation for histological analysis of newly formed bone. The results of the study showed peaks of bone growth in all groups since the first week, however, only groups with incorporated BMP2 were able to sustain the peak on the following timepoints [124].

Also, in a study by Sachse et al., Ti implant healing was supported in the presence of BMP2 in vivo using an aged sheep model [125]. The aged sheep showed significant histological and radiographical signs of osteoporosis, however, bone healing was observed along with higher mechanical stability (up to 50% higher) in the groups coated with BMP2, which highlighted the potential of its use in compromised bone healing situations [125]. These examples, along with the ones discussed in the previous section 1.2.2 of this thesis), and many others, establish the clinical significance of BMP2 administration in fortifying peri-implant bone healing.

Despite the obvious benefits of BMP2 administration and the fact that it is approved as treatment for few bone indications by the American Food and Drug Administration (FDA), many side effects have been reported in correlation to its use [14,126,127]. A systematic review done by Haimov et al., analysed the data produced over 10 years of osteointegration improvement around Ti implants by BMP2 [14]. They have concluded that the fast release and very high concentrations of BMP2 should be avoided to prevent many of the side effects (such as excessive bone formation, bleeding, hematoma, inflammation, oedema, bone resorption, and implant failure) [14]. Moreover, its high price, short half-life in vivo, and the fact that safe dosage, and remote systemic effects of BMP2 are still under investigation, have limited the routine clinical use of this recombinant growth factor [61,127,128]. To overcome these issues, alternative modalities, such as using local gene therapy and transcript therapy techniques, have been developed [16,123,129–132].

1.3.2. Gene therapy

In local BMP2 gene therapy, the gene encoding the growth factor is used instead of the degradable protein to activate the metallic implant surface and induce bone formation. The gene, used as its cDNA form, transfects the target cells turning them into tiny bioreactors that produce the coded protein. Such process leads to intrinsic BMP2 production and regulation, hence reducing excessive dose side effects and ensuring the functionality of the produced protein [127].

Plasmid DNA could be delivered to the target cells using viral or non-viral vectors [127]. The gene vectors generally are used to target specific cells without disrupting their natural function and facilitate the gene entry through the cell membrane and into the nucleus, all while evading the host's immunity [127]. Different viral vectors such as adeno-, retro-, and lentiviruses have been used due to their high transfection/transduction efficiency and their natural tropism, however, high immunogenicity and disruption of normal gene function have been reported [127,133]. Therefore, non-viral vectors such as dendrimers, and polycation (i.e., polymers or lipids) are considered a safer alternative for gene delivery, yet, not as efficient as viral vectors [129,134,135]. The cationic polymers or cationic lipids are widely used as non-viral vectors for genetic materials as they can bind to DNA to form polyplexes or lipoplexes to protect it against nucleases and facilitate its uptake by the negatively charged cell membrane [135].

Many studies that tested BMP2 gene-activated Ti implants, confirmed its ability to induce osteointegration both in vitro and in vivo. For example, Chen et al. reported that functionalization of Ti surface with the layer-by-layer technique of naked BMP2 plasmid DNA, and poly (amidoamine) dendrimer/EGFP-BMP2 led to the expression of both genes in seeded osteoblasts in vitro [136]. Elevations of alkaline phosphatase activity, collagen secretion, and extracellular matrix (ECM) mineralization were also observed. This was confirmed by the histologic and radiographic findings in vivo, showcasing peri-implant bone formation in both subcutaneous and femoral implants in rats [136].

Many other examples from the literature and the ones mentioned in section 1.2.2 of this thesis confirm the validity of the gene therapy approach for osteogenic functionalization of Ti [61,77,78,137]. However, limitations such as the inability to transfect postmitotic cells, unwanted or prolonged effects, and the potential risks associated with viral vectors such as insertional mutagenesis, oncogenesis, and immunogenicity in addition to its high coast might restrict its clinical use [128,138]. Such concerns have driven researchers to explore messenger RNA (mRNA) or transcript therapy as a potentially safer alternative for gene therapy.

1.4. Transcript therapy

Messenger RNA (mRNA) is produced in eukaryotic cells via DNA gene transcription; its main function is to communicate the genetic information from DNA to the ribosomes [139]. In the cytoplasm, ribosomes translate mRNA into the encoded protein [139]. In recent decades, the use of RNA polymerases in vitro allowed the recreation of the DNA transcription process in the laboratory, leading to the production of in vitro transcribed mRNA (IVT mRNA) that can transfect cells leading to the production of the selected protein [140]. This opened the gates for a new era of mRNA therapeutics or transcript therapy.

Transcript therapy shares some advantages with gene therapy, such as controlled intrinsic production of the proteins, whilst overcoming some of the disadvantages [129]. For instance, the function of IVT mRNA is conducted exclusively in the cells' cytoplasm; this eliminates the need to cross the nuclear membrane, thus making it transfect non-dividing cells easier, and eliminating the risk of insertional mutagenesis, which presents it as a safer treatment alternative. Additionally, its rapid results and transient nature allow the possibility of multiple applications without long-term effects, which is considered advantageous, especially for regenerative medicine applications [129].

1.4.1. Chemically modified messenger RNA (cmRNA)

In eukaryotic cells, the transcribed mRNA undergoes a series of modifications to become mature, stable, and translatable. The modifications include RNA splicing, capping at the 5′ end, and polyadenylation at the 3′ end (poly-A tail) aiming to protect the mature mRNA from enzymatic degradation and further improve its translatability [141–144]. Demonstrated in Figure 7 is the basic structure of eukaryotic mRNA. Similar to naturally occurring mature mRNA, IVT mRNA must be capped, and poly adenylated, however, splicing is not required, as it is included in the design of the DNA plasmid template along with certain UTR modifications to ease translation. In addition to that, it should undergo further chemical modifications to the IVT mRNA backbone as well as it being highly purified to further decrease its immunogenicity and instability in the extracellular environment [145,146].

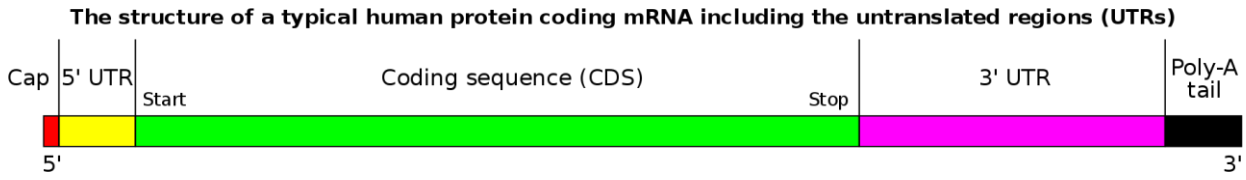

Figure 7: Structure of mature eukaryotic mRNA. Reproduced from Wikipedia [147]

In vitro poly adenylation is usually done by adding a poly-T tail in the plasmid DNA template, which helps control the length of the produced poly-A tail. The length of the poly-A tail ranges between 100-250 nucleotides according to the target cell type; however, it was found that IVT mRNA poly-A tails longer than 120 nucleotides are more likely to get translated [148]. Polyadenylation could also be done later after transcription using a poly-A polymerase. The presence of poly-A tail increases the translational efficiency and stability of the produced IVT mRNA [148].

IVT mRNA triphosphate portion at the 5'end (which is also characteristic of viral RNA) can be recognized in the cytoplasm by pattern recognition receptors (PRRs) and cause a type-1 interferon reaction (IFN1) [149]. This mandates in vitro capping process as the cap helps the mRNA to be recognized as self-RNA (not viral-), thus decreasing its immunogenicity [149]. In vitro capping is done by removing the triphosphate portion and adding inverted 7-methylguanosine instead [150]. Such process could be done co- or post-transcriptionally. Capping co-transcriptionally is done by adding cap analogues to the transcription mix; however, this could lead to capping at the 3'end instead, leading to untranslatable strands of mRNA [151]. This was rectified by using anti-reverse cap analogues (ARCA) which prevent the elongation of faulty capped strands and lead to high capping efficiency and better translatability [151]. Post-transcriptional capping is also possible via removing the triphosphate with a phosphatase enzyme and adding inverted 7-methylguanosine by a 2'-O-methyltransferase [151]. Still, the incomplete capping risk is present in both methods hence the high immunogenicity of IVT mRNA [149].

Additionally, DNAs and RNAs can stimulate the innate immune response as they can be recognized by the Toll-like receptors [152]. To overcome this issue and further decrease IVT mRNA immunogenicity, chemical modifications to the nucleotides were presented as a solution [152]. This also aids in increasing the stability of the IVT mRNA [152]. Karikó et al. were the first to report that in naturally occurring RNAs, selected nucleotides are methylated or otherwise modified, consequently, they tested some of the modifications by including them in IVT mRNA and found that it ablated the immune response and significantly decrease cytokines release [152,153]. Following in their footsteps, many chemically modified RNA nucleotides were investigated to further stabilize IVT mRNA and decrease its immunogenicity [140,153,154].

Rudolph et al. have patented that the substitution of 5-50% of IVT mRNA uridines and cytidines nucleotides in the transcription mix, with chemically modified ones (such as thiouridine and 5-methyl-cytidine - to name an example), created a more stable less immunogenic chemically modified mRNA (cmRNA) [154]. Kormann et al. used a single intra-muscular injection of erythropoietin cmRNA, which increased the haematocrit value in mice from 51.5% to 64.2% after 28 days [140]. Additionally, it showed curative potential in the treatment of congenital surfactant B deficiency in mice when inhaled twice daily until the end of the study. These experiments paved the way to explore more potential of the proposed cmRNA [140].

Local delivery of cmRNA (transcripts) can be achieved either using naked nucleic acid, physical methods (e.g. gene gun, and electroporation), or non-viral vectors; this represents another safety advantage over gene therapy carried out mostly with viral vectors to ensure efficiency [18]. While naked mRNA delivery showed a lack of therapeutic benefits, physical methods and non-viral vectors gave the most remarkable results [155–160]. The non-viral vectors are the most used method of delivery due to their safety and simplicity; they are usually polycations (i.e., polymers, or lipids). Few studies have investigated the use of cmRNA with polymeric non-viral vectors (i.e., polyplexes) - the most established is polyethyleneimine (PEI) [159]. These studies established PEI's ability to transfect cells in vitro, delivering different mRNA molecules, as well as yielding good results in vivo compared to plasmid DNA[161,162]. However, cationic polymers are not as heavily investigated as cationic or ionizable lipids which makes them less clinically advanced in comparison [163]. Cationic or ionizable lipids have a lower charge density as many cationic polymers. Nevertheless, they can bind and condense nucleic acids to nanoparticles which in addition to electrostatic interactions are held together by hydrophobic interaction. Lipoplexes protect nucleic acids against nucleases and facilitate its uptake by the cell membrane. Other molecules are added to the cationic or ionizable lipids to further stabilize the

complexes (e.g., cholesterol) and protect them in the extracellular environment (e.g., Polyethylene glycol) [145]. Numerous studies have established cationic lipids as efficient non-viral vectors for mRNA delivery [18–20,131,164–169]. These features present lipid-delivered cmRNA as a very promising therapeutic tool with exciting potential in the field of bone regeneration, which is addressed in the following section of this thesis.

1.4.2. Transcript therapy and bone regeneration

Recently, the utilization of transcript therapy for bone regeneration has gained considerable attention [131]. Its therapeutic potency, both in vitro and in vivo, was demonstrated repeatedly, as well as its ability to be combined with different biomaterials (vehicles) forming transcript-activated matrices (TAM). Badieyan et al., have loaded cmRNA lipoplexes into collagen sponges creating TAMs, which yielded 6 days of steady protein production and 11 days of residual production after transfection in vitro [20]. Additionally, using the same technique, sponges loaded with BMP2 encoding cmRNA (BMP2-cmRNA) led to osteogenic differentiation in vitro and induced healing in a non-critical defect in rat femur model in vivo [20]. The same research group successfully used cmRNA magnetic lipoplexes (i.e., magnetically targeted strategy for cmRNA delivery or magnetofection) [170,171]. This allowed them to transfect muscle, fat, and endothelial tissues of the carotid artery in an ex-vivo model [171].

Balmayor et al. used BMP2-cmRNA in vitro to transfect MSCs and loaded it in fibrin glue creating TAM for in vivo treatment of rats' femoral defect model [19]. In both cases, the treatment showed osteogenic activity demonstrated by elevated levels of alkaline phosphatase (ALP), upregulated osteogenic markers, and evident mineralization in vitro, while inducing new bone formation in vivo [19]. This further confirmed transcript therapy's capabilities in bone regeneration. Furthermore, the same group developed BMP2-TAMs using fibrin gel and micro-macro biphasic calcium phosphate granules (MBCP), which demonstrated sustained release capabilities over 7 days for both materials with varying

rates - MBCP being faster [17]. Interestingly, MSCs cultured in vitro on both materials showed similar osteogenic markers expression, with higher collagen-I and osteocalcin in the MBCP group. Mineralization was evident in both groups, also favouring the MBCP group [17]. These results further proof the potency of BMP2-cmRNA in the induction of MSCs osteogenic differentiation.

To improve BMP2-cmRNA osteogenic features, Zhang et al., further developed the cmRNA construct by removing certain undesirable sequence elements that may have reduced the downstream translation of the mRNA and its stability [169]. The removed elements were an upstream open reading frame (uORF) at the 5′ ends untranslated region (UTR), polyadenylation signal (PAS), and AU-rich region in the 3′UTR. Additionally, they introduced new elements namely translation initiator of short UTRs (TISU) and 5-iodo modified pyrimidine nucleotides to further increase mRNA's translational efficiency and stability. This new construct showed robust BMP2 production, MSCs osteogenic as well as angiogenic markers upregulation in vitro. Moreover, its potency was demonstrated in vivo in a critical-sized-defect femur in a rat model. The animals were treated with the new BMP2-cmRNA loaded into collagen sponges (TAMs); they showed superior evidence of new bone formation as well as improved vascularization, especially in the groups treated with the highest BMP2-cmRNA concentrations [169]. The same cmRNA construct was used by Balmayor and Evans who in a collaborative effort demonstrated, for the first time, a dose response effect of BMP2-cmRNA on healing bone tissue, as well as its ability to remain local at the administration site without leakage to other organs or the circulation [172]. This pioneer study also showed a superior biomechanics and tissue remodelling of the cmRNA-healed bones when compared to its recombinant protein counterpart. Despite the extensive research of transcript therapy in the bone regeneration field, none have researched its application in combination with Ti implants - till the time of writing this thesis. One paper by Xing et al., used a small interfering RNA (siRNA), not transcript mRNA, to create a hierarchical nanostructured coating for

orthopaedic titanium implants [173]. The siRNA was designed to target cathepsin K regulation and loaded on nanoparticles which were then assembled on the implant's surface. The coating revealed the ability to regulate gene expression via controlling mRNA transcription, leading to improved vascularization and cell viability on the bone-implant interface in both rat and dog in vivo models [173].

1.5. Thesis aim and objectives.

In the study presented in this thesis, we aimed to utilize cmRNA technology to create BMP2 transcript-activated coating for Titanium (Ti) implants. To achieve that, we used physical functionalization coating strategies, and we evaluated the effect of coating type and composition on the BMP2 translation efficiency, kinetics over time, as well as cell viability, and proliferation in vitro. Finally, we tested if the optimized transcript-activated Ti was able to induce osteogenic differentiation of C2C12 cells in vitro.

Our objectives were to:

1) Produce functional IVT cmRNAs.
2) Formulate and characterize cmRNA lipoplexes and test them for transfection efficiency.
3) Optimize transcript-activated coating via physical adsorption on cell culture plastic and on Ti discs, using a cmRNA reporter system.
4) Optimize transcript-activated coating via different physical entrapment methodologies using synthetic (PDLLA) and natural (fibrin) polymers by means of a cmRNA reporter system and Ti discs.
5) Understand the relationship between cmRNA concentration and coating methodology in terms of cmRNA release, transfection efficiency, and cytotoxicity.
6) Incorporate osteogenic BMP2 cmRNA into the optimized Ti coatings to demonstrate the bioactivity of the resulting coated implant in terms of osteogenic potential by using cell culture methods.

Chapter 2: Materials and methods

2.1. Materials

Table 1: Materials and chemicals for titanium discs preparation

Material	**Description**	**Provider**
Titanium	Grade IV 0.5 mm thick foil	Ankuro (Germany)
Teflon inserts	Polytetrafluoroethylene (PTFE) Teflon® 3D printer tubes	StickandShine (Germany)
Polystyrene 96 wells cell culture plates	Flat-bottom transparent - TPP® tissue culture plates	Sigma Aldrich (Germany) Product no.# Z707902
Polypropylene 96 wells plates	Flat-bottom, clear, Sterile plates Greiner®	Greiner Bio-One (Germany) Product no.# 655261
Acetone	99.7% concentration	Carl Roth (Germany) Product no.# CP40.1
Ethanol	99% concentration	Carl Roth (Germany) Product no.# 0911.2

Table 2: Materials for cmRNA preparation

Material	**Description**	**Provider**
Ribonucleoside triphosphate (ATP, CTP, GTP, and UTP)	The different mRNA building blocks in 99% purity and 100 mM ± 2% in concentration	Jena Bioscience (Germany)
Modified ribonucleotides (5-methyl-CTP, 2-thio-UTP, 5-Iodo-CTP, and 5-Iodo-UTP)	99% purity and 100 mM ± 2% in concentration	Jena Bioscience (Germany)
T7 RNA polymerase	10^5 U/mL	Thermo Fisher scientific (USA)
DNase	10^3 U/mL	Thermo Fisher scientific (USA)
Ammonium acetate	5 M solution	Sigma Aldrich (Germany) Product no.# 09691
ARCA	99% purity and 100 mM ± 2% in concentration	Jena Bioscience (Germany)
Water for injection (WFI)	N.A.	B. Braun Medical inc. (USA)

Table 3: Materials for lipoplexes preparation

Material	**Description**	**Provider**
Lipofectamine 2000	Lipid non-viral vector	Thermo Fisher Scientific (USA) Product no.# 11668019
dl_05 (R)®	Proprietary cationic lipid 50 mg/mL solution	Ethris GmbH (Germany)
DPPC	Dipalmitoyl phosphatidylcholine 20 mg/mL	Ethris GmbH (Germany)
Cholesterol	20 mg/mL	Ethris GmbH (Germany)
DMG-PEG2k	1,2-Dimyristoyl-rac-glycero-3-methylpolyoxyethylene PEGylated lipid 20 mg/mL	Ethris GmbH (Germany)
2-Propanol	Isopropanol ROTISOLV® HPLC grade	Carl Roth (Germany) Product no.# 7343.1

Citrate buffer	- Citrate 10 mM	Ethris GmbH (Germany)
D-(+)-Trehalose dihydrate	50% w/v Solution in WFI	Sigma life science (Germany) Product no.# T0167

Table 4: Coating materials

Material	**Description**	**Provider**
PDLLA	poly (D, L-lactide) Resomer R 203 H	Sigma Aldrich (Germany) Product no.# 719943
Ethyl acetate	HPLC grade 99.8%	Sigma Aldrich (Germany) Product no.# 270520
Fibrin glue kit (Tissucol®)	- Freeze-dried fibrinogen 66 mg/mL - Freeze-dried thrombin 100 IU/mL components	Baxter Healthcare (USA)

Table 5: Cells and cell culture materials

Material	**Description**	**Provider**
NIH3T3 cell line	Mouse embryonic fibroblast	ATCC (USA) Product no.# CRL-1658
C2C12 cell line	Murine myoblast cell line	DSMZ (Germany) Product no.# ACC 565
Dulbecco`s Modified Eagle Media (DMEM) - high glucose	containing 4.5 g/l glucose, 0.584 g/l L-glutamine	Sigma Aldrich (Germany) Product no.# D5796
DMEM - low glucose	1 g/l glucose, 0.584 g/l L-glutamine	Thermo Fisher Scientific, Gibco (USA) Product no.# 21885025
Foetal bovine serum (FBS)	N.A.	PAA cell culture company (UK)
Penicillin/Streptomycin	N.A.	PAA cell culture company (UK)

Trypsin-EDTA	1X	PAA cell culture company (UK)
L-ascorbic acid 2-phosphate sesquimagnesium salt hydrate	0.2 M solution	Sigma Aldrich (Germany) Product no.# A8960
β-glycerophosphate disodium salt hydrate	10 mM final concentration	Sigma Aldrich (Germany) Product no.# G9422

Table 6: Materials for Metridia Luciferase (MetLuc) expression assay

Material	**Description**	**Provider**
Coelenterazine	10 mg	SynChem (Germany) Product no.# S053
Methanol	99.9%	Sigma Aldrich (Germany) Product no.# 34860
Buffer solutions	- Na_2HPO_4 (MW: 141,96g/mol)	Carl Roth (Germany)

	- NaH_2PO_4 $X2H_2O$ (MW: 156,01g/mol)	Na_2HPO_4: Product no.# 7558-79-4 NaH_2PO_4: Product no.# 13472-35-0
White measurement plates	Corning® Costar white polystyrene flat-bottom non-treated 96 well plates	Sigma Aldrich (Germany) Product no.# CLS3912

Table 7:cell viability assays materials

Material	**Description**	**Provider**
Alamar blue	Alamar blue staining solution	MyBioSource (USA) Product no.# MBS638941
Picogreen assay kit	Quant-iT™ Picogreen® dsDNA assay kit	Molecular Probes-Life Technologies / Thermo Fisher Scientific (USA) Product no.# P7589

Black measurement plates	Nunc black non-treated no lid flat bottom	Thermo Fisher Scientific (USA) Product no.# 237108

Table 8: Release and stability assays materials

Material	**Description**	**Provider**
Ribogreen stain	Quant-iT™ Ribogreen® RNA reagent	Thermo Fisher Scientific (USA) Product no.# R11491
Detergent mixture	- Heparin sodium salt from porcine intestinal mucosa (40 mg/mL) - Triton-X 100	Fisher Scientific (USA) Heparin sodium salt: Product no.# 9041-08-1 Triton-X 100: Product no.# 85112
Black measuring plates	Black polystyrene 96 well assay plates Corning®	Sigma Aldrich (Germany) Product no.# CLS3991

Table 9: BMP2 expression and osteogenic detection assays materials

Material	**Description**	**Provider**
BMP2 ELISA	Human BMP2 Duo Set ELISA	R&D Systems (USA) Product no# DY355
Alkaline phosphatase activity (ALP)	- 10 mM 4-Nitrophenyl Phosphate di-Sodium salt hydrate pNPP - 4-Nitrophenol pNP 10 mM solution	Sigma Aldrich (Germany) pNPP: Product # 333338-18-4 pNP: Product # 100-02-7
Alizarine red assay	- Alizarine red staining solution 0.5% - 10% Hexadecylpyridiniumchloride	Sigma Aldrich (Germany) Alizarine red: Product no# 130-22-3 Hexadecylpyridiniumchloride: Product no# 6004-24-6

2.2. Methods

2.2.1. cmRNA preparation and characterization

2.2.1.1. cmRNA preparation

Chemically modified RNAs (cmRNAs) for Metridia Luciferase (MetLuc) and Bone Morphogenetic protein 2 (BMP2) were synthesized via in vitro transcription (IVT) according to the method described by Kormann et al. [140].

At first, the ribonucleotides (NTPs) mixtures for both RNAs were prepared as usual by mixing: adenosine-triphosphate (ATP), uridine-triphosphate (UTP), guanosine triphosphate (GTP) and cytosine-triphosphate (CTP). In addition, chemically modified ribonucleotides were added; 5-methyl-CTP, and 2-thio-UTP for MetLuc cmRNA mixture [20], and 5-Iodo-CTP and 5-Iodo-UTP for BMP2 cmRNA mixture [169].

Anti-reverse cap analogue (ARCA) was added to the prepared NTPs mixtures. ARCA acts by replacing the 3' hydroxyl group with OCH3 during RNA polymerization reaction, which allows the RNA polymerase to initiate transcription in the direction of the remaining 5' hydroxyl group [174]. This leads to proper capping of the prepared cmRNA in a forward orientation, preventing the growth of untranslatable reverse capped fragments. This in turn leads to better capping efficiency and consequently better translation of the prepared cmRNAs [174].

After that, linearized plasmid DNA template for each cmRNA was added to the corresponding NTPs mixture. Then T7 RNA polymerase was added to allow the in vitro transcription reaction to occur. After IVT was completed, the plasmid template was degraded using DNase enzyme.

The resulting MetLuc and BMP2 transcripts were not subjected to enzymatic 3'-polyadenylation, as they had the poly-A tail encoded into the used plasmid templates. The average poly-A tail was approximately 200 nucleotides in length for both prepared cmRNAs.

The transcripts were then purified via ammonium-acetate precipitation and resuspension in water for injection (WFI). The purified transcripts were filtered multiple times using Vivaspin 6 centrifugal concentrator (Sartorius, Germany). Finally, the filtered cmRNAs were diluted to the desired concentration in WFI. The cmRNA concentration was measured using NanoDrop 2000C spectrophotometer (Thermo Fisher Scientific, USA). The produced cmRNAs were stored in a -80°C fridge.

2.2.1.2. cmRNA characterization and biological testing

cmRNA integrity and purity assessment

The integrity and purity of the produced cmRNAs were assessed via automated capillary electrophoresis (Fragment Analyzer, Agilent Technologies, USA). The fluorescent labelled nucleic acid is separated according to its size by capillary electrophoresis in reference to an internal standard (i.e., ladder). The result of this analysis is usually represented by a graph showing a sharp peak that corresponds to the expected number of nucleotides (nt.) of the prepared cmRNA - including the poly-A tail. The presence of extra humps or noise around the sharp peak usually signifies fragments either from degradation or the presence of impurities – it is referred to as a smear. The sharper the peak of fluorescence and the smaller smear percentage of the total the better the purity of the measured sample.

cmRNA quality assessment

As for the quality of the prepared cmRNAs, it was evaluated by nucleotide analysis using High-Performance Liquid Chromatography (HPLC) (Agilent 1260 Infinity HPLC, Agilent Technologies,

USA). HPLC analysis highlights qualities such as chemically modified nucleotides incorporation rate, capping efficiency, as well as the length of the poly-A tail.

cmRNA biological activity assessment

The activity of the cmRNAs was tested via standard 2D transfection. For that, NIH3T3 cells and Lipofectamine 2000 lipid vector were used following the manufacturer's protocol. This allowed us to confirm their ability to transfect the cells and translate into the coded protein, as well as understand the kinetics of translation over time. The transfection experiments were all done in triplicates.

2.2.2. Lipoplexes formulation and characterization

Non-viral lipid vector was formulated using proprietary cationic lipid with Dipalmitoyl phosphatidylcholine (DPPC), cholesterol helper lipids, and 1,2-Dimyristoyl-rac-glycero-3-methylpolyoxyethylene PEGylated lipid (DMG-PEG). The Lipoplexes (lipid-cmRNA complexes) was formulated utilizing the solvent exchange method [20,175]. The self-assembled lipid vector in isopropanol solution was injected rapidly into an aqueous solution of cmRNA in 10 mM citrate buffer/150 mM sodium chloride. The mixture was then vortexed for 15 seconds and incubated at RT for 30 minutes to form the complexes. The lipoplexes were then dialyzed overnight against ddH_2O using a dialysis membrane of 7 kDa cut-off molecular weight (Thermo Fisher Scientific, USA) to remove excess isopropanol. The final cmRNA approximate concentration in lipoplexes solution was 100-120 µg/ml with an N/P ratio of 8 (ratio of amino groups of the lipid to phosphate groups in cmRNA).

For cryopreservation, 5% volume trehalose sugar was added to the prepared lipoplexes solution then it was stored at -20°C until used. The average size and zeta potential of the lipoplex particles were measured via dynamic light scattering and zeta sizer respectively, using a particle size analyser (Malvern Nanosizer, Malvern Panalytical Ltd., UK).

The produced lipoplexes were tested via standard 2D transfection of NIH3T3 cells in triplicates to confirm lipoplexes' ability to transfect the cells. Consequently, the cmRNA will translate into the coded, measurable protein. Different lipoplexes concentrations/well (serial 1:1 dilution from 500-7.5 ng/well) were used to understand the dose-effect relationship. The best concentration of lipoplexes was then used to optimize the cell number and understand kinetics over/time. The statistical analysis of the resultant data was done using ordinary one-way ANOVA with multiple comparisons between the different groups using Tukey's correction and 95% confidence intervals.

2.2.3. cmRNA lipoplexes stability

The stability of the lipoplexes was evaluated by assessing their size and zeta potential over time. For this, lipoplexes formed in WFI were analysed for a period of 8 days. In addition, cmRNA encapsulation efficiency, and cmRNA integrity over time at 37° C were also studied. To achieve that, 100 µg/ml cmRNA lipoplex solution was incubated at 37 C° for 8 days in separate, sealed Eppendorf tubes for each time point. A total of 10 time points (i.e., 0 hrs, 2 hrs, then daily up to 8 days) were analysed. In addition to the analysed lipoplexes, blanks, and positive control (i.e., reference naked cmRNA) were prepared. Each time point was analysed by measuring both size and zeta potential using Malvern Nanosizer apparatus (Malvern Panalytical Ltd., UK).

The cmRNA encapsulation efficiency evaluation was done to quantify how much of the cmRNA was encapsulated via the lipid vector. It was analysed using Ribogreen staining. This was done via comparing untreated lipoplex samples (which represent the free or non-encapsulated cmRNA) with samples treated with the detergent solution mix (which represent the total cmRNA). The detergent solution contains 1:14 Heparin 40mg/ml to Triton X-100 2% vol/vol, which was used to release the cmRNA from the lipid complexes to be detected via the Ribogreen staining. The Ribogreen stain was prepared and added according to the manufacturer's instructions, and the fluorescence was measured

via the micro-plate reader (Tecan®, infinite M200 Pro, Switzerland). The results of samples with and without the detergent extraction were compared to determine encapsulated cmRNA using Equation 1. Furthermore, the efficiency percentage was calculated in comparison to the reference cmRNA sample according to Equation 2.

Equation 1: Encapsulated cmRNA calculation

$$Encapsulated\ cmRNA = Treated\ (total)cmRNA - Untreated\ (free)cmRNA$$

Equation 2: equation to calculate encapsulation efficiency %

$$Encapsution\ efficiency\ \% = \frac{\text{Encapsulated cmRNA} \times 100}{\text{Reference cmRNA}}$$

Finally, cmRNA integrity was evaluated via automated capillary electrophoresis (Fragment Analyzer, Advanced Analytical, USA) comparing the detergent-treated lipoplex samples at different time points to the reference cmRNA in terms of the presence and percentage of pre- and post-smear. The pre-smear represents smaller fragments of RNA while the post-smear represents larger contaminants. These values were calculated automatically in percentage via the fragment analyser software (Advanced Analytical Technologies, Inc., USA). Later, the sum of smears was subtracted from the main peak of the intact cmRNA at each time point and then plotted against the reference cmRNA sample for comparison.

2.2.4. Coating process optimization using MetLuc cmRNA reporter system.

In this section, the experimental set-up, the methods for Ti discs preparation, and the different methodologies used to physically incorporate MetLuc cmRNA lipoplexes on the Ti surface are explained in detail.

2.2.4.1. Coating optimization on cell culture plates

This step was done to optimize the physical adsorption coating process to prevent wasting titanium. Thus, polystyrene 96 well plates were coated instead. For this coating, 50 µl of 500 ng/well MetLuc cmRNA lipoplexes solution prepared in 20% ethanol were used to speed up the drying process. The coated wells were dried at room temperature (Dry/RT) or on ice (Dry/ice) in the cell culture flow hood in sterile conditions overnight (8-12 hrs). Thereafter, the coated wells were seeded with 10^4 cells/well using NIH3T3, which were then tested for MetLuc transfection at 24 hrs after seeding to compare the two methods. The resultant data were analysed using ordinary one-way ANOVA with multiple comparisons between the different groups using Tukey's correction and 95% confidence intervals.

2.2.4.2. Titanium discs preparation

Titanium (grade IV, 50 microns-thick foil) was cut into 6 mm diameter circular discs to fit inside the wells of 96 wells plate. The discs were de-greased in 99.7% Acetone for 10 minutes in an ultrasonic bath at room temperature (RT). Then they were washed 3 times in double distilled water (ddH_2O), then 3 times with ethanol 80% with the last wash in an ultrasonic bath for 10 min at RT to sterilize. The excess ethanol was removed, and the discs were left to air-dry in the cell culture flow hood. The dry Ti discs were kept in air-tight containers until used.

2.2.4.3. Experimental set-up

Teflon circular inserts were used to immobilize the Ti discs previously placed inside the 96 well plates, and to confine the coating to the exposed Ti surfaces as shown in the photographs in Figure 9. The inserts were cut from Polytetrafluoroethylene (PTFE) Teflon® 3D printer tubes with 7mm outer diameter and 5mm inner diameter. The tubes were cut into 2mm thick pieces using a 3D printed cutting

guide self-designed and fabricated[1] that is shown in Figure 8. The inserts were also de-greased with Acetone 99.7% and washed 3 times with ddH_2O and 3 times with ethanol 80%, then finally autoclaved to sterilize. Under the cell culture hood, Ti discs were placed in 96 wells plates and fixed in place using the sterilized inserts as shown in Figure 9, followed by irradiation with ultraviolet light for 1 hour to sterilize.

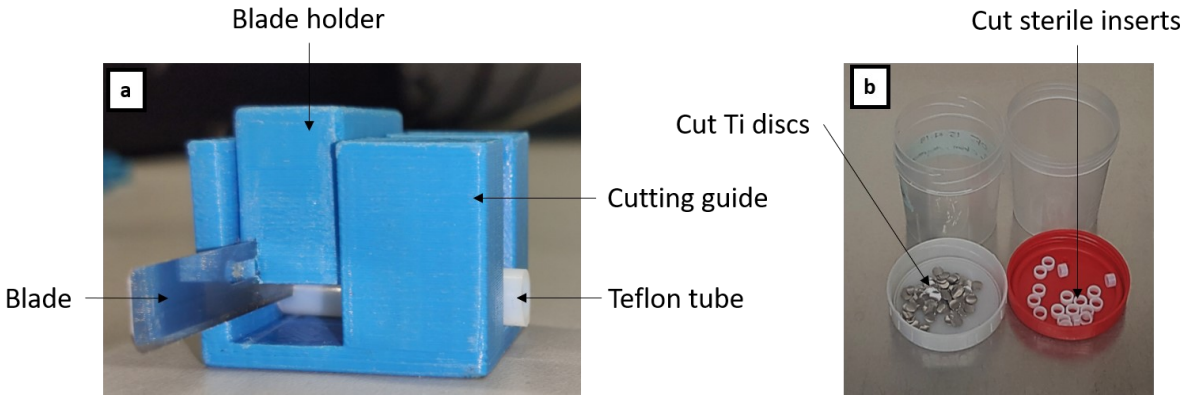

Figure 8: Photographs of the cutting guide, Ti discs and inserts.(a.) Photograph of the 3-D printed cutting guide used to cut the Teflon into equal-sized inserts. (b.) Photograph showing the Ti discs and Teflon inserts cut to size.

[1] The cutting guide was designed and fabricated by Dr. Jan Lang, researcher at the department of orthopedics and sport orthopedics, "Klinikum rechts der Isar" from the technical university of Munich.

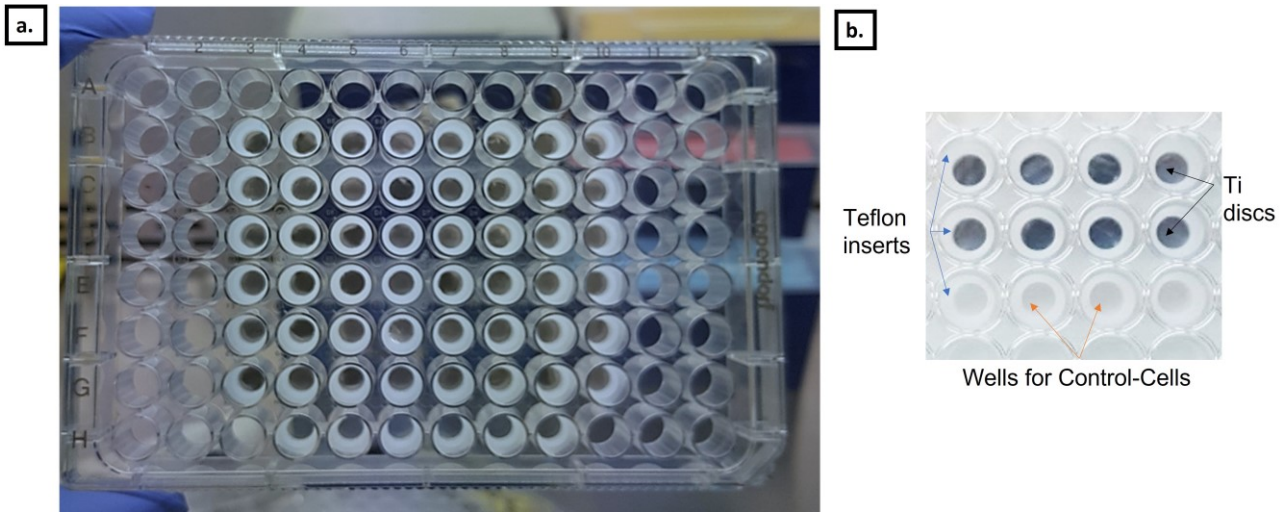

Figure 9: Photographs showing the experimental set-up with the cleaned Ti discs at the bottom of 96 wells plate and fixed in place with sterile Teflon inserts. On the left (a.), a photo of the whole plate, and on the right (b.) a zoomed photo with labels identifying the inserts and the discs for better appreciation of the used setup.

2.2.4.4. Coating via physical adsorption

Sterilized Ti discs (from the previous step 2.2.4.2 of this thesis) were coated by adding 30µl of previously prepared MetLuc-lipoplexes in 20% volume ethanol solution in a 1:1 serial dilution, starting at 500 ng/well MetLuc cmRNA until 62.5 ng/well. Then the coated discs were left to air-dry overnight (8-10 hrs) at RT under the cell culture flow hood. The lipoplex-coated Ti is referred to as (MetLuc-Ti) and uncoated clean Ti was used as control referred to as (Control-Ti), as illustrated in Figure 10. The experiment was done in triplicates. The resultant MetLuc luminescence data were processed by deducting blanks and correcting for total volume. The processed data were analysed using two-way ANOVA with multiple comparisons between the different cmRNA concentration groups using Tukey's correction and 95% confidence intervals.

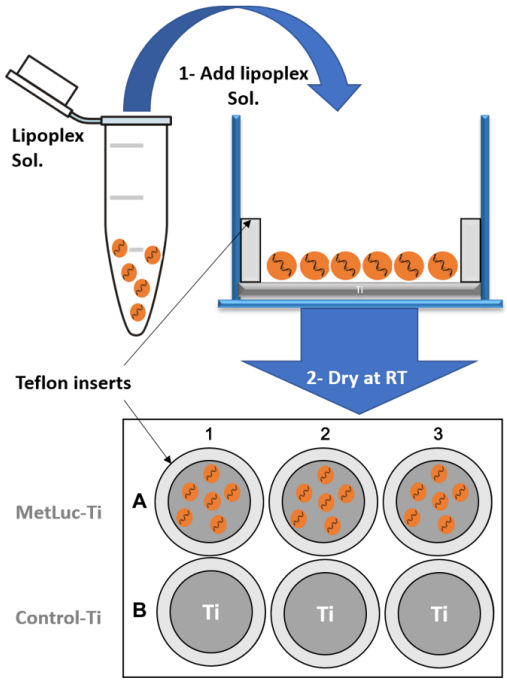

Figure 10: Illustration showing the physical adsorption coating process of Ti discs in the experimental setup.

2.2.4.5. Coating via physical entrapment using poly (D, L-lactide)

For poly (D, L-lactide) PDLLA coating, the best cmRNA concentration result from the physical adsorption method experiments was selected. The Ti discs were first coated with MetLuc-lipoplexes as described in the previous section 2.2.4.4 of this thesis. Then the dry samples were further coated with PDLLA (poly (D, L-lactide) Resomer R 203 H) dissolved in 99.8% Ethyl acetate. The PDLLA-coated Ti discs were left to dry under the chemical hood for 3 hrs. Thereafter, the drying process was allowed to continue under partial vacuum (500 Torr) in a closed desiccator for one more hour at RT. The polymer coating thickness was optimized by testing different PDLLA concentrations (3, 2, 1, 0.5, and 0.25 mg/well) based on calculations from previous data reported in Kolk et al.'s work [61]. The resultant groups were named MetLuc-PDLLA 3, MetLuc-PDLLA 2, MetLuc-PDLLA 1, MetLuc-PDLLA 0.5, and MetLuc-PDLLA 0.25, with the numeric value indicating the PDLLA concentration used for the coating. The corresponding controls had the same coating thicknesses but did not contain MetLuc lipoplexes and were similarly named Control-PDLLA 3, 2, 1, 0.5, and 0.25. The samples were

prepared also in triplicates as illustrated in Figure 11. The resultant MetLuc luminescence data of the different PDLLA groups were processed by deducting blanks and correcting for total volume. The processed data were analysed using ordinary two-way ANOVA with multiple comparisons between the different PDLLA thicknesses groups within each time point using Tukey's correction and 95% confidence intervals.

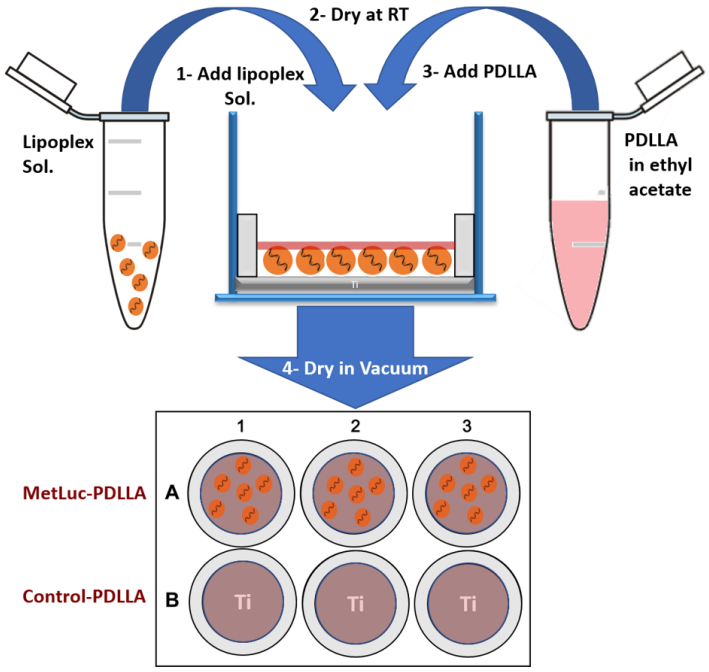

Figure 11: Illustration showing the steps of coating Ti with lipoplexes and PDLLA polymer via the physical entrapment method.

2.2.4.6. Coating via physical entrapment (Fibrin/Fibrinogen)

Like for the PDLLA coating, the best cmRNA concentration resulting from the physical adsorption method was chosen to test different compositions of fibrin. Subsequently, the best fibrin composition was tested with different cmRNA concentrations to determine a possible dose effect. Tissucol® fibrin

glue kit consisting of a fibrinogen component (F, 66 mg/ml) and a thrombin component (T, 100 IU/ml) was used.

First, MetLuc-lipoplexes aqueous solution was mixed with F component, and was used to cover the Ti surface with 15 µl of the mixture solution, setting the final concentrations at 500 ng/well cmRNA and 0.33 mg/well F. Then, an equal volume of thrombin solution (0.5 IU/well) was added to the MetLuc-fibrinogen mixture and mixed gently on the surface. The coated Ti discs were then incubated for 30 min in a 5% CO2 37°C incubator to allow for coagulation to occur creating the fibrin (FT) network.

To create different compositions of FT, different concentrations of T solution were used; the final coating volume ratios of fibrinogen (F) to thrombin (T) were 1F:1T, 1F:0.5T, 1F:0.25T, and 1F:0T, creating the groups (MetLuc-FT, MetLuc-F0.5T, MetLuc-F0.25T, and finally the group MetLuc-F - which was coated with MetLuc-fibrinogen only) in addition to their corresponding controls. The numeric value in the groups' nomenclature indicates the ratio F:T that was used in each case.

After incubation, the coated samples were frozen for 1 hour at -80°C. Subsequently, the coated samples were freeze-dried (Alpha 2-4, Martin Christ, Germany) for 48 hrs primary drying cycle with shelf-temperature at -30°C and 0.05 mbar vacuum, and 24 hrs for secondary drying at 4°C and 0.025 mbar vacuum. The coating steps are illustrated in Figure 12a and b. Then the coated samples were stored in vacuum bags at 4°C until the time of the experiment. These experiments were done in biological triplicates and repeated 3 times. The data was processed as mentioned in the previous section 2.2.4.5 of this thesis. The statistical analysis was done using ordinary two-way ANOVA with multiple comparisons of the different fibrin compositions within each time point using Tukey's correction and 95% confidence intervals.

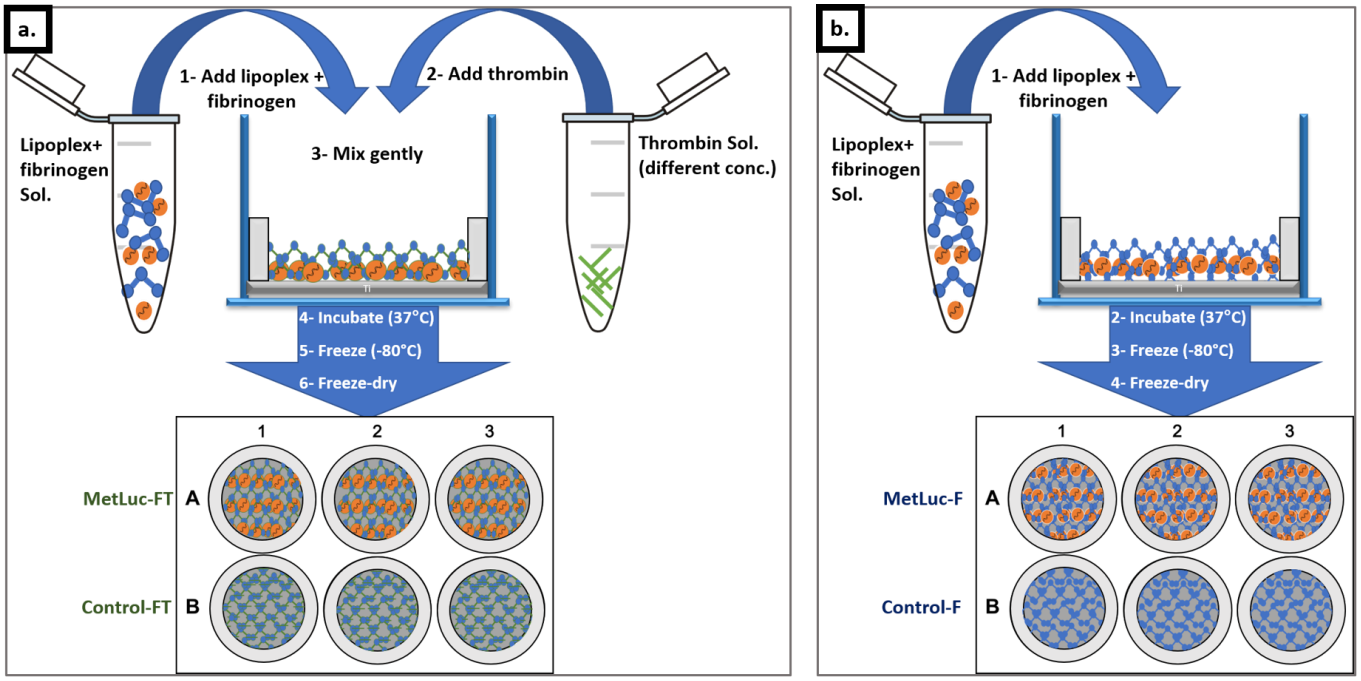

Figure 12: Illustrations of Ti coating process with fibrin (FT) and fibrinogen (F), (a.) showing the steps for coating Ti with fibrin, while (b.) is showing Ti coating with fibrinogen.

2.2.4.7. Cell culture of NIH3T3 cells

The NIH3T3 cell line was in vitro cultured in Dulbecco`s Modified Eagle Media (DMEM) containing 4.5 g/l glucose, 0.584 g/l L-glutamine and supplemented with 10% foetal bovine serum (FBS), and 1% penicillin/streptomycin (P/S) antibiotics. The cell density seeded on the coated Ti discs and the controls was 10^4 cells/well in 96 wells plates. The cells were cultured and kept at 37°C in a humidified 5% CO_2 cell culture incubator.

2.2.4.8. MetLuc translation and kinetics

MetLuc cmRNA reporter translation and kinetics were evaluated via collecting 100 µL of the medium supernatant daily starting 24 hrs after seeding the cells. The medium collection continued for up to 7 to 10 days (according to the coating type). The collected medium was replaced with fresh medium daily. The collected supernatant from the different samples was frozen at -20°C until measured. MetLuc translation was measured by adding 20 µL of 0.05 mM Coelenterazine to 50 µl of the collected

supernatant in Costar® white 96 well plates, and the luminescence was measured in relative light units (RLU) using microplate reader (Tecan®, infinite M200 Pro, Switzerland). The results were calculated minus the blank (un-transfected cells supernatant with Coelenterazine) and corrected to the total volume (100 µl).

2.2.4.9. Cell metabolic activity and proliferation

To gauge cell viability, Alamar blue assay was used to evaluate cells' metabolic activity via oxidation-reduction reaction. Living cells (i.e., metabolically active cells) have the ability to reduce the non-fluorescent resazurin dye (Alamar blue assay active ingredient) via mitochondrial reductase enzyme to fluorescent resorufin dye [176]. The fluorescence could then be measured to calculate cell vitality.

On the other hand, Picogreen assay was used to evaluate cells' growth and proliferation via staining of double-stranded DNA (dsDNA) content of each well. For these experiments, the cells were seeded on the coated Ti discs in 96 wells plates, as described before, and cell metabolic activity and proliferation were measured on the 1st, 3rd, 7th, and 14th days after seeding.

For Alamar blue assay, the cell culture medium was removed from wells and replaced with 10% Alamar blue solution in a cell culture medium. The plates were then incubated for 3 hrs at 37°C in 5% CO_2 humidified incubator (until the blue solution turns into a red/purple colour). Then the Alamar blue solution was transferred to black 96 wells plate and the fluorescence was measured at the excitation wavelength of 544 nm and emission at 590 nm with FLUOStar Omega plate reader (BMG Labtech, Germany). Then the results were calculated and normalized to the material's control. The samples were cells seeded on cmRNA coated functionalized Ti surface and their corresponding controls. As positive control, we used cells seeded in 96 wells plate with Teflon inserts (Control-Cells), as shown in the setup photograph Figure 9b. The blank was the incubated 10% Alamar blue solution with no cells. The

blank was deducted from all samples and normalized activity was calculated as shown in Equation 3. The samples were then washed with 3 times PBS and used for Picogreen assay. The statistical analysis of the processed fluorescence data was done via 2-way ANOVA followed by Tukey's correction.

Equation 3: Alamar blue results calculation.

$$Metabolic\ activity\ normalized\ to\ control = \frac{(sample\ reading - blank)}{Average\ (control\ readings - blank)}$$

For the Picogreen assay, Quant-iT™ Picogreen® dsDNA assay kit was used. After washing the cells, the Ti discs were removed from the 96 wells plates and were placed each into a separate Eppendorf tube. Then each disc was covered with 250 µl ddH_2O and froze them at -80 °C. The frozen samples were exposed to 3 cycles of freezing and rapid thawing at 37°C in a water bath, and the tubes were vortexed in-between to break down the cells forcing the release of their DNA content. For the Control-cells samples, ddH_2O was added to the wells containing the cells and was pipetted vigorously until the cells were all detached (checked via light microscope). Then the solution was transferred to the Eppendorf tube and subjected to the freeze-thaw cycles to breakdown the cells, as described before. The dsDNA concentration was measured for 50 µl of each sample using Picogreen stain following the manufacturer's instructions. The results were calculated according to the standard curve in dsDNA pg/ml. Then the samples were corrected for the total volume used (250 µl). The resultant data were normalized to material control. The data were analysed using 2-way ANOVA followed by Tukey's test for statistical significance calculation. Both Alamar blue and Picogreen experiments were done in biological triplicates and measured in technical duplicates.

2.2.5. Lipoplexes in vitro release from BMP2-F and BMP2-FT coated Ti

The transcript-activated fibrin and fibrinogen coated Ti discs were prepared as described before then incubated at 37 °C in DMEM medium supplemented with 1% P/S antibiotics and without serum. The

medium was collected and replaced after 2 hrs then daily for 7 days. The collected supernatant was frozen at -80°C until analysed at the end of the experiment. On the 7th day, the remaining F and FT coatings were digested by incubating the coated Ti discs in 100 µl of 0.05% Trypsin at 37°C for 1 hour, then the digest was collected for analysis.

To quantify the released cmRNA, a treatment with a detergent mixture (1:14 Heparin 40mg/ml to Triton X-100 2% vol/vol) must be done to release the cmRNA from the lipid complexes. For this, 50 µl of the samples containing cmRNA lipoplexes were mixed with an equal volume of the detergent mix and covered with a sticky foil in a black polystyrene 96 wells plate. The mixture was then incubated in a Thermomixer (Eppendorf, Germany) for 15 minutes at 70 °C and 300 rpm for mixing. The plate was then centrifugated at 3000 rpm for a minute to recover the evaporated water droplets.

Then Ribogreen (Thermo Fisher Scientific) assay was done according to the manufacturer's instructions to quantify cmRNA. The fluorescence of Ribogreen was measured using a microplate reader (Tecan®, infinite M200 PRO, Switzerland). The results were calculated as percent of the positive control (which was 500 ng/well cmRNA lipoplex solution in serum-free DMEM medium) and were analysed using 2-way ANOVA followed by Sidak correction.

2.2.6. BMP2 transcript activated Ti.

2.2.6.1. Ti Coating via Fibrin or Fibrinogen

The coating method yielding the best result from the optimization phase (i.e., fibrinogen coating (F)) was selected for further experiments. However, fibrin coating group (FT) was added for the sake of comparison and relevance.

2.2.6.2. Cell culture of C2C12

For this phase of experiments, C2C12 cell line was used, which is an immortalized mouse myoblast cell line that is capable to differentiate into osteoblasts in the presence of BMP2 [177]. C2C12 cells were cultured in DMEM containing 4.5 g/L glucose, 0.584 g/l L-glutamine, supplemented with 10% FBS, and 1% P/S antibiotics. The same medium was used for BMP2 translation experiments.

However, for the in vitro differentiation experiments, an osteogenic differentiation medium was used. The osteogenic differentiation medium is necessary to allow the cells to produce extracellular matrix and mineralization in an in vitro setting. It was prepared as DMEM containing 1 g/l glucose, 0.584 g/l L-glutamine, supplemented with 2% FBS, 1% P/S antibiotics, 1.18 g of β-glycerophosphate disodium hydrate salt and finally, added freshly each medium change, 1 µl/ml l-ascorbic acid 2-phosphate sesquimagnesium 0.2 mM solution. This medium did not contain dexamethasone. Thereby, the osteogenic induction will be provided by the secreted BMP2 upon cells transfection with BMP2-cmRNA. The medium was freshly prepared before each medium change. The cells were cultured and kept at 37°C in a humid 5% CO_2 cell culture incubator.

2.2.6.3. BMP2 translation and kinetics

C2C12 cells were seeded at a density of 2×10^4 cells/well on the surface of the BMP2 activated fibrin and fibrinogen coated Ti discs (i.e., BMP2-FT and BMP2-F). Two different concentrations of 500 and 250 ng/Ti disc BMP2 cmRNA for each coating type were investigated. The medium was collected and replaced daily for 4 days after cells seeding. BMP2 translation was measured in the collected supernatant using a human BMP2 ELISA kit (R&D systems, USA) following the manufacturer's instructions. The experiment was done in biological triplicates. The statistical analysis of the ELISA data was done using 2-way ANOVA followed by multiple comparisons with Tukey’s correction.

2.2.6.4. ALP activity

Alkaline phosphatase (ALP) is an early marker for osteogenic differentiation that could be detected using an alkaline phosphatase activity assay. ALP activity was measured on the 5th, 7th, and 10th days after C2C12 cells were seeded on the BMP2-F and BMP2-FT coated Ti (1.5×10^4 cells/well). The method described by Katagiri et al. [178,179] was slightly modified and used. The medium was removed from the plates and cells were washed 3 times with PBS, then frozen at -80°C for 2 hrs. After thawing the cells, they were covered with 50 mM Tris-HC1 containing 0.1% Triton X-100 buffer (pH 7.5), and the plates were shaken for 20 minutes to lysate the cells. 25 µl of the cell lysate was transferred to a transparent 96 wells plate and topped with 100 µl of 10 mM 4-Nitrophenyl phosphate di-Sodium salt hydrate pNPP dissolved in ALP buffer (50 mM Glycine, 100 mM Tris-base containing 2 mM $MgCl_2$ and NaOH to adjust the pH to 10.5 in ddH_2O). The mixture was incubated at RT for 1 hour, then quenched with 0.2 M NaOH. The absorbance was measured at wavelength 405 nm using Tecan® (Infinite M200 Pro, Switzerland). The ALP activity was then calculated according to the standard curve of p-nitrophenol pNP in ALP buffer in (pNP µmol/ml/hour) after blank deduction and then normalized to material control (uncoated Ti). The experiment was done in biological quadruplets. The statistical analysis was done using ordinary 2-way ANOVA with multiple comparisons within each timepoint using Tukey's correction.

2.2.6.5. Alizarine red staining and quantification

Similar to the above described, C2C12 cells were seeded on the BMP2-F and BMP2-FT coated Ti discs with a cell density of 1.5×10^4 cells/well in 96 well plates. The cells were cultured in an osteogenic differentiation medium, and the medium change was done every 2-3 days for 35 days. Alizarine red staining solution 0.5% was added to detect mineralization after the cells were fixed with ice-cold 96% ethanol for 30 minutes. After 10 minutes of incubation in alizarin red stain, the cells were washed 5

times for 5 minutes with ddH_2O to remove excess dye. After that, photos were taken for qualitative evaluation, then the stain was retrieved through 1.5 hrs of incubation in 10% Hexadecylpyridiniumchloride solution. The solution was then transferred to a transparent 96 well plate and the absorbance was measured at λ 562 nm using Tecan® (Infinite M200 Pro, Switzerland) plate reader for quantitative evaluation. The results were calculated in mg/ml Alizarin red according to a standard curve of 0.5% Alizarine red stain diluted 1:1 in 10% Hexadecylpyridiniumchloride solution in 1:1 serial dilution. The results were normalized to material control. This experiment was done in biological quadruplets. The statistical analysis was done using ordinary 2-way ANOVA with multiple comparisons within each timepoint using Tukey's correction.

2.2.7. Statistical analysis

The statistical analysis was done using GraphPad Prism 6 software (GraphPad, USA). All methods and corrections were as recommended by the statistical analysis software. The outlier values of all our data were identified via the "identify outliers" function in the software using the ROUT method, which can identify any number of outliers with the Q value set to 10%. Sample size (n) varied between different assays (3-8 biological repeats) and was mentioned in each result's graph.

Chapter 3: Results

3.1. cmRNA preparation and testing

Prepared cmRNAs were examined via automated electrophoresis (fragment analyser) and a nucleotide analysis via HPLC was performed to evaluate the samples' integrity and composition respectively. Then a standard transfection experiment was done to confirm the biological activity of the prepared cmRNAs.

3.1.1. cmRNA purity and integrity results

The fragment analysis was done using automated capillary electrophoresis. The capillary electrophoresis results are typically represented as a graph showing the peaks of fluorescence corresponding to the labelled nucleic acid. The resulting graph usually includes a small peak of fluorescence on the left side that represents the lower limit (smallest range of measurement), and a bigger sharp peak corresponds to the prepared cmRNA at the expected number of nucleotides (nt.) - including the poly-A tail. The presence of extra noise around the sharp peak usually signifies fragments either from degradation or the presence of impurities – it is referred to as a smear. Smearing is calculated automatically by the devices' software as a percent of the total analysed sample; it is calculated as pre-smear (fragments smaller than the tested sample), post-smear (fragments larger than the tested sample) and finally, the summation of both types of smears is the total smear. Our results showed sharp peaks corresponding to the expected number of nucleotides for both prepared cmRNAs (i.e., coding for MetLuc and BMP2) with minimal smearing as shown in Figure 13 a and b. MetLuc's peak was at 964 nt. with a total smear of 11.5%, while BMP2 was 1394 nt. with an 11% total smear.

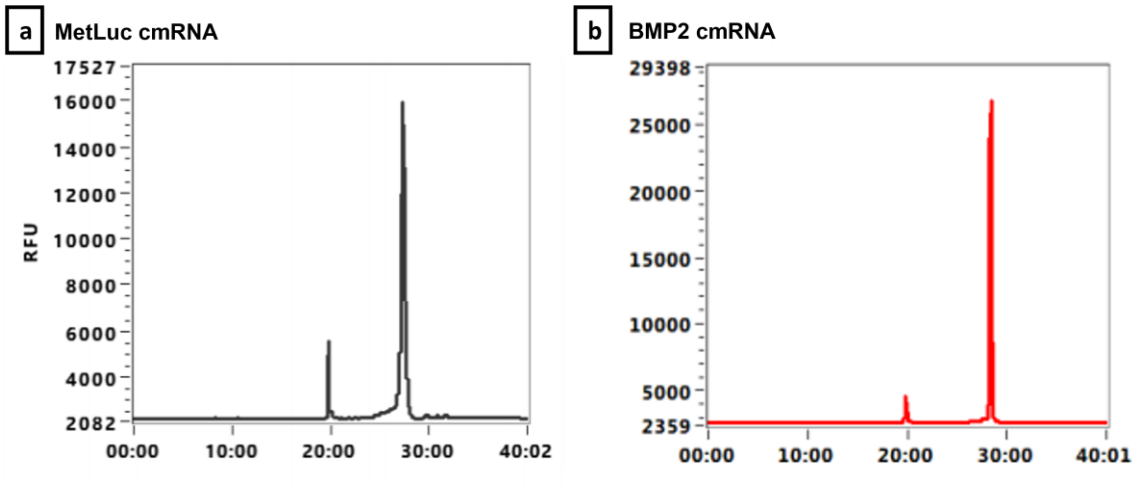

Figure 13: Fragment analysis results graphs showing the sharp fluorescence peaks for both MetLuc cmRNA (a / grey) and BMP2 cmRNA (b / red) at the expected nucleotides number ranges for each cmRNA, also both graphs show minimal smearing before and after the peaks indicating the integrity of the prepared cmRNAs.

3.1.2. cmRNA composition analysis results

The nucleotide analysis was performed via HPLC to assess the capping efficiency and incorporation rate of the modified nucleotides. Our results showed proper capping efficiency (>75%), and proper poly-A tail length (~200 nucleotides) for both prepared cmRNAs. Additionally, MetLuc cmRNA showed modified CTP (i.e., 5-methyl-CTP) incorporation rate of 28% of total CTPs and modified UTP (i.e., 2-thio-UTP) incorporation rate of 2.1% of total UTPs. As for BMP2 cmRNA, the results showed modified CTP (i.e., 5-Iodo-CTP) incorporation rate of 6.1% of the total CTPs and the modified UTP (i.e., 5-Iodo-UTP) incorporation rate was 54.9% of the total UTPs.

3.1.3. cmRNA biological activity results

After the analyses, standard transfection experiments were performed for both cmRNAs to check their biological activity. Lipofectamine 2000 (LF2000) was used as a lipid mRNA vector and the NIH3T3 cell line as the target cells. The supernatant was collected for four days and measured for protein expression. The experiment's results confirmed the activity of both cmRNAs. It demonstrated the

ability of both cmRNAs to transfect cells leading to the translation of the encoded proteins over several days.

The luminescence results measured in relative light units (RLU) of MetLuc translation in MetLuc-LF2000 group supernatant, had the peak of expression on the first day after transfection, then a sharp decline followed in the later days, as shown in Figure 14 a. Similarly, the BMP2 group (BMP2-LF2000) ELISA results measured in pg/ml, showed the largest peak of expression on the first day then a sharp decline followed, however, the protein was not detectable after the second day, as shown in Figure 14 b.

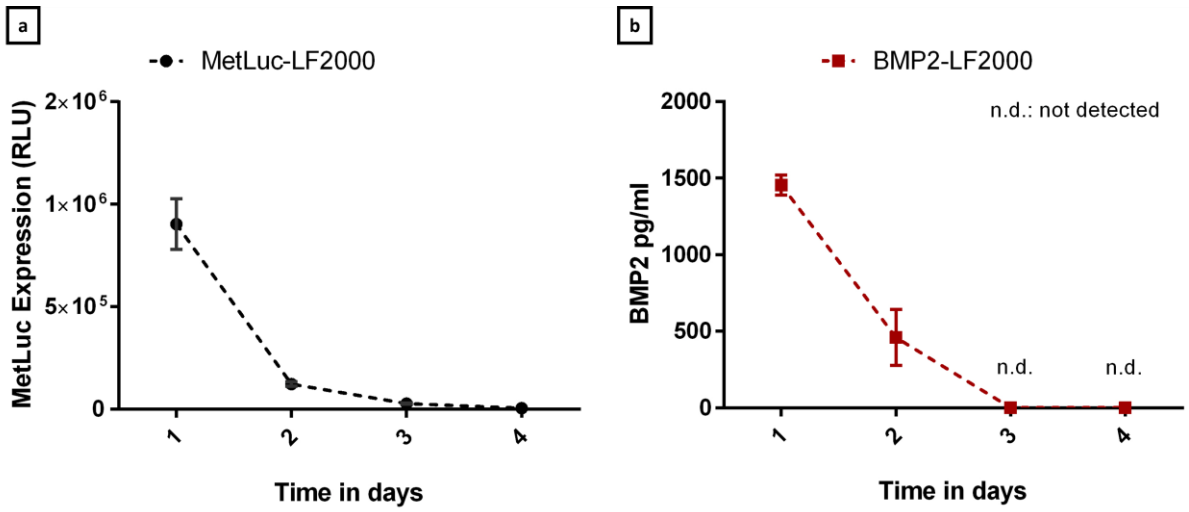

Figure 14: Graphs showing the MetLuc and BMP2 cmRNA (500 ng/well) translation kinetics/time results in standard transfection using Lipofectamine 2000 on NIH3T3 cells, both graphs showed a high peak of expression on the first day after transfection which sharply declined on the later time points. (a) showing MetLuc translation kinetics/ time results measured in relative light units (RLU). While (b), is showing the translation kinetics/ time results of BMP2 measured via ELISA in pg/ml with the protein detected only on the first 2 days with the largest peak on the 1st day.

3.2. Lipoplexes formulation and testing

After the cmRNAs preparation, characterization, and quality control testing, cmRNA-lipoplexes were formulated using a proprietary lipid-based vector. The particle size of the prepared lipoplexes was

measured via dynamic light scattering in nanometres, and the measured size ranged between 60-150 nm – according to the batch and type of cmRNA. Meanwhile, the measured zeta potential ranged between 16-25 mV for MetLuc and 0-2 mV for BMP2, a variation was noted according to the preparation conditions and type of cmRNA. Nevertheless, both ranges are within known ranges for each nucleic acid. The results shown in Figure 15 showcase one batch of each prepared cmRNA as an example.

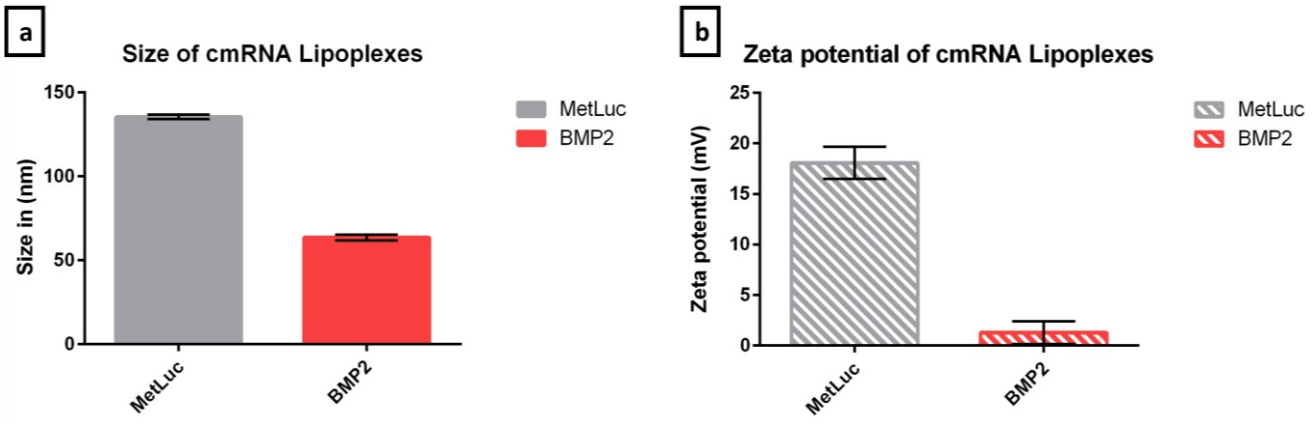

Figure 15: Figures showing size and zeta potential measurements of the prepared lipoplexes (a) Figure showing the size of MetLuc and BMP2 lipoplexes measured via dynamic light scattering in nm, and (b) shows the corresponding zeta potential for each cmRNA measured in mV.

3.2.1. Optimization of cmRNA transfection using NIH3T3 cells

These pilot experiments were done to optimize the cell seeding number used for transfection, as well as to understand both the dose/effect relationship and the kinetics/time for the prepared lipoplexes. They were done using MetLuc reporter cmRNA at first then the optimized results were confirmed using BMP2 cmRNA.

3.2.1.1. Optimization of the cell density

For this experiment, 500 ng/well MetLuc cmRNA in lipoplex formulation was used to determine the optimal NIH3T3 cell density for transfection. Different cell numbers (3000, 5000, 7000, and 10000 cells/well) were seeded in 96 well plates 24 hrs before transfection. Transfection was then performed following described standard methodology followed by a supernatant collection after 24 hrs that was kept at -20°C until measured. The results shown in Figure 16 demonstrated the improvement of transfection with the increase in cell number. The MetLuc-Lipoplexes showed the highest MetLuc expression with 10000 cells/well, which was significantly higher than all the other cell densities (p-value <0.001). Thus, the cell density of 10000 (or 10^4) cells/well was selected for the later experiments. Statistical analysis results are shown in detail in (Appendix 1 - 7.1.1).

3.2.1.2. Optimization of cmRNA concentration: Dose/effect relationship

Using 10^4 NIH3T3 cells/well, a standard transfection experiment was done to understand the dose/effect relationship of the prepared MetLuc-lipoplexes. The MetLuc luminescence results measured in RLUs showed that the highest MetLuc expression belonged to the 500 ng/well cmRNA concentration group, as shown in Figure 16 b, with statistical significance in comparison to all other groups (p-value <0.0001). Additionally, the 250 ng/well group was significantly higher than the lesser concentration groups (p-value <0.001 compared to125 ng/well and 62.5 ng/well, and p-value <0.0001 compared to 31.250, 15.125, and 7.8 ng/well groups). These results confirmed the presence of a positive correlation between the dose and effect in the tested concentrations. Hence, the 500 and 250 ng/well cmRNA concentrations were highlighted in the later experiments. The statistical analysis results are presented in (Appendix 1 - 7.1.2).

3.2.1.3. Kinetics/time

This experiment was done as described before, using only the 500 ng/well cmRNA concentration, and the supernatant was collected and replaced daily for 4 days. The results showed that the peak of expression was on the 1st day, which dropped sharply after that, as illustrated in Figure 16 c, which is consistent with the MetLuc-LP2000 results in Figure 14 a.

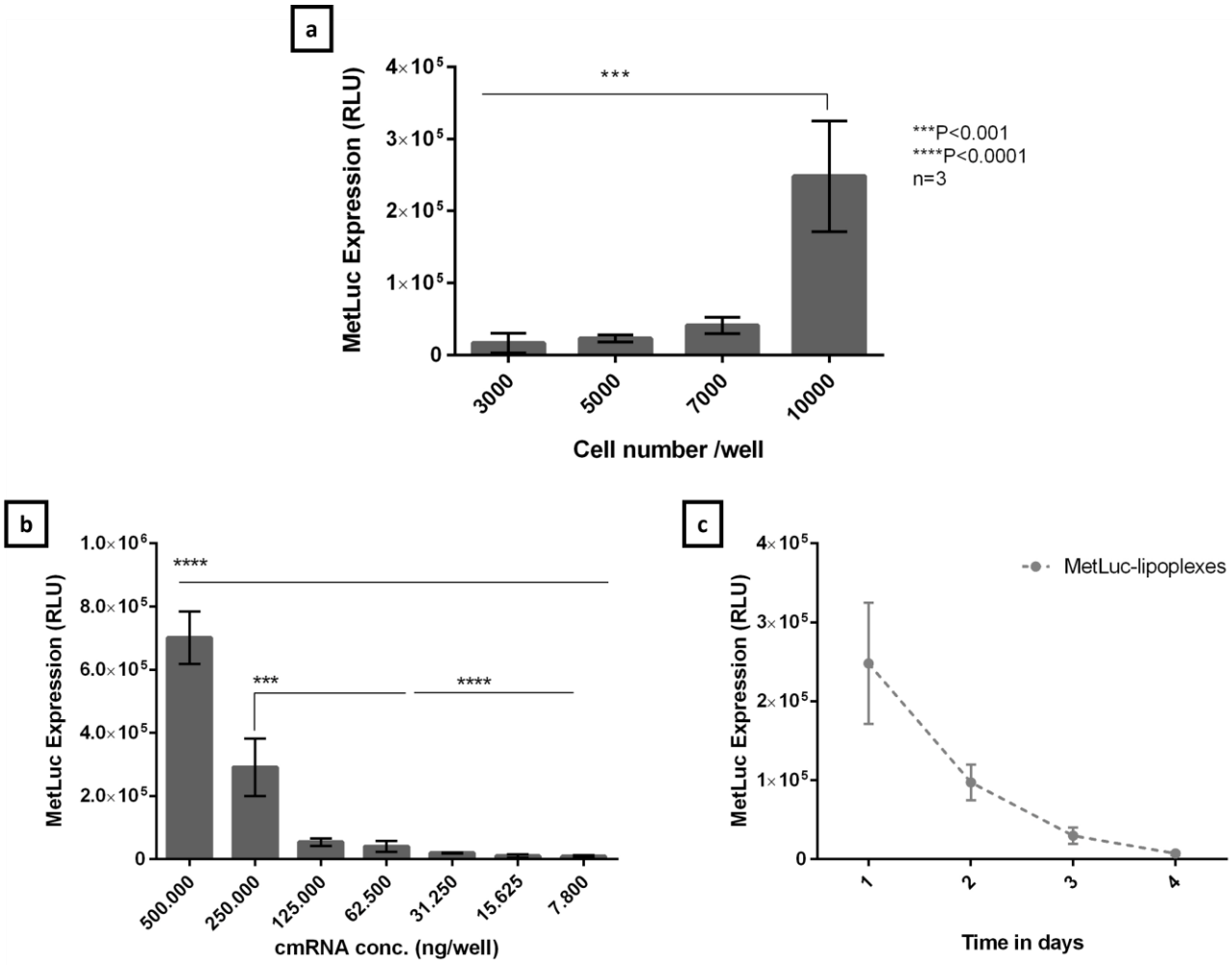

Figure 16: Graphs showing cell number optimisation, dose/effect relationship and kinetics/time of the prepared lipoplexes. (a) Graph showing the results of MetLuc standard transfection with different cell densities (3000, 5000, 7000, and 10000 cells/well). The transfection was done using 500ng/well MetLuc cmRNA lipoplexes formulations (MetLuc-lipoplexes). The results showed that the 10000 cells/well was remarkably higher than the other cell densities. (b) : Graph that highlights the dose/effect relationship between cmRNA concentration in MetLuc-Lipoplexes and the MetLuc expression 24 hrs. after standard transfection. The results showed different peaks of MetLuc expression corresponding to

different concentrations. The MetLuc-lipoplexes had the highest peak of expression with 500 ng/well cmRNA concentration in contrast to all other concentrations, in addition, 250 ng/well was significantly higher than the lesser concentrations as well. (c) : Graph showing the results of a standard transfection experiment that was done using 500 ng/well cmRNA MetLuc-Lipoplexes and the supernatant was collected daily for 4 days to assess the kinetics/time, the results showed that the peak of expression was on the first time point, which dropped sharply after that.

3.2.2. BMP2-lipoplexes results

Finally, the optimized cell number, and cmRNA concentration were used to check if the prepared BMP2-lipoplexes behave similarly to MetLuc-lipoplexes. However, it was found that BMP2-lipoplexes did not lead to detectable BMP2 translation and only the BMP2-LP2000 group showed positive results. This was demonstrated before in cmRNA preparation and testing 3.1 Figure 14 b.

3.3. Stability of the prepared cmRNA-Lipoplexes (at 37° C)

The nanoparticles' stability was evaluated at 37° C by measuring the size and zeta potential over time. The encapsulation efficiency of the lipids to the cmRNA was evaluated by measuring free (non-encapsulated) vs total cmRNA. Finally, the cmRNA integrity was evaluated via capillary electrophoresis.

3.3.1. Size and zeta potential

The size and zeta potential of the prepared lipoplexes showed non-significant size variance (P-value >0.05 BMP2 lipoplexes mean 64.8 ± 1.7 nm, and MetLuc lipoplexes mean 139.5 ± 2.9 nm) over the 8 days' time of the experiment, as shown in Figure 17 a. On the other hand, zeta potential measurements showed some changes with BMP2 average 0.9 ± 1 mV, which fluctuated from 2 to -0.19 measurement towards the end of the experiment, while MetLuc stayed positive (average 21.3 ± 2.3 mV), shown in Figure 17 b. These results indicated the stability of the prepared lipoplexes size throughout the experiment.

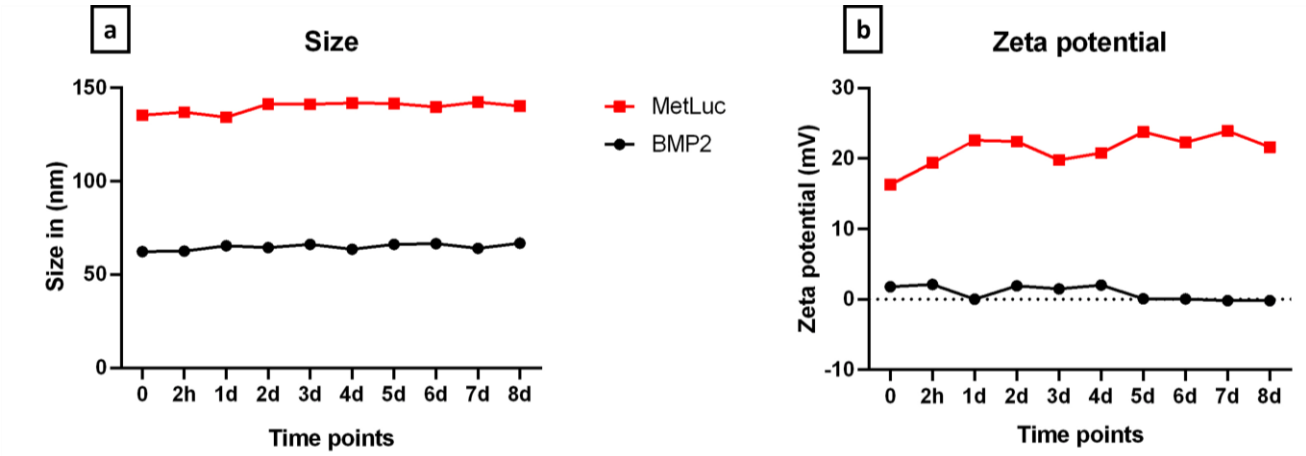

Figure 17: Graphs showing the size and zeta potential stability overtime of the prepared lipoplexes. (a) Graph represents the size measurements of BMP2 lipoplexes and MetLuc lipoplexes. Both graphs show high stability of the particle size over time with minimal variation. (b) Graph represents the corresponding zeta potential measurements.

3.3.2. Encapsulation efficiency

The encapsulation efficiency results indicate the percentage of encapsulated cmRNA (cmRNA forming complexes with the used lipid vector) compared to total cmRNA. The results showed a tendency to improve towards the end of the experiment for both BMP2 and MetLuc lipoplexes (Figure 18).

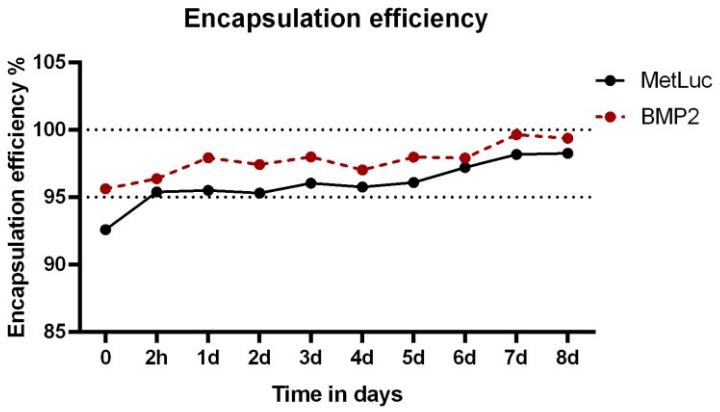

Figure 18: Graph showing the encapsulation efficiency results in percent of total cmRNA. it signifies the tendency of gradually increasing towards the later time points for both BMP2 and MetLuc lipoplexes.

3.3.3. cmRNA integrity

The relative integrity (quality) results were above 80% until the 6th day of incubation for both BMP2 and MetLuc cmRNAs, which indicates low degradation of the cmRNA after lipoplexes formation. The minimal quality was measured at end of the experiment (8th day timepoint) with BMP2 at 73% while for MetLuc at 69%. This result has indicated the ability of the developed cmRNA formulations to relatively keep the integrity of the cmRNA over the course of the experiment (Figure 19).

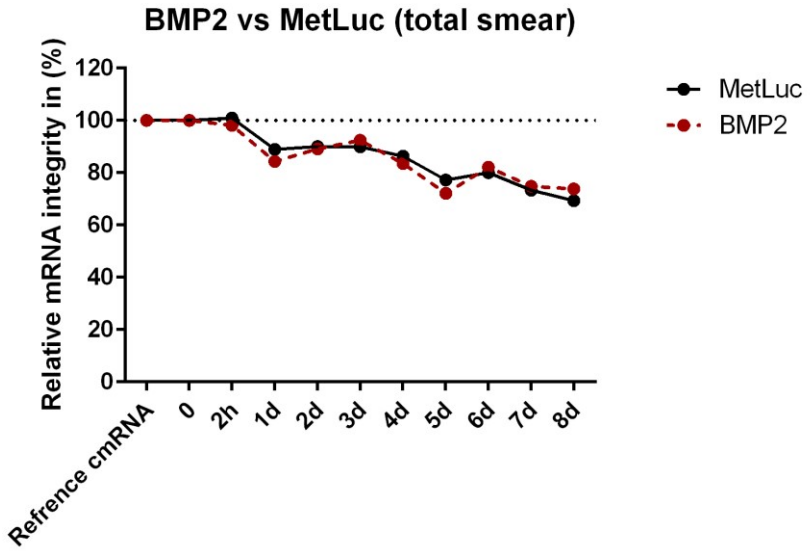

Figure 19: Graph showing the relative cmRNA integrity results.

3.4. Optimization of the surface coating of Ti discs

3.4.1. Coating via physical adsorption

3.4.1.1. Optimization on cell culture plastic

Before coating was attempted on Ti discs, a pilot experiment was conducted, in which the surface of 96 well cell culture plates were coated with MetLuc-lipoplexes via physical adsorption. The experiment aimed to check if the coated surfaces would transfect the cells and to optimize the coating method as well as the cmRNA concentrations used.

The wells were coated using 3 different MetLuc-cmRNA concentrations (i.e., 500, 250, and 125 ng/well) of MetLuc-lipoplexes aqueous solution utilizing 2 different drying methods: drying on ice (Dry/ice); drying at room temperature (Dry/RT) - as shown in (Table 10). After that, cells were seeded, and supernatant was collected 24 hrs after seeding to be measured for the MetLuc expression.

Table 10: Drying methods optimization samples

Samples	**cmRNA**	**cmRNA conc. (ng/well)**	**Coating method**	**Coating temperature**	**Coating material**
Dry/ice	MetLuc	500 250 125	Physical adsorption	On ice pad	MetLuc lipoplexes
Dry/RT	MetLuc	500 250 125	Physical adsorption	At room temperature (RT)	MetLuc lipoplexes

The results showed no significant differences between the two drying methods (Dry/ice and Dry/RT), which was not the case for the cmRNA concentration, as shown in Figure 20. The 500 ng/well cmRNA concentration showed significantly higher MetLuc expression with p-value <0.05 and <0.001 in contrast to 250 and 125 ng/well groups, respectively for both drying methods. Statistical details are presented in Appendix 1 - 7.1.

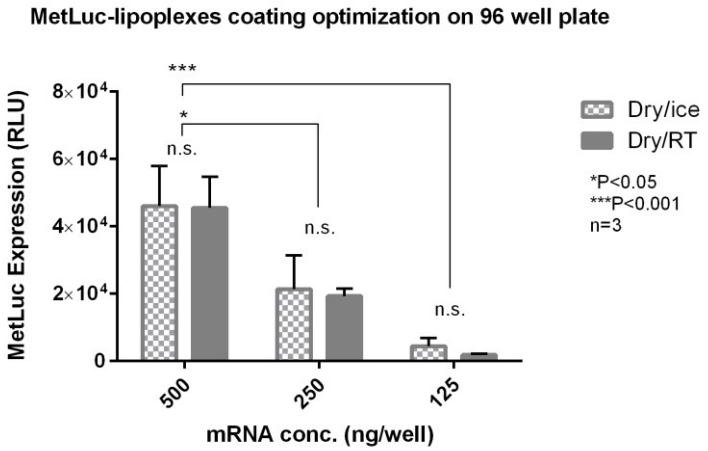

Figure 20: Graph showing the results of MetLuc expression using 2 different methods: drying on ice (Dry/ice) and drying at room temperature (Dry/RT). NIH3T3 cells were seeded on 96 well plates coated with MetLuc-Lipoplexes via physical

adsorption The results showed no significant differences between the 2 methods while showing statistical significance of the highest expression with 500 ng/well cmRNA concentration in contrast to all the other concentrations for both drying methods.

3.4.1.2. Coating on Ti discs

The Ti discs were coated with MetLuc lipoplexes via physical adsorption at RT (samples details in Table 11). NIH3T3 cells were seeded on the coated Ti discs then the supernatant was collected and replaced daily with fresh medium. The collected supernatant was measured for MetLuc translation and processed the resultant luminescence data as mentioned in the methods section of this thesis. The statistical analysis details were covered in Appendix 7.2.2.

Table 11: samples of physical adsorption coating on Ti

Sample	**cmRNA**	**cmRNA conc. (ng/Ti disc)**	**Coating method**	**Coating material**
MetLuc-Ti	MetLuc	500 250 125 62.5	Physical adsorption on Ti via drying at RT in the cell culture hood	MetLuc lipoplexes

The results showed that Ti discs coated with MetLuc lipoplexes via physical adsorption (MetLuc-Ti) were able to transfect cells seeded on them across the different cmRNA concentrations tested (i.e. 500, 250, 125, and 62.5 ng/well), as shown in Figure 21 a and b. The samples containing 500 ng/well cmRNA have shown the highest MetLuc translation. While the translation kinetics/time showed a high peak on the first day, then it rapidly decreased in the following days (Figure 21 a), which is similar to the standard transfection results shown previously in 3.2.1.2 and 3.2.1.3 sections of this thesis.

Focussing on the first time point, the 500 ng/well cmRNA concentration group showed higher MetLuc translation compared to all other tested concentrations. The difference was statistically significant compared to 250 ng/well group with p-value <0.01 and compared to the 125 and 62.5 ng/well groups the p-value was <0.0001. Additionally, it was noted that the 250 ng/well group showed significantly higher MetLuc translation than 62.5 ng/well cmRNA concentration group with p-value <0.05.

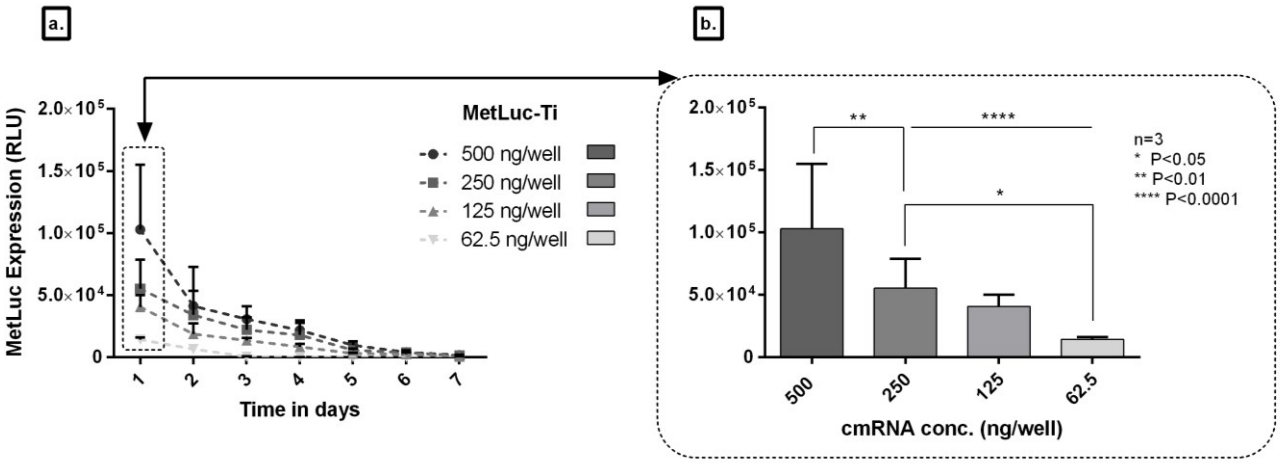

Figure 21: Graphs showing the results lipoplexes physical adsorption method on Ti discs. (a.) Graph showing the MetLuc translation measured in relative light units (RLU) of MetLuc-Ti samples (Ti discs coated with MetLuc-lipoplexes via physical adsorption method) dose-dependence on translation kinetics of the cmRNA concentrations 500-62.5 (ng/well) and over 7 days, while (b.) a graph that shows a comparison between the different cmRNA concentrations 24 hrs after cell seeding. Both graphs indicate that 500ng/well had the highest MetLuc translation.

3.4.2. Coating via physical entrapment

3.4.2.1. PDLLA coating

Using the optimal cmRNA concentration from the previous experiments (i.e., 500 ng/well MetLuc cmRNA), Ti discs were coated with the MetLuc lipoplexes via physical adsorption, then a layer of PDLLA was added to physically trap the lipoplexes underneath it. Different PDLLA concentrations were tested (i.e., 3, 2, 1, 0.5, 0.25, and 0 mg/well PDLLA) to optimize the coating thickness (samples

details in Table 12). Thereafter, NIH3T3 cells were seeded on the different coated-Ti discs, then the supernatant was collected and replaced daily for 7 days to evaluate the MetLuc translation over time. The daily translation measurements were processed, and statistical analysis was performed as mentioned in the materials and methods section of this thesis.

Table 12: samples details of coating via physical entrapment (PDLLA) on Ti discs

Samples	**cmRNA conc. (ng/Ti disc)**	**Coating methods**	**PDLLA conc. mg/Ti disc**	**Coating materials**
MetLuc-Ti	MetLuc 500 ng/Ti disc	Lipoplexes physical adsorption	0 mg/Ti disc	MetLuc lipoplexes
MetLuc-PDLLA 0.25	MetLuc 500 ng/Ti disc	Physical entrapment in PDLLA	0.25 mg/Ti disc	MetLuc lipoplexes and PDLLA protective layer
MetLuc-PDLLA 0.5	MetLuc 500 ng/Ti disc	Physical entrapment in PDLLA	0.5 mg/Ti disc	MetLuc lipoplexes and PDLLA protective layer
MetLuc-PDLLA 1	MetLuc 500 ng/Ti disc	Physical entrapment in PDLLA	1 mg/Ti disc	MetLuc lipoplexes and PDLLA protective layer
MetLuc-PDLLA 2	MetLuc 500 ng/Ti disc	Physical entrapment in PDLLA	2 mg/Ti disc	MetLuc lipoplexes and PDLLA protective layer
MetLuc-PDLLA 3	MetLuc 500 ng/Ti disc	Physical entrapment in PDLLA	3 mg/Ti disc	MetLuc lipoplexes and PDLLA protective layer

Figure 22 shows the plotted daily MetLuc translation data in RLU, highlighting the statistical significance of the different time points. On the first day, MetLuc-PDLLA 3 showed significantly lower MetLuc expression when compared to all other groups (denoted on the graph by the letter **a** with p-value <0.05). While, the MetLuc-PDLLA2 sample showed significantly lower expression when compared to MetLuc-PDLLA 0.5, MetLuc-PDLLA 0.25, and MetLuc-Ti discs (denoted on the graph by the letter **b** with p-value <0.001). At the same time, MetLuc-PDLLA 1 showed significantly lower MetLuc expression when compared to MetLuc-PDLLA 0.25 and MetLuc-Ti (denoted on the graph by the letter **c** with p-value < 0.0001). Meanwhile, no significant differences were found between MetLuc-Ti and MetLuc-PDLLA 0.5, however, MetLuc-PDLLA 0.25 showed significantly higher MetLuc expression in contrast to MetLuc-PDLLA 0.5 (p-value <0.01).

After the 1st day, MetLuc-Ti results dropped dramatically in the later time points, which is consistent with the previous results mentioned in 3.4.1 section of this thesis. Meanwhile, MetLuc-PDLLA 3, 2, and 1 sample sustained significantly lower MetLuc expression in the later time points denoted on the graph by the letter **d** on the 2nd and 4th days (p-value <0.001, and <0.05, respectively, in contrast to MetLuc-PDLLA 0.5 and 0.25 samples), and by the letter **e** on the 3rd day in contrast to MetLuc-PDLLA 0.25 (p-value <0.001). No significant differences were found after the 4th day timepoint.

These results demonstrated the dependence of MetLuc translation on PDLLA coating thickness. The highest translation was obtained for the lowest PDLLA concentration used for coating (i.e., MetLuc-PDLLA 0.25 group). The results also demonstrated the improvement of the translation kinetics/time in the presence of physical protection by PDLLA (up to the 4th day), such improvement was also dependent on PDLLA thickness (statistical tables in appendix 7.3.1).

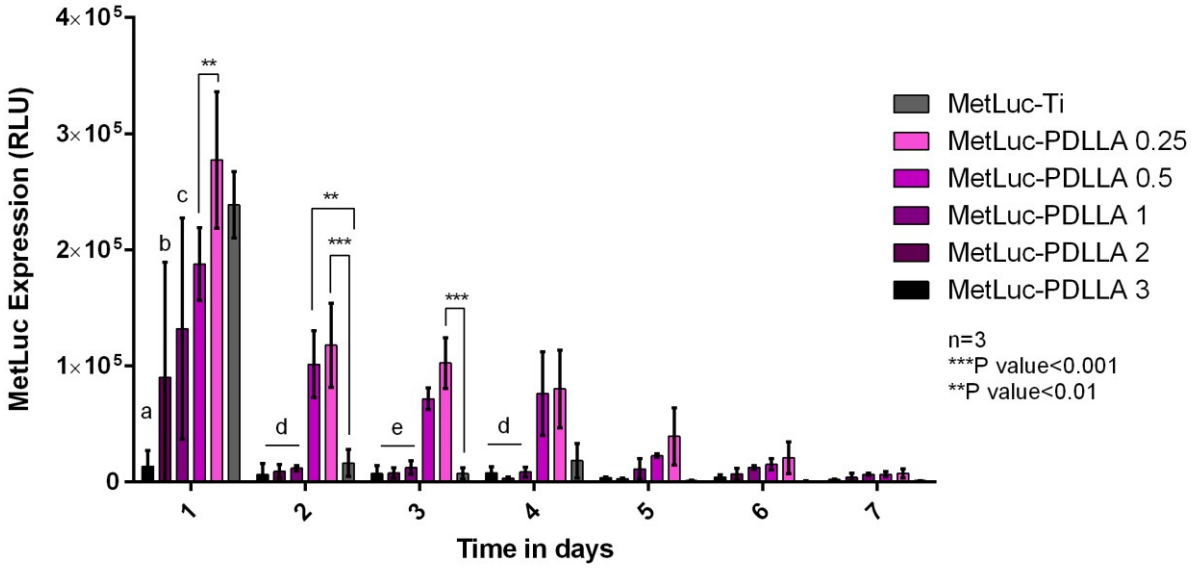

*Figure 22: A column chart represent the MetLuc translation over time comparing Ti discs coated with MetLuc lipoplexes physically adsorbed vs. entrapped in different PDLLA concentrations. It shows the translation/day for MetLuc-PDLLA different concentrations from 0.25 up to 3 mg/well and MetLuc-Ti highlighting the significant difference in MetLuc translation (especially through the first 4 days) between the different groups. The statistical significance was highlighted on the graph using ** ($p<0.01$) and *** ($p<0.001$)as well as letters from a - e. (a) indicate significantly lower expression for MetLuc-PDLLA 3 when compared to all other groups ($p \leq 0.0109$); (b) indicates a significantly lower expression for MetLuc-PDLLA 2 when compared to MetLuc-PDLLA 0.5, MetLuc-PDLLA 0.25, and MetLuc-Ti disks ($p \leq 0.0001$); (c) indicates a significantly lower expression for MetLuc-PDLLA 1 when compared to MetLuc-PDLLA 0.25 and MetLuc-Ti disks ($p \leq 0.0001$). On day 2, (d) indicates a significantly lower expression for MetLuc-PDLLA 3, MetLuc-PDLLA 2, and MetLuc-PDLLA 1 when compared to MetLuc-PDLLA 0.5 and MetLuc-PDLLA 0.25 ($p \leq 0.001$). On day 3, (e) indicates a significantly lower expression for MetLuc-PDLLA 3, MetLuc-PDLLA 2, and MetLuc-PDLLA 1 when compared to MetLuc-PDLLA 0.25 ($p \leq 0.001$). Like day 2, on day 4, (d) indicates a significantly lower expression for MetLuc-PDLLA 3, MetLuc-PDLLA 2, and MetLuc-PDLLA 1 when compared with MetLuc-PDLLA 0.5 and MetLuc-PDLLA 0.25 ($p \leq 0.05$).*

To further visualize the improvement in the translation kinetics/time, the data of MetLuc-PDLLA 0.25 (physical entrapment coated Ti discs showing the highest test results) was plotted in contrast to MetLuc-Ti (physical adsorption coated Ti discs) which clearly shows the improvement of the translation starting 2nd to 4th days as shown in Figure 23. A significant difference was found starting the 2nd until the 4th day with p-value <0.001 for the 2nd and 3rd days and p-value <0.05 on the 4th day.

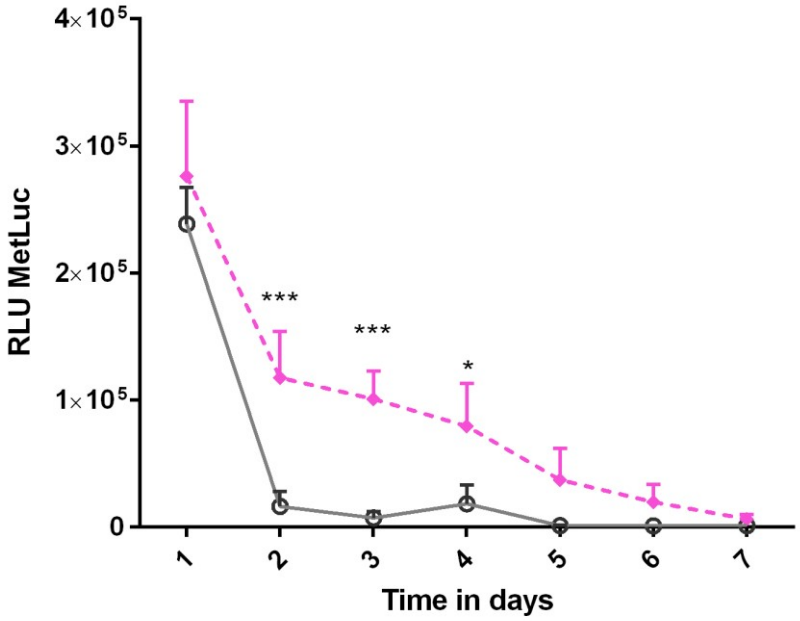

Figure 23: Graph showing the MetLuc translation over time comparing MetLuc-PDLLA 0.25 samples with MetLuc-Ti. A significant difference was found starting the 2nd until the 4th day with p-value<0.001 for the 2nd and 3rd days and p-value<0.05 on the 4th day.

3.4.2.2. Fibrin/-ogen coating

For this coating, fibrin/-ogen was used to entrap MetLuc lipoplexes within the coating at the surface of the Ti discs, then the coating was tested for protein translation efficiency and kinetics over time. First, a screening of different fibrinogen to thrombin ratios was done. Thereafter, the optimized fibrin composition was utilized to screen different cmRNA lipoplexes concentrations testing for protein translation over time.

a. *The effect of fibrinogen to thrombin ratio on the cmRNA transfection efficiency*

The MetLuc expression was detectable up to 10 days and higher than both physical adsorption and entrapment in PDLLA, also the peak of expression was delayed up to 5 days after cells seeding for the same cmRNA concentration (500 ng/well) as shown in Figure 24. The different formulations of fibrin had a strong effect on MetLuc's translation and kinetics/time. The results showed that, as the

concentration of thrombin (T) decreased in the final coating, the translation of MetLuc increased. Moreover, using only fibrinogen (F) for coating resulted in a significant improvement in MetLuc translation and kinetics/time (Figure 24). Investigated sample groups are detailed in Table 13.

Table 13: samples details of different fibrin formulation screening experiment

Samples	**cmRNA conc. (ng/Ti disc)**	**Coating methods**	**F:T ratio**	**Coating materials**
MetLuc-Ti	MetLuc 500 ng/Ti disc	Lipoplexes physical adsorption	N.a.	MetLuc lipoplexes
MetLuc-PDLLA 0.25	MetLuc 500 ng/Ti disc	Physical entrapment in PDLLA 0.25	N.a.	MetLuc lipoplexes and PDLLA 0.25 protective layer
MetLuc-FT	MetLuc 500 ng/Ti disc	Physical entrapment in Fibrin	1F:1T	MetLuc lipoplexes and Fibrin (1F:1T)
MetLuc-F0.5T	MetLuc 500 ng/Ti disc	Physical entrapment in Fibrin	1F:0.5T	MetLuc lipoplexes and Fibrin (1F:0.5T)
MetLuc-F0.25T	MetLuc 500 ng/Ti disc	Physical entrapment in Fibrin	1F:0.25T	MetLuc lipoplexes and Fibrin (1F:0.25T)
MetLuc-F	MetLuc 500 ng/Ti disc	Physical entrapment in Fibrinogen	1F:0T	MetLuc lipoplexes and Fibrinogen (1F:0T)

Figure 24 is showing the MetLuc translation of different compositions of fibrin over 10 days. On the 3rd day, statistical significance was evident (p-value <0.05) between MetLuc-F0.5T samples and MetLuc-FT samples. While on the 4th day MetLuc expression from MetLuc-F0.25T samples was

significantly higher than MetLuc-F0.5T and MetLuc-FT samples (p-value <0.01). The MetLuc expression was the highest significantly on the 5th day from MetLuc-F samples compared to the other formulations with the p-values <0.05, <0.01, and <0.001 in contrast to MetLuc F0.25T, MetLuc-F0.5T, and MetLuc-FT, respectively. Similarly, on the 7th day, MetLuc-F expression was significantly higher than all other fibrin formulations with a p-value <0.05 in contrast to MetLuc-F0.25T and MetLuc-F0.5T samples, and p-value <0.01 compared to MetLuc-FT samples (statistical details in appendix 7.3.2.1).

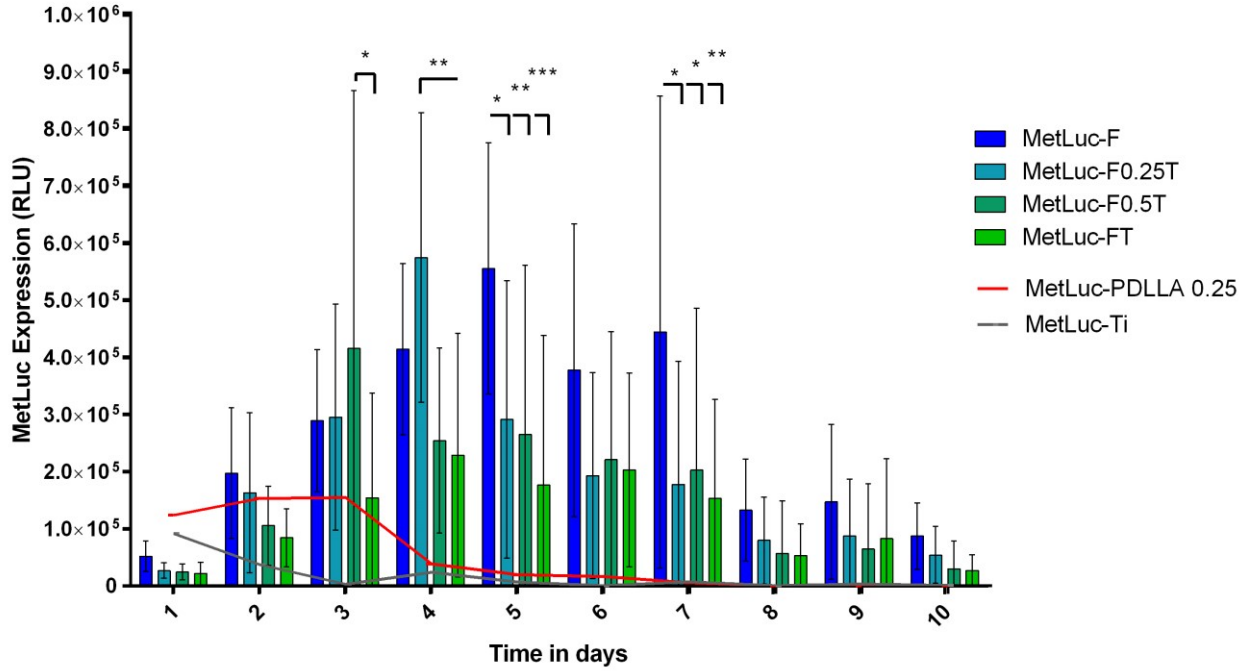

Figure 24: Column chart showing MetLuc translation of different formulations of MetLuc-fibrin coatings for 10 days. MetLuc-Ti and MetLuc-PDLLA 0.25 Ti disks were used for comparison as a line chart on top. 500 ng/well MetLuc cmRNA was used in this experiment with NIH3T3 cells. Significant differences were noted between the different groups on the 3rd day (P <0.05 for MetLuc-F0.5T vs. MetLuc-FT), 4th day (P <0.01 for MetLuc-F0.25T vs. MetLuc-F0.5T and MetLuc-FT), 5th day (MetLuc-F took the lead with P <0.05, <0.01, and <0.001 vs. MetLuc-F0.5T, MetLuc-F0.25T, and MetLuc-FT, respectively) and finally 7th day (MetLuc-F was the highest with P <0.05, vs. MetLuc-F0.5T and MetLuc-F0.25T, and P<0.01 vs. MetLuc-FT).

b. Effect of cmRNA concentration on transfection efficiency

Following the fibrin formulation optimization, the dose/effect relationship of the cmRNA concentration entrapped in the optimized fibrin coating was investigated. To do that, different MetLuc-cmRNA concentrations (i.e., 500, 250, 125, and 62.5 ng/well) were compared using the fibrin coating that showed the highest expression from the previous experiment, which was the Ti discs coated with only fibrinogen 1F:0T (MetLuc-F). The samples coated with fibrin 1F:1T (MetLuc-FT) were used for contrast. Samples and details are in Table 14.

Table 14: fibrin/-ogen coating cmRNA dose/effect relationship samples

Samples	**cmRNA conc. (ng/Ti disc)**	**Coating methods**	**F:T ratio**	**Coating materials**
MetLuc-FT	MetLuc 500 ng/Ti disc 250 ng/Ti disc 125 ng/Ti disc 62.5 ng/Ti disc	Physical entrapment in Fibrin	1F:1T	MetLuc lipoplexes and Fibrin (1F:1T)
MetLuc-F	MetLuc 500 ng/Ti disc 250 ng/Ti disc 125 ng/Ti disc 62.5 ng/Ti disc	Physical entrapment in Fibrinogen	1F:0T	MetLuc lipoplexes and Fibrinogen (1F:0T)

Although the time kinetics and transfection efficiency have greatly improved with FT and F coatings in comparison to the other investigated methods (Figure 24), the time kinetics between F and FT were quite similar, and the peak of translation was shifted to the 3rd day in all concentrations (Figure 25 a-

d). At the same time, the transfection efficiency differed significantly in favour of the MetLuc-F group as shown in Figure 25.

Figure 25 (a-d) showcased the superiority of the fibrinogen coating (MetLuc-F) to the fibrin coating (MetLuc-FT) independent of the cmRNA concentration used. In Figure 25 a (500 ng/well cmRNA concentration) MetLuc-F showed significantly higher MetLuc expression than MetLuc-FT with p-value <0.0001 on days 1 to 4 and <0.001 on days 5 and 7. While Figure 25 b (250 ng/well cmRNA concentration) MetLuc-F had higher MetLuc expression than MetLuc-FT with p-value <0.01 in days 1, 3, and 6, <0.001 in days 2, 5 and 7, and <0.0001 in day 4. Similarly, Figure 25 c (125 ng/well cmRNA concentration) MetLuc-F had significantly higher expression than MetLuc-FT with p-value <0.001 on days 1 and 4, <0.01 on days 2 and 3, and <0.0001 on days 5 and 7. Finally, Figure 25 d (62.5 ng/well cmRNA concentration) MetLuc-F samples MetLuc expression had similar superior tendencies compared to MetLuc-FT with p-values of <0.01 on day 3, and <0.001 on day 4 (Statistical details in appendix 7.3.2.2).

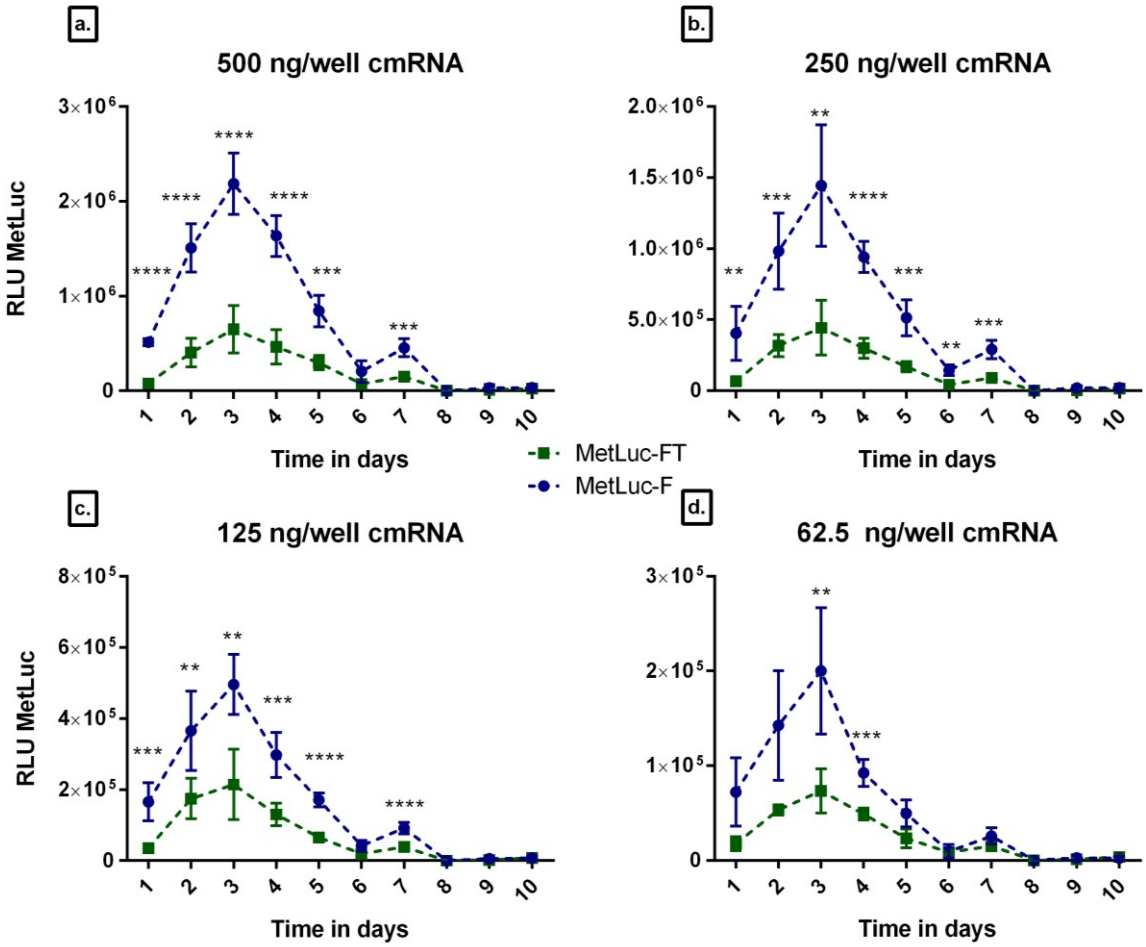

Figure 25: Graph showing the time kinetics of MetLuc translation for the F and FT coated Ti with different concentrations of cmRNA over 10 days highlighting the superiority of MetLuc-F samples independent of the cmRNA concentration. (a) showing a comparison of MetLuc-F vs. MetLuc-FT both containing 500 ng/well. MetLuc-F showed significantly higher MetLuc expression than MetLuc-FT with p-value <0.0001 on days 1 to 4 and <0.001 on days 5 and 7. While, (b) (250 ng/well cmRNA concentration) MetLuc-F was higher than MetLuc-FT with p-value <0.01 in days 1, 3, and 6, <0.001 in days 2, 5 and 7, and <0.0001 in day 4. Similarly, (c) (125 ng/well cmRNA concentration) MetLuc-F was significantly higher than MetLuc-FT with p-value <0.001 in days 1 and 4, <0.01 in days 2 and 3, and <0.0001 in days 5 and 7. Finally, (d) (62.5 ng/well cmRNA concentration) MetLuc-F showed the same tendencies with p-value <0.01 in day 3, and <0.001 in day 4. The statistical analysis was done using multiple t-tests with the statistical significance determined using the Holm-Sidak method to correct for the multiple comparisons.

When evaluating the effect of cmRNA concentration within the MetLuc-F group, the best performance was observed for 500 ng/well and 250 ng/well cmRNA concentrations (Figure 26). Upon comparing the different cmRNA concentrations of MetLuc-F on the peak expression day (day 3), no significant differences were found between the 500 and 250 ng/well groups in terms of MetLuc expression. Yet, the MetLuc-F 500 ng/well group had significantly higher expression than the 125 and 62.5 ng/well groups with p-values <0.01 and <0.001, respectively. Whereas the MetLuc-F 250 ng/well group showed significance in terms of MetLuc expression compared to lesser cmRNA concentration groups (p-value <0.05). Finally, MetLuc-F 125 ng/well group had significantly higher MetLuc expression than the 62.5 ng/well group (p-value <0.01) - all shown in Figure 26.

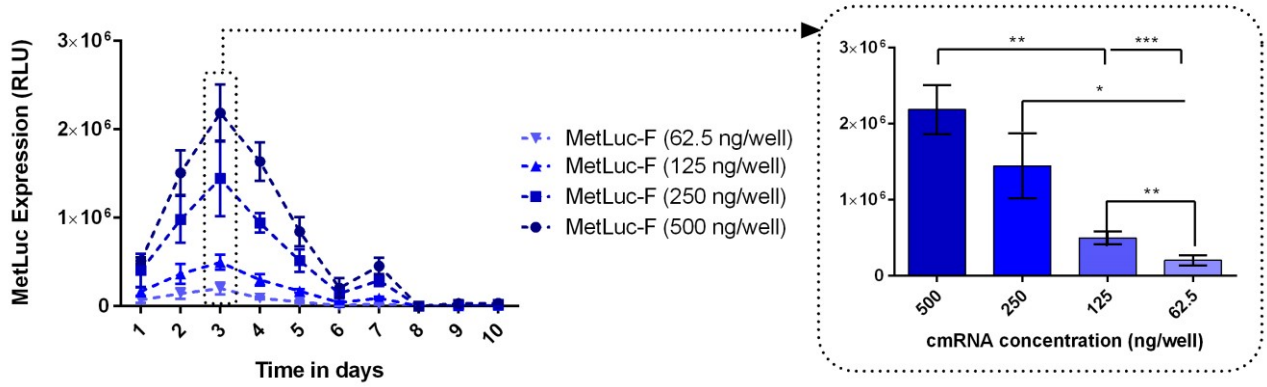

*Figure 26: Graph shows MetLuc translation over time of 4 different MetLuc cmRNA concentrations physically entrapped in fibrinogen-coated Ti (500, 250, 125, and 62.5 ng/well) highlighting the dose-dependent MetLuc expression as well as the shift in the peak of expression from the first and second days (from the MetLuc-Ti and MetLuc-PDLLA groups) to the 3rd day. On the left is a graph showing the MetLuc expression in all the time points. On the right, a graph highlighting MetLuc expression on day 3 (expression peak) for the MetLuc-F disks loaded with different cmRNA concentrations. The significance on the graph (*p <0.05, **p < 0.01, and ***p <0.001). Repeated measures of one-way ANOVA, followed by Tukey's test were performed for data analysis.*

3.4.3. Cell viability

NIH3T3 cell viability was assessed by conducting 2 assays: Alamar blue and Picogreen. The Alamar blue was used to evaluate the cells' metabolic activity while the Picogreen was used to determine the cells' proliferation. The different coating methods and materials tested before were compared using the cmRNA concentration that showed the best results (500 ng/Ti disc MetLuc cmRNA). Samples details are in Table 15.

Table 15: the samples details of the cells' viability test

Samples	**cmRNA** **conc. (ng/Ti disc)**	**Coating methods**	**Coating materials**
MetLuc-Ti	MetLuc 500 ng/Ti disc	Lipoplexes physical adsorption	MetLuc lipoplexes
MetLuc-PDLLA 0.25	MetLuc 500 ng/Ti disc	Lipoplexes physical adsorption Physical entrapment with PDLLA 0.25	MetLuc lipoplexes and PDLLA 0.25 protective layer
MetLuc-FT	MetLuc 500 ng/Ti disc	Physical entrapment in Fibrin	MetLuc lipoplexes and Fibrin (1F:1T)
MetLuc-F	MetLuc 500 ng/Ti disc	Physical entrapment in Fibrinogen	MetLuc lipoplexes and Fibrin (1F:0T)

3.4.3.1. Cell metabolic activity

To test cell viability when seeded on the coated Ti discs, the cells' metabolic activity was measured via Alamar blue. The cells seeded on MetLuc-PDLLA 0.25 samples demonstrated higher metabolic

activity on day 1 timepoint, however, no significant difference compared to the other groups in all time points, as shown in Figure 27 a. This indicated that the type of Ti coating did not significantly affect the cells' metabolic activity. Statistical details are in appendix 7.3.3.1.

3.4.3.2. Cell proliferation

The cell proliferation was tested via Picogreen staining. Significant differences were notable in the early time points (days 1 and 3) indicating the superiority of both fibrin (MetLuc-FT) and fibrinogen (MetLuc-F) coatings in the cell's proliferation front; however, this effect decreased in the later time points. On day 1, MetLuc-FT and MetLuc-F groups supported significantly higher cell proliferation compared to MetLuc-Ti and MetLuc-PDLLA 0.25 groups (p-values <0.0001). On day 3 timepoint, cell proliferation on MetLuc-PDLLA 0.25 samples improved, however, it was still significantly lower than that observed on MetLuc-F group. Simultaneously, cell proliferation on MetLuc-Ti remained significantly lower than on both fibrin and fibrinogen coated samples (p-values <0.001 and <0.0001 respectively). No significant differences were noted between all the different coatings on day 7. Interestingly, by the last timepoint (day 14 of cell seeding), MetLuc-Ti coating supported the lowest cells proliferation in contrast to all other groups (p-values < 0.0001 compared to MetLuc-PDLLA 0.25 and <0.001 compared to MetLuc-FT) as shown in Figure 27b. Meanwhile, MetLuc-PDLLA 0.25 supported significantly higher cell proliferation than MetLuc-F group (p-value <0.05), as shown in Figure 27b. Statistical details are in appendix 7.3.3.2.

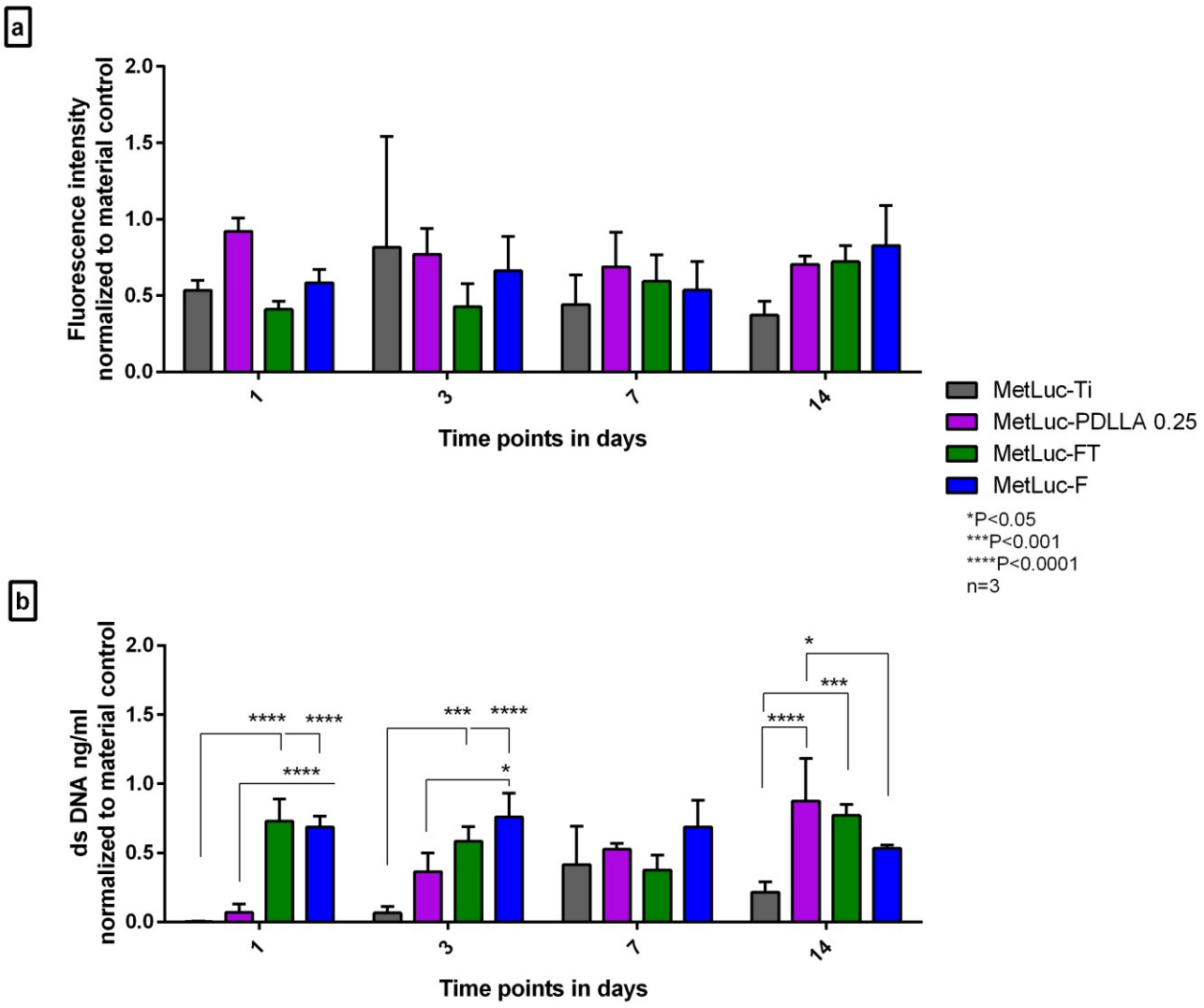

Figure 27: Results of NIH3T3 cells' metabolic activity and proliferation seeded on coated titanium discs. The coating contained 500 ng/well cm RNA MetLuc lipoplexes physically adsorbed (MetLuc-Ti) or physically entrapped in biocompatible coating (MetLuc-PDLLA 0.25, MetLuc-FT, and MetLuc-F), (a.) the cell viability results showed no significant differences between all the tested groups all the time points (1, 3, 7 and 14 days). (b.) the cell proliferation results for the same groups were measured at the same time points. Both MetLuc-FT and MetLuc-F showed significantly higher proliferation than MetLuc-Ti and MetLuc-PDLLA 0.25 on day 1 and day 3 time points then no significant differences were noticed by day 7, however, on day 14 MetLuc-Ti showed the least cells proliferation compared to MetLuc-PDLLA 0.25 and MetLuc-FT. P values are highlighted on the graph.

3.4.4. Lipoplexes released from fibrin and fibrinogen Ti coatings.

This experiment was done using BMP2 cmRNA in lipoplex formulation at 500 ng/Ti disc concentration and comparing the fibrin vs. fibrinogen coatings. The samples details are shown in Table 16.

Table 16: the samples details for the lipoplexes release test

Samples	**cmRNA** **conc. (ng/Ti disc)**	**Coating methods**	**Coating materials**
BMP2-FT	BMP2 500 ng/Ti disc	Physical entrapment in Fibrin	MetLuc lipoplexes and Fibrin (1F:1T)
BMP2-F	BMP2 500 ng/Ti disc	Physical entrapment in Fibrinogen	MetLuc lipoplexes and Fibrin (1F:0T)

The results showed a burst of release of the lipoplexes on the first timepoint (2 hrs) from the fibrinogen-coated samples (BMP2-F), while the fibrin samples (BMP2-FT) showed minimal release, which was statistically significant (p-value <0.01). After that initial time point, both coatings showed similar release patterns, however, BMP2-F samples' peak release was on the 3rd day (p-value <0.0001), while the release from BMP2-FT peaked on the 4th day (p-value < 0.001). The peaks were followed by a drop 2 days later for both samples (Figure 28). After the 6th day there was almost no release and the digested coating after 7 days also had minimal cmRNA residual. Statistical details are in appendix 7.3.4.

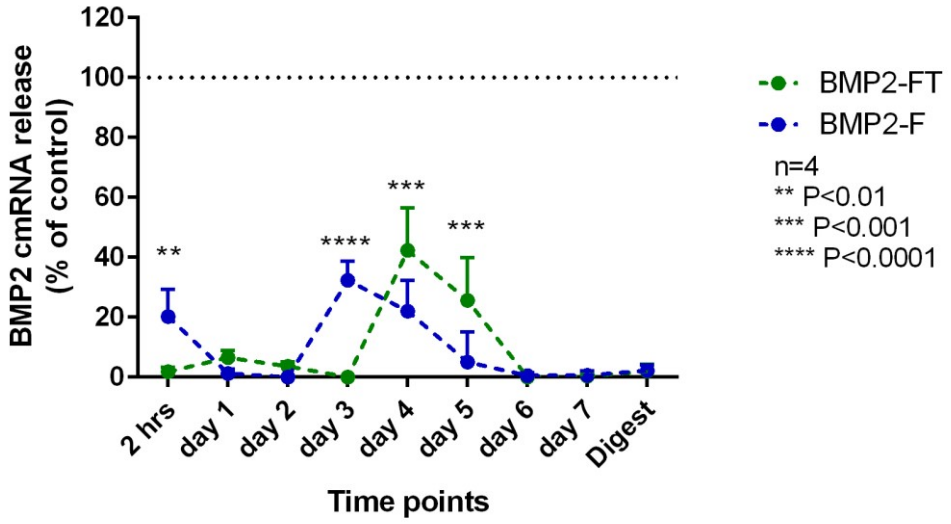

Figure 28: Graph showing the release of BMP2 lipoplexes from fibrin (BMP2-FT) and fibrinogen (BMP2-F) coated titanium discs. The results showed a burst of release from the fibrinogen coating in the 2 hrs. timepoint followed by a drop and it peaked on the 3rd day .on the other hand, fibrin showed minimal release in the beginning until it peaked on the 4th day. Both coatings had similar release patterns after the initial timepoint.

3.5. BMP2 transcript activated Ti coating.

The same experimental setup and cmRNA concentrations described for the optimization phase (section 2.2.4 of this thesis) were used here. BMP2 cmRNA was used instead of the MetLuc reporter, also C2C12 cell line was used instead of NIH3T3. However, only fibrin and fibrinogen coatings were compared as they yielded the best results in the optimization experiments.

3.5.1. BMP2 Expression from fibrin and fibrinogen coated Ti discs.

The translation of BMP2 was evaluated via ELISA in the supernatant of the fibrinogen and fibrin coated Ti discs both containing 500 and 250 ng/Ti disc cmRNA concentrations (i.e., BMP2-F 500 ng/Ti disc, BMP2-F 250 ng/Ti disc, BMP2-FT 500 ng/Ti disc and BMP2-FT 250 ng/Ti disc). Samples details in Table 17.

Table 17: the samples details for the BMP2 expression from fibrin and fibrinogen coated Ti discs.

Samples	**cmRNA** **conc. (ng/Ti disc)**	**Coating methods**	**Coating materials**
BMP2-FT	BMP2 500 ng/Ti disc 250 ng/Ti discs	Physical entrapment in Fibrin	MetLuc lipoplexes and Fibrin (1F:1T)
BMP2-F	BMP2 500 ng/Ti disc 250 ng/Ti discs	Physical entrapment in Fibrinogen	MetLuc lipoplexes and Fibrin (1F:0T)

BMP2 expression was detectable only with BMP2-F coated Ti discs. The BMP2 expression was the highest during the first 2 days after cell seeding, with statistical significance, the p-values were <0.001 and <0.0001 of the 1st and 2nd days compared to the 3rd respectively. No BMP2 expression was detected after the 3rd day. The BMP2-F 500 ng/well cmRNA concentration group had significantly higher BMP2 expression than BMP2-F 250 ng/well group with a p-value <0.01 on days 1 and 2. BMP2-FT showed no detectable protein expression in the supernatant at all the time points (Figure 29). The statistical details in appendix 7.3.5.

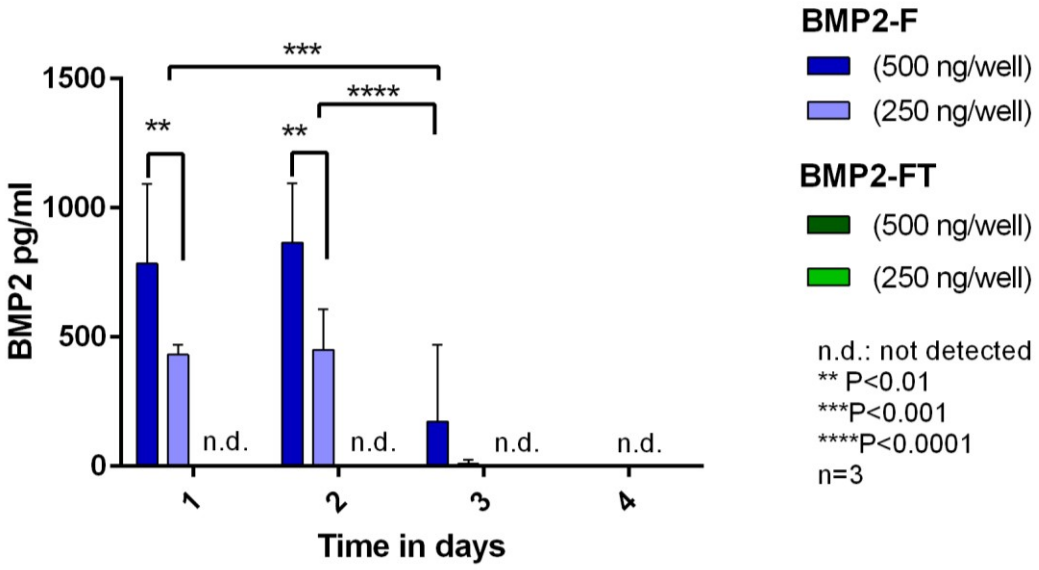

Figure 29: Graph that presents the data of BMP2 translation kinetics/time from BMP2-F and BMP2-FT coated Ti with 2 cmRNA concentrations (500 and 250 ng/well) measured via ELISA in BMP2 pg/ml. The results showed BMP2 expression on the 1st and 2nd days after cell seeding, with significance on both days in favour of the 500 ng/well MetLuc-F group (p value<0.01 and n=3). The fibrin-coated titanium disc BMP2-FT had no detectable expression at all the time points.

3.5.2. Osteogenic activity

Alkaline phosphatase assay (ALP) was used to detect the osteogenic activity of the cells seeded on coated Ti. Moreover, alizarine red staining (AR) was used to detect the resultant ossification. Samples details in Table 18.

Table 18: the samples details for osteogenic activity in vitro

Samples	**cmRNA** **conc. (ng/Ti disc)**	**Coating methods**	**Coating materials**
BMP2-FT	BMP2 500 ng/Ti disc 250 ng/Ti disc	Physical entrapment in Fibrin	MetLuc lipoplexes and Fibrin (1F:1T)

	125 ng/Ti disc 62.5 ng/Ti disc		
BMP2-F	BMP2 500 ng/Ti disc 250 ng/Ti disc 125 ng/Ti disc 62.5 ng/Ti disc	Physical entrapment in Fibrinogen	MetLuc lipoplexes and Fibrin (1F:0T)

3.5.2.1. Alkaline phosphatase (ALP) activity

The results showed a consistent significant increase in ALP activity of the cells seeded on (BMP2-F 500 ng/well) Ti surface at all the time points vs. all other groups except (BMP2-F 250 ng/well) at all the time points (Figure 30). On the first timepoint (5 days after cell seeding), the cells seeded on the (BMP2-F 500 ng/well) group had significantly higher ALP activity than (BMP2-F 125 ng/well) and (BMP2-FT 250 ng/well) groups with p-value < 0.05, and (BMP2-F 62.5 ng/well), and (BMP2-FT 500, 125, and 62.5 ng/well) groups with p-value <0.01. Similarly, on the second timepoint (7 days after cell seeding), the cells seeded on (BMP2-F 500 ng/well) samples had significantly higher ALP activity than (BMP2-F 125 ng/well) with a p-value <0.01, (BMP2-F 62.5 ng/well), (BMP2-FT 500 and 250 ng/well) groups with p-value <0.001, and (BMP2-FT 125, and 62.5 ng/well) groups with p-value <0.0001. At the same time point, (BMP2-F 250 ng/well) cells had significantly higher ALP activity than (BMP2-F 125 ng/well) group with a p-value <0.01 and all the remaining groups with a p-value <0.001. Finally, at the last timepoint (10 days after cell seeding), only cells seeded on 500 ng/well fibrinogen coated Ti group (BMP2-F 500 ng/well) showed significantly higher ALP activity than (BMP2-F 62.5 ng/well)

and (BMP2-FT 250 ng/well) with p-value <0.05. All are shown in Figure 30. The statistical analysis details in appendix 7.3.6.

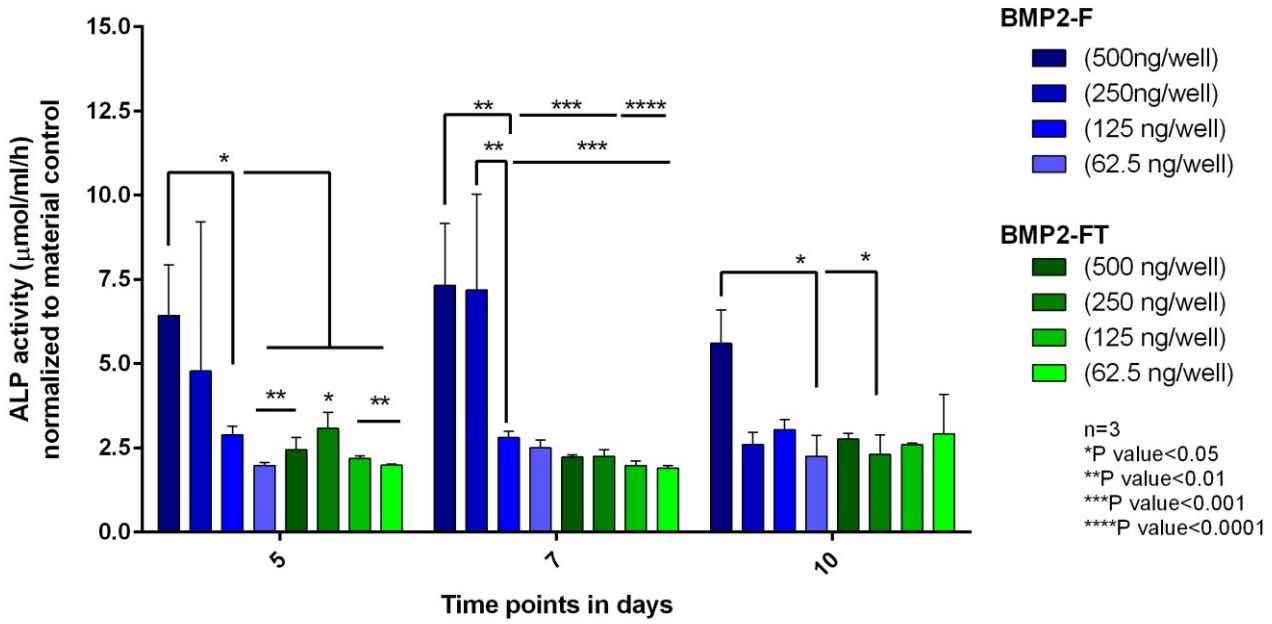

Figure 30: Graph shows ALP activity in C2C12 cells on the 5th, 7th, and 10th days after seeding on the surface of F and FT coated Ti containing different concentrations of BMP2 cmRNA (500-62.6 ng/well), as determined using pNP assay. The graph highlights the significant increase in ALP activity in the groups coated with BMP2-F (500 ng/well and 250 ng/well) especially on the 5th and 7th days, while 500 ng/well concentration still showed a significant increase vs. other concentrations on the 10th day. On the other hand, BMP2-FT samples showed lower ALP activity.

3.5.2.2. Alizarine red staining (AR)

After 35 days of incubation of C2C12 cells on the coated Ti discs in osteogenic medium, the AR staining had confirmed the formation of calcified nodules on the surface of BMP2-transcript activated fibrinogen coated Ti discs (i.e., BMP2-F) compared to controls, as shown in Figure 31. However, BMP2-transcript activated fibrin coated Ti discs (i.e., BMP2-FT) had no visual calcification nodules on their surfaces. The AR dye was later retrieved and quantified to demonstrate the difference in calcification on the surface of the different coated groups. The results showed a significant difference in the amount of the retrieved dye between the BMP2-F samples containing 500, 250, and 125 ng/Ti

disc cmRNA concentration cmRNA vs. the same cmRNA concentrations in the BMP2-FT group with p-values <0.0001, <0.0001, and <0.05, respectively. Among the different cmRNA concentrations tested, the BMP2-F containing 500 ng/Ti disc cmRNA group showed significantly higher AR dye concentration than BMP2-F containing 250 and 125 ng/Ti disc groups with p-value <0.001, and BMP2-F 62.5 ng/Ti disc with p-value <0.0001, as illustrated in Figure 32. Meanwhile, BMP2-F 250 and 125 ng/Ti disc samples both had significantly higher AR dye concentration than BMP2-F 62.5 ng/Ti disc with p-values <0.01 and <0.05 respectively. On the other hand, BMP2-FT samples showed low AR dye concentration results across all tested cmRNA concentrations at all the time points Figure 32.

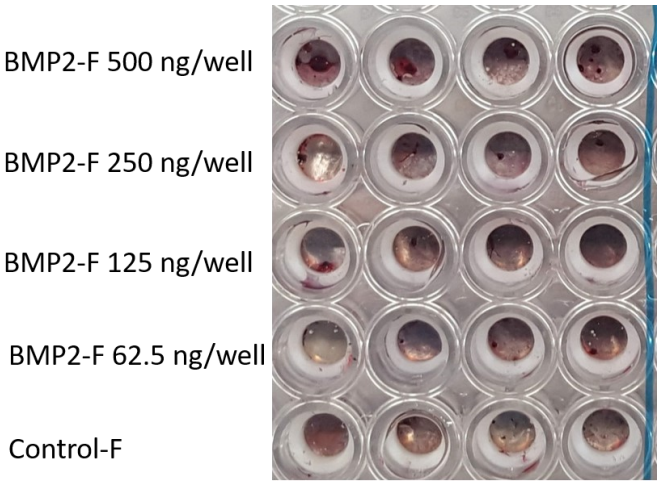

Figure 31: Photograph showing the alizarine red stained calcified nodules formed by C2C12 cells on Ti surface coated with BMP2 lipoplexes-activated fibrinogen coating containing different concentrations of cmRNA. The nodules seemed to be the highest with the BMP2-F 500ng/well group.

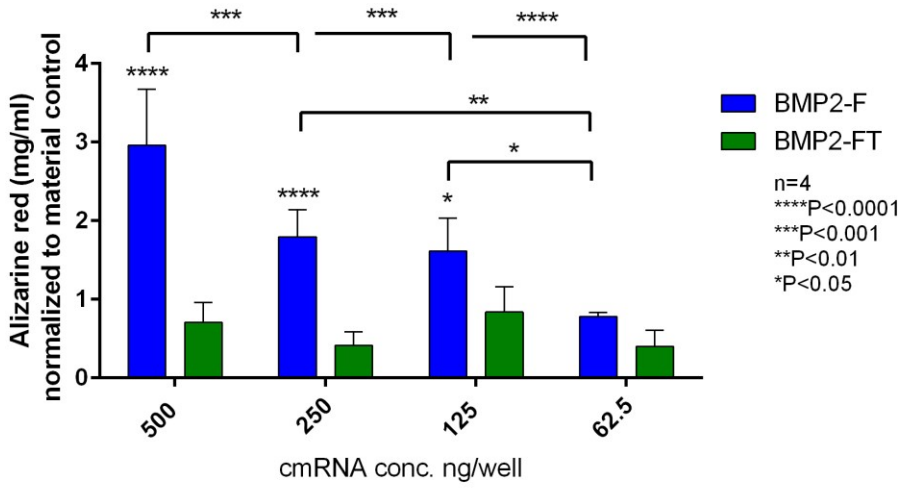

Figure 32: Graph representing the results of alizarine red stain retrieval measured in mg/ml. (a.) shows the significant increase of the retrieved stain from samples coated with fibrinogen especially the 500 ng/well samples in contrast to other concentrations and controls (p values <0.001 and <0.0001, n=4). On the other hand, (b.) shows the different FT coated groups all with equal or less than control indicating negative results.

Chapter 4: Discussion

Metallic implants' success is greatly reliant on the integration with the surrounding bone [180]. However, in many cases, having optimal bone quality and quantity is difficult to come by, thus, bio-functionalizing the surface of metallic implants to induce bone formation has become a hot topic of research. In this work, we attempted the development of biocompatible, osteogenic BMP2 transcript-activated coatings for titanium implant surfaces.

One of the most investigated osteogenic biomolecules for implant surface functionalization is BMP2. Although BMP2's role in the osteogenic differentiation of osteoblasts and the induction of bone formation is well known, the supra-physiological concentrations used in the local protein application can lead to many side effects such as ectopic bone formation, inflammation, bleeding, hematoma, oedema, erythema, and implant failure [14,181,182]. Therefore, other strategies such as gene therapy and transcript therapy have been developed to overcome the potential side-effects of BMP2 protein applications.

Transcript therapy, which is using mRNA to translate into therapeutic proteins, has been introduced as an attractive solution for bone healing applications [16,19,130,169]. In many ways, transcripts (mRNA) have advantages over protein therapy and gene therapy. Its ability to transfect postmitotic cells and its transient nature are some of the advantages over gene therapy, which requires crossing the nuclear membrane with the increased risk of insertional mutagenesis. In contrast to protein therapy, mRNA therapy leads to the translation of the encoded protein by the transfected cells, which means, the produced protein is internally folded and regulated, making it highly functional [183,184]. In a recent in vivo study, it was demonstrated that when BMP is synthesized internally, it aids bone formation

without the need for prolonged application or high concentrations [183], which added to the appeal of using transcript therapy for bone healing.

Still, mRNA applications have been limited due to its high immunogenicity and sensitivity to degradation via nuclease enzymes. To overcome such issues, many mRNA chemical modifications were introduced. For example, Kormann et al., [140] introduced modifications by substituting 5-50% of the uridines and cytidines with modified ones, which increased the stability of mRNA and decrease its immunogenicity. Such modifications resulted in preventing the recognition of the cmRNA by the toll-like receptors, thus preventing the inflammatory reaction responsible for detecting viral infections [185]. Also, Carlsson et al., reported that the substitution of uridine with N1-methylpseudouridine in VEGF-A mRNA led to the production of a nonimmunogenic functional mRNA [183]. In our study, we introduced cmRNA with chemically modified cytidine and uridine and substituted up to 50% of the ribonucleotides with chemically modified ones.

Chemically modified mRNA (cmRNA) has been receiving a lot of attention lately in bone tissue engineering and it has proven potency in inducing bone formation both in vitro and in vivo. Studies by our group and others depicted cmRNA coding for BMP2 [19–21,162,169] and BMP9 [161,186] to have remarkable osteogenic activity in vitro and in vivo. For instance, transcript-activated collagen sponges loaded with BMP2 cmRNA were able to induce osteogenic differentiation in vitro and in vivo critical and non-critical defects in rat femur [20,169]. Therefore, in our work, we incorporated BMP2-encoding cmRNA onto the Ti implant surface to induce bone formation in vitro using the C2C12 cell line.

Additionally, based on our previous findings, we introduced some modifications to the BMP2 transcript sequence such as the translation initiator of the short 5′UTR (TISU) sequence, we deleted an upstream open reading frame and an extra polyadenylation signal, followed by an adenylate−uridylate

rich region as part of the mRNA modifications to improve the translational efficiency [169]. By adopting these modifications, we were able to obtain functional cmRNAs that encoded MetLuc and BMP2. In our work, we were able to produce the required cmRNAs with high integrity that were able to demonstrate high transfection efficiency when administered to NIH3T3 and C2C12 cell lines. This agrees with previous work by Langenbach et al., Zhang et al., as well as Kormann et al.[140,169,187] that showed improved mRNA stability and translational efficiency after such modifications have been done. We produced MetLuc and BMP2 cmRNAs via in vitro transcription and the selection of a proper delivery vector was the next step.

cmRNA delivery has been achieved through the use of viral vectors and non-viral vectors (cationic lipids and polymers) and nanoparticles [188,189]. Among those methods, cationic lipids were the most used delivery vectors for transcript therapy. Their safety was advantageous, as well as, their ease of use, demonstrated by their ability to form lipoplexes automatically due to electrostatic attraction forces. They also provide moderate attachment to the negative backbone of the RNA, which helps stabilize the complex and aid the uptake via the negatively charged cell membrane [190]. Multiple studies have reported a significantly higher transfection efficiency of the cationic lipid vectors when compared to other non-viral vectors [166,190]. The efficacy of cationic lipid delivery systems was also supported by our results in which the in vitro transcribed cmRNA was able to transfect NIH3T3 and C2C12 cells in a 2D standard transfection setting using lipofectamine 2000 lipid vector. However, we did not achieve the same success with the in-house prepared proprietary lipoplexes (lipidoid vector with cmRNA) in a similar standard transfection setting. These results could be attributed to the polyethylene glycol (PEG) shielded design of the in-house prepared lipoplexes. Although it is well established that PEG grafting on lipoplexes has increased their extracellular stability, circulation time, and water solubility (which led to higher efficiency in vivo), it is also reported that PEGylation strongly hinders cellular uptake

and endosomal escape, which may decrease the efficiency of the delivery system in vitro [191,192]. This may explain the difference in our standard transfection results, PEGylated (in-house prepared lipoplexes), and non-PEGylated lipid (lipofectamine 2000). Nevertheless, it is a delicate balance to achieve extracellular stability whilst preserving transfection efficiency, and our selection was supported by reports of successful use of PEGylated lipid vector design in transcript-activated matrixes for bone regeneration both in vitro and in vivo [19,20,169].

Sugar cytoprotectants have been used in tandem with lipoplexes to protect their structure during the freeze/thaw cycles in addition to protecting the complexes during dehydration/rehydration cycles, like in lyophilization or drying for physical adsorption coating. The sugar particles replace the water inside the lipid bilayer, thus preserving the lipoplexes integrity during rehydration. Many sugars have been used such as sucrose, maltose, and trehalose [193,194]. Many reports supported that the use of sugar cryoprotectants has effectively preserved particle size and surface charge of many non-viral vectors [195–198]. Based on that, we used 5% v/v trehalose sugar as a cryoprotectant to preserve our lipoplexes through the freeze/thaw and dry/rehydration cycles.

Once our lipoplexes were formed, they featured small size (<150 nm) and low zeta potential (<0.2). This matched the observations from our group's previous work as well as that of Li et al. [199], in which, the authors obtained the highest expression with lipoplexes that had zeta potential close to zero. They concluded that size is a more important factor for lipofection success rather than the surface charge. Despite the size and charge effects being controversial [200], the impact of lipoplex size on transfection efficiency has been reported highlighting that smaller particles lead to higher transfection [201].

To incorporate the prepared cmRNA lipoplexes onto the Ti surface, different physical incorporation methods were investigated. We employed physical methods (physical adsorption and physical

entrapment) due to their simplicity, ease, and lack of interference with the structure of the used biomolecules [48]. The available literature supports our selection to utilize physical methods as they have been used successfully in functionalizing the surface of Ti implants with therapeutics (e.g. analgesics and antibiotics) and biomolecules (e.g. proteins, and nucleic acids) [26,65,202].

Physical adsorption mainly depends on weaker electrostatic attraction, van der Waal forces, hydrogen bonds, and hydrophobic interactions [48] and is usually achieved via immersing the surface of the titanium with a solution containing bioactive molecules. For example, BMP2 adsorbed on porous Ti implants was able to induce bone formation in an ectopic rat model [107]. Additionally, gene activation was attempted via adsorbing DNA lipoplexes in layer-by-layer technique [203] as well as simply via adsorbing DNA complexes like in the case of co-polymer protected BMP2-DNA complexes coated medullary stabilization wires in rat tibia model that induced fracture healing in vivo [74]. Also, small interference RNA lipoplexes have been adsorbed on the surface of Ti implants leading to enhancing peri-implant cellular osteogenic function [204]. This was further confirmed by our success in transfecting the cells seeded on the surface of Ti functionalized with MetLuc cmRNA lipoplexes via physical adsorption.

Although the physical adsorption method has been employed successfully in our work, the yielded transfection efficiency and kinetics over time were quite low in contrast to incorporating the cmRNA lipoplexes in a biomaterial. This could be attributed to many reasons. First, physical adsorption is sensitive to the material concentration and surrounding environmental factors, such as temperature and pH [205]. Secondly, the drying of the lipoplexes in the air exposes them to the risk of RNase degradation. Lastly, the lipoplexes can desorb in a fast and uncontrolled manner. Such fast release of the lipoplexes may increase the risk of toxicity to the cells seeded on the coated surface due to exposure to a high

dose of lipoplexes in a short time. The latter toxicity concern was confirmed with our cell viability and proliferation results that showed MetLuc-Ti discs resulted in the worst cell proliferation in comparison to the other tested methods. Other studies have also reported that the use of lipoplexes can induce toxicity by inhibiting some proteins such as protein kinase C, inducing changes in the cell like shrinking and vacuolization of the cytoplasm, and reducing mitoses [134]. So, as expected the incorporation of cmRNA lipoplexes via physical entrapment in biomaterial coatings led to better results than directly depositing cmRNA complexes on Ti. In our study, we used PDLLA, fibrin, and fibrinogen as biomaterials for cmRNA surface incorporation to further protect the lipoplexes from the surrounding environment and create a sustained release platform.

PDLLA polymer is a well-established implant coating material known for its safety, biocompatibility, and biodegradability [206]. It has the ability of drug and biomolecule delivery, and its mechanical properties are favourable for endosseous implant applications. Current literature supports our PDLLA material selection for this work. A study by Schmidmaier et al. used a medullary nail coated with BMP2 protein incorporated in PDLLA which led to fracture healing in rats' tibia [76]. Recently, researchers have developed (mRNA)-bearing poly(lactide-co-glycolide acid) (PLGA) coating for a surgical suture that can transfect adjacent cells and accelerate wound healing [207]. Kolk et al. used PDLLA together with co-polymer-protected BMP2-DNA polyplexes to develop a Ti-implant coating [61] that could induce bone formation in a critical size defect in a rat jaw model [77]. Inspired by Kolk et al. work, we established a coating with PDLLA and cmRNA, yet, as we are using a lipid-based delivery vector that requires cryoprotectant sugar for storage, mixing our sugar-containing lipoplexes with PDLLA dissolved in ethyl acetate was not possible as the used trehalose sugar does not dissolve in ethyl acetate. This technical difficulty was overcome by functionalizing the surface of Ti first with the

lipoplexes solution via physical adsorption, then we added different concentrations of PDLLA in ethyl acetate solution to establish different coating thicknesses when the solvent evaporates.

The results of our MetLuc-PDLLA coating showed similar tendencies to Kolk's work with DNA [61]. In our results, the use of the least amount of PDLLA coating for Ti (MetLuc-PDLLA 0.25) yielded better transfection efficiency compared to the higher PDLLA concentrations and MetLuc-Ti. Based on the previous reports and our results, we can assume that polymeric coatings with low polymer concentrations may allow for a faster release of lipoplexes, thereby increasing cellular uptake and transfection. These improved results could also be correlated with the cell proliferation assay, which showed an improvement in samples coated with MetLuc-PDLLA in comparison MetLuc-Ti. This indicated that PDLLA coating has improved the biocompatibility of the functionalized implant surface.

Our other physical entrapment strategy was based on incorporating cmRNA lipoplexes within a natural polymer coating material, namely, fibrin (FT). Fibrin is reported to have many advantages as a coating material, being the body's natural healing scaffold, it supports cell attachment, growth and differentiation, the flow of signals and nutrients, and cell-cell communication [84]. It has been long used in tissue engineering applications for its ability as a carrier for different biomolecules. The most common form of use is fibrin hydrogels which were used by our group [17], as cmRNA carriers that were capable of controlled release and the induction of stem cell osteogenic differentiation in vitro, in addition to improving cell viability when compared to standard 2D transfection. Although the mechanical properties of FT are very low, which can limit its use as a metallic implant coating. However, this disadvantage could be overcome by the use of porous metallic implants that can shield the coating within its pores until their function is done. Van der Stok et al. [82] used porous Ti implant filled with BMP2 loaded fibrin to induce healing in critical size defect in a rat's femur. Additionally,

fibrin glue activated with BMP2-DNA polyplexes was able to induce chondrogenesis in vitro [88]. Thus, given the literature support and its many advantages, we used transcript-activated fibrin and fibrinogen as Ti coating materials.

Interestingly, our results revealed that titanium coated with fibrin and fibrinogen yielded better transfection efficiency than that of PDLLA. However, establishing a direct comparison between these two coating materials is difficult as the physical entrapment strategies employed are completely different. Moreover, we could not find any reports that directly compare these materials as metallic implant coating. Yet, in terms of biocompatibility, PDLLA, fibrin, and fibrinogen seem to improve cell proliferation in contrast to uncoated Ti. These biomaterials may have stimulated cells' attachment on them, in addition to preventing the fast exposure of the cells to high concentrations of lipoplexes, which may be toxic to the cells.

The 3D structure of fibrin and fibrinogen coating could explain their superior transfection efficiency in contrast to PDLLA and uncoated Ti. This 3D network allows for better drug entrapment and cell colonization. It has been reported that plasmid DNA complexes loaded into 3D matrices show reduced toxicity [199,208]. Because, in such 3D structures, the cells are gradually exposed to the lipoplexes due to their co-localization on the matrix. Identically, in our study, cmRNA lipoplexes are not delivered at once into the cells but rather in a sustained manner from the transcript-activated fibrin and fibrinogen Ti coatings.

To our surprise, fibrinogen-coated samples generated better transfection efficiency compared to fibrin, and the best in our work. This finding could be attributed to the open and homogenous microstructure of fibrinogen in comparison to the cross-linked fibrin [209], which allows for better more homogenous cell distribution. Additionally, the PEG shielded design of the used lipoplexes may have played a role

in increasing the transfection efficiency. Besides its role in protecting the lipoplexes in the extracellular environment, PEG grafting was reported to decrease fibrinogen adsorption to a surface [210], which may have contributed to the easier release of the lipoplexes from the fibrinogen matrix as they would be loosely bound to it. In contrast, it was reported that un-PEGylated lipoplexes strongly bind to fibrinogen components which may hinder their release from the matrix [211].

Moreover, fibrinogen also supported higher transfection efficiency and prolonged production of BMP2 protein by transfected cells. This could be attributed to the effect of thrombin concentration on the final structure of fibrin. As the thrombin concentration decreases, a thicker less branched more open fibrin structure is formed, that is characterized by larger pores and consequently lower surface area for cell attachment in comparison to higher concentrations which has more tight pores, more branching, and larger surface area [212–214]. Fibrinogen forms a gel-like structure in the absence of thrombin that features thin fibrils [215,216]. This may result in a faster diffusion of entrapped molecules. Furthermore, it has excellent adsorption on Ti [217], which can make it a more stable coating. Another aspect to consider is the biocompatibility and cell-attractant properties of fibrinogen as well as its ability to promote cell attachment and proliferation [218]. These cellular features of fibrinogen may have increased the cellular attachment to the fibrinogen-coated titanium, thereby increasing the transfection efficiency. Such differences could explain the discrepancies between the fibrin and fibrinogen results in terms of transfection, release, and later osteogenesis.

Looking at our BMP2 lipoplexes release results from the fibrin and fibrinogen coatings, we can see a significant difference. Although fibrin and fibrinogen had similar release patterns, fibrinogen had a characteristic initial burst, as well as being slightly faster in terms of lipoplexes release than fibrin. One explanation for this observation may be because of fibrin's 3D network structure. In agreement with

our observations, Jeon et al. reported that by increasing thrombin in the composition of fibrin, the release rate of entrapped drugs decreased [214].

After screening the different transcript-activated coating methods for Ti, we chose the coatings that yielded the best transfection efficiency results (i.e., fibrin and fibrinogen coated Ti discs) to functionalize with BMP2 cmRNA lipoplexes (BMP2-FT and BMP-F, respectively). C2C12 cells are a well-established mouse pre-myocyte cell line that can differentiate into osteoblasts in the presence of BMP2 and starts expressing markers for initial differentiation (e.g. alkaline phosphatase)[178,219,220], Therefore, we used them to assess the BMP2 transcript-activated Ti coatings bioactivity in vitro.

Our results showed that the C2C12 cells transfected by BMP2 cmRNA fibrinogen coated Ti expressed BMP2 in vitro and underwent the subsequent osteogenic differentiation, while fibrin coated Ti did not. Fibrinogen coated samples increased ALP activity and showed evident mineralization. Both ALP activity and mineralization appeared to be dependent on the cmRNA amount present on the coating. These results corroborate our group's previously published data, both in vivo and in vitro, in which osteogenesis strongly depends on the cmRNA dose used [19,169]. That published work has established that 20 pg of BMP2 cmRNA/cell (human mesenchymal stem cell monolayers) is osteogenic in vitro [19]. Yet, in this work, we developed a 3D coating instead of the cell monolayers used previously. Also, we used different cells type. However, higher doses of BMP2 cmRNA (>5 μg) have been reported to be necessary to heal a 5 mm critical bone defect in rats [169]. The optimal dose of cmRNA for in vivo implant osteointegration will be the subject of future research. However, the cmRNA can be easily produced at a low cost [221]. The GMP-grade cmRNA production for clinical use was reported to be up to 10-folds lower than its protein counterpart [184]. Yet, to fully assess the feasibility of these newly developed implants, their biomechanical performance in vivo should be evaluated. Limitations of our

work include the lack of these biomechanical studies. It was reported that the biomechanical performance of fibrinogen- or PLGA-coated Ti screws [222,223] as well as PDLLA-coated Ti [224] was improved after in vivo implantation. Remarkably, these reports demonstrated a tight integration of the coating material to the implant surface regardless of the implantation method used.

Up till the time of writing this work, cmRNA transcript-activated metallic implants have not been reported before. One study by Wu et al. [204], described functionalizing the surface microporous titanium oxide using microRNA to enhance its osteogenic activity. Recently, another study by Lui et al. [222], incorporated microRNA (miR-204)−gold nanoparticles into a PLGA coating on titanium surfaces also to boost the osteogenic activity. Along with these two studies, our work pioneers the demonstration of RNA therapeutics potency in the field of metallic implants' integration for dental and orthopaedic applications. Additionally, our work shines a light on the potential of fibrinogen as an implant coating and a carrier material for cmRNA, which can have various potential applications in the field of tissue engineering and implantology.

Chapter 5: Conclusion

We have investigated different methods for coating cmRNA on titanium surfaces. We found that the use of biomaterials to coat cmRNA lipoplexes onto the Ti surface further improved the transfection efficiency of the coating, as well as the cellular response to it. It was highlighted in our work that transcript-activated fibrinogen coating provided sustained delivery of the loaded cmRNA lipoplexes, increased the transfection efficiency and attracted cells to the coating layer, and thereby improved the overall outcome. BMP2 transcript-activated fibrinogen coating on Ti expressed the coded protein in vitro and induced the osteogenic differentiation of C2C12 cells, evident by the elevation of ALP activity and the subsequent mineralization. Overall, our findings support the use of fibrinogen as a carrier for RNA therapeutics that can be used on metallic implant surfaces. Especially, in the areas requiring bone regeneration, this biomaterial−nucleic acid combination allows for obtaining transcript-activated matrices with outstanding features.

Chapter 6: References

1. Thiagarajan, S., Rajkumar, M. & Chen, S. Nano TiO 2 -PEDOT Film for the Simultaneous Detection of Ascorbic Acid and Diclofenac. *Int. J. Electrochem. Sci.* **7**, 2109–2122 (2012).
2. W. Nicholson, J. Titanium Alloys for Dental Implants: A Review. *Prosthesis* **2**, 100–116 (2020).
3. Listgarten, M. A., Lang, N. P., Schroeder, H. E. & Schroeder, A. Periodontal tissues and their counterparts around endosseous implants. *Clin. Oral Implants Res.* **2**, 1–19 (1991).
4. Stanford, C. M. & Schneider, G. B. Functional behaviour of bone around dental implants. *Gerodontology* **21**, 71–77 (2004).
5. Anil, S., Anand, P. S., Alghamdi, H. & Janse, J. A. Dental Implant Surface Enhancement and Osseointegration. in *Implant Dentistry - A Rapidly Evolving Practice* 544 (InTech, 2011). doi:10.5772/16475
6. Wang, Y., Zhang, Y. & Miron, R. J. Health, Maintenance, and Recovery of Soft Tissues around Implants. *Clinical Implant Dentistry and Related Research* **18**, 618–634 (2016).
7. De Bruyn, H., Vandeweghe, S., Ruyffelaert, C., Cosyn, J. & Sennerby, L. Radiographic evaluation of modern oral implants with emphasis on crestal bone level and relevance to peri-implant health. *Periodontol. 2000* **62**, 256–270 (2013).
8. Yeo, I.-S. L. Modifications of Dental Implant Surfaces at the Micro- and Nano-Level for Enhanced Osseointegration. *Materials (Basel).* **13**, 89 (2019).
9. Le Guéhennec, L., Soueidan, A., Layrolle, P. & Amouriq, Y. Surface treatments of titanium dental implants for rapid osseointegration. *Dent. Mater.* **23**, 844–854 (2007).
10. Hendra Jubhari, E., Dammar, I., Launardo, V. & Goan, Y. Implant Coating Materials to Increase Osseointegration of Dental Implant: A Systematic Review. *Syst. Rev. Pharm.* **11**, 35–41 (2020).
11. Priyadarshini, B., Rama, M., Chetan & Vijayalakshmi, U. Bioactive coating as a surface modification technique for biocompatible metallic implants: a review. *J. Asian Ceram. Soc.* **7**, 397–406 (2019).
12. Jung, H.-D. *et al.* Novel strategy for mechanically tunable and bioactive metal implants. *Biomaterials* **37**, 49–61 (2015).
13. Reckhenrich, A., Koch, C., Egaña, J. & Plank, C. The use of non-viral gene vectors for bioactive poly-(D,L-lactide) implant surfaces in bone tissue engineering. *Eur. Cells Mater.* **23**, 441–448 (2012).
14. Haimov, H., Yosupov, N., Pinchasov, G. & Juodzbalys, G. Bone Morphogenetic Protein Coating on Titanium Implant Surface: a Systematic Review. *J. Oral Maxillofac. Res.* **8**, e1 (2017).
15. Wang, J., Guo, J., Liu, J., Wei, L. & Wu, G. BMP-Functionalised Coatings to Promote Osteogenesis for Orthopaedic Implants. *Int. J. Mol. Sci.* **15**, 10150–10168 (2014).
16. D'Mello, S. *et al.* Bone Regeneration Using Gene-Activated Matrices. *AAPS J.* **19**, 43–53 (2017).
17. Balmayor, E. R. *et al.* Modified mRNA for BMP-2 in Combination with Biomaterials Serves as a Transcript-Activated Matrix for Effectively Inducing Osteogenic Pathways in Stem Cells. *Stem Cells Dev.* **26**, 25–34 (2017).
18. Badieyan, Z. S. Establishing mRNA Delivery Systems for Conversion of Cell Differentiation Status. *thechnical university of munich* (2016).
19. Balmayor, E. R. *et al.* Chemically modified RNA induces osteogenesis of stem cells and human tissue explants as well as accelerates bone healing in rats. *Biomaterials* **87**, 131–146 (2016).

20. Badieyan, Z. S. *et al.* Transcript-activated collagen matrix as sustained mRNA delivery system for bone regeneration. *J. Control. Release* **239**, 137–148 (2016).
21. R., B. *et al.* Modified mRNA for BMP-2 in Combination with Biomaterials Serves as a Transcript-Activated Matrix for Effectively Inducing Osteogenic Pathways in Stem Cells. *https://home.liebertpub.com/scd* **26**, 25–34 (2017).
22. Smeets, R. *et al.* Impact of Dental Implant Surface Modifications on Osseointegration. *Biomed Res. Int.* **2016**, 6285620 (2016).
23. Zhang, R. *et al.* Fabrication of micro/nano-textured titanium alloy implant surface and its influence on hydroxyapatite coatings. *J. Wuhan Univ. Technol. Sci. Ed.* **31**, 440–445 (2016).
24. Kuroda, K. & Okido, M. Osteoconductivity Control Based on the Chemical Properties of the Implant Surface. *J. Biomater. Nanobiotechnol.* **09**, 26–40 (2018).
25. Yeo, I.-S. Reality of Dental Implant Surface Modification: A Short Literature Review. *Open Biomed. Eng. J.* **8**, 114–119 (2014).
26. Civantos, A. *et al.* Titanium Coatings and Surface Modifications: Toward Clinically Useful Bioactive Implants. *ACS Biomater. Sci. Eng.* **3**, 1245–1261 (2017).
27. Glauser, R., Schüpbach, P., Gottlow, J. & Hämmerle, C. H. F. Periimplant Soft Tissue Barrier at Experimental One-Piece Mini-implants with Different Surface Topography in Humans: A Light-Microscopic Overview and Histometric Analysis. *Clin. Implant Dent. Relat. Res.* **7**, s44–s51 (2005).
28. Nothdurft, F. P. *et al.* Differential Behavior of Fibroblasts and Epithelial Cells on Structured Implant Abutment Materials: A Comparison of Materials and Surface Topographies. *Clin. Implant Dent. Relat. Res.* **17**, 1237–1249 (2015).
29. Cochran & Cochran, D. L. Attachment and growth of periodontal cells on smooth and rough titanium. *Int. J. Oral Maxillofac. Surg.* **9**, (1994).
30. Junker, R., Dimakis, A., Thoneick, M. & Jansen, J. A. Effects of implant surface coatings and composition on bone integration: A systematic review. *Clin. Oral Implants Res.* **20**, 185–206 (2009).
31. Zhao, L., Mei, S., Chu, P. K., Zhang, Y. & Wu, Z. Biomaterials The in fl uence of hierarchical hybrid micro / nano-textured titanium surface with titania nanotubes on osteoblast functions. *Biomaterials* **31**, 5072–5082 (2010).
32. Brunette, D. M., Tengvall, P., Textor, M. & Thomsen, P. *Titanium in Medicine*. *Springer-Verlag: Heidelberg and Berlin* (Springer-Verlag, 2001). doi:10.1007/978-3-642-56486-4
33. Hirano, T. *et al.* Proliferation and osteogenic differentiation of human mesenchymal stem cells on zirconia and titanium with different surface topography. *Dent. Mater. J.* **34**, 872–80 (2015).
34. Krishna Alla, R. *et al.* Surface roughness of implants: A review. *Trends in Biomaterials and Artificial Organs* **25**, 112–118 (2011).
35. Nicolas-Silvente, A. I. *et al.* Influence of the titanium implant surface treatment on the surface roughness and chemical composition. *Materials (Basel).* **13**, 314 (2020).
36. Potdar, R. & Ramesh, A. Current Concepts of Surface Topography of Implants: A Review. *J. Heal. Allied Sci. NU* **12**, 208–211 (2022).
37. Wang, F., Li, C., Zhang, S. & Liu, H. Tantalum coated on titanium dioxide nanotubes by plasma spraying enhances cytocompatibility for dental implants. *Surf. Coatings Technol.* **382**, 125161 (2020).
38. Liu, Z., Liu, X. & Ramakrishna, S. Surface engineering of biomaterials in orthopedic and dental implants: Strategies to improve osteointegration, bacteriostatic and bactericidal activities. *Biotechnol. J.* **16**, 2000116 (2021).

39. Trueba, P. *et al.* Fabrication and characterization of superficially modified porous dental implants. *Surf. Coatings Technol.* **408**, 126796 (2021).
40. Cervino, G. *et al.* Sandblasted and Acid Etched Titanium Dental Implant Surfaces Systematic Review and Confocal Microscopy Evaluation. *Materials (Basel).* **12**, 1763 (2019).
41. Luke Yeo, I.-S. Dental Implants. *Dent. Clin. North Am.* **66**, 627–642 (2022).
42. Iwaya, Y. *et al.* Surface properties and biocompatibility of acid-etched titanium. *Dent. Mater. J.* **27**, 415–421 (2008).
43. Ban, S., Iwaya, Y., Kono, H. & Sato, H. Surface modification of titanium by etching in concentrated sulfuric acid. *Dent. Mater.* **22**, 1115–1120 (2006).
44. Zahran, R., Rosales Leal, J. I., Rodríguez Valverde, M. A. & Cabrerizo Vílchez, M. A. Effect of Hydrofluoric Acid Etching Time on Titanium Topography, Chemistry, Wettability, and Cell Adhesion. *PLoS One* **11**, e0165296 (2016).
45. Juodzbalys, G., Sapragoniene -Phd, M., Wennerberg -Phd, A., Sapragoniene, M. & Wennerberg, A. New Acid Etched Titanium Dental Implant Surface. *Balt. Dent. Maxillofac. J.* **5**, 101–105 (2003).
46. Guo, J., Padilla, R. J., Ambrose, W., De Kok, I. J. & Cooper, L. F. The effect of hydrofluoric acid treatment of TiO2 grit blasted titanium implants on adherent osteoblast gene expression in vitro and in vivo. *Biomaterials* **28**, 5418–5425 (2007).
47. Stewart, C., Akhavan, B., Wise, S. G. & Bilek, M. M. M. A review of biomimetic surface functionalization for bone-integrating orthopedic implants: Mechanisms, current approaches, and future directions. *Prog. Mater. Sci.* **106**, 100588 (2019).
48. de Jonge, L. T., Leeuwenburgh, S. C. G., Wolke, J. G. C. & Jansen, J. A. Organic–Inorganic Surface Modifications for Titanium Implant Surfaces. *Pharm. Res.* **25**, 2357–2369 (2008).
49. Sevilla, P., Godoy, M., Salvagni, E., Rodríguez, D. & Gil, F. J. Biofunctionalization of titanium surfaces for osseintegration process improvement. *J. Phys. Conf. Ser.* **252**, 012009 (2010).
50. Meng, H.-W. W., Chien, E. Y. & Chien, H.-H. H. Dental implant bioactive surface modifications and their effects on osseointegration: a review. *Biomark. Res.* **4**, 24 (2016).
51. Rupp, F., Liang, L., Geis-Gerstorfer, J., Scheideler, L. & Hüttig, F. Surface characteristics of dental implants: A review. *Dent. Mater.* **34**, 40–57 (2018).
52. Ghanem, A. *et al.* Role of osteogenic coatings on implant surfaces in promoting bone-to-implant contact in experimental osteoporosis: A systematic review and meta-analysis. *Implant Dent.* **26**, 770–777 (2017).
53. Yamaguchi, S., Spriano, S. & Cazzola, M. Fast and effective osseointegration of dental, spinal, and orthopedic implants through tailored chemistry of inorganic surfaces. in *Nanostructured Biomaterials for Regenerative Medicine* 337–377 (Elsevier, 2020). doi:10.1016/B978-0-08-102594-9.00013-9
54. Damerau, J.-M. *et al.* A systematic review on the effect of inorganic surface coatings in large animal models and meta-analysis on tricalcium phosphate and hydroxyapatite on periimplant bone formation. *J. Biomed. Mater. Res. Part B Appl. Biomater.* (2021). doi:10.1002/JBM.B.34899
55. Kumar, M., Kumar, R. & Kumar, S. Coatings on orthopedic implants to overcome present problems and challenges: A focused review. *Mater. Today Proc.* **45**, 5269–5276 (2021).
56. Goodman, S. B., Yao, Z., Keeney, M. & Yang, F. The future of biologic coatings for orthopaedic implants. *Biomaterials* **34**, 3174–3183 (2013).
57. Bosco, R. *et al.* Instructive coatings for biological guidance of bone implants. *Surf. Coat. Technol.* **Complete**, 91–98 (2013).

58. Vanderleyden, E., Mullens, S., Luyten, J. & Dubruel, P. Implantable (Bio)Polymer Coated Titanium Scaffolds: A Review. *Curr. Pharm. Des.* **18**, 2576–2590 (2012).
59. Fuchs, T. F. *et al.* Local delivery of growth factors using coated suture material. *ScientificWorldJournal.* **2012**, 109216 (2012).
60. Auras, R. A., Lim, L.-T. T., Selke, S. E. M. & Tsuji, H. *Poly(lactic acid): Synthesis, Structures, Properties, Processing, and Applications*. (Wiley, 2011).
61. Kolk, A. *et al.* A strategy to establish a gene-activated matrix on titanium using gene vectors protected in a polylactide coating. *Biomaterials* **32**, 6850–9 (2011).
62. Lucke, M. *et al.* Gentamicin coating of metallic implants reduces implant-related osteomyelitis in rats. *Bone* **32**, 521–531 (2003).
63. Vester, H., Wildemann, B., Schmidmaier, G., Stöckle, U. & Lucke, M. Gentamycin delivered from a PDLLA coating of metallic implants. *Injury* **41**, 1053–1059 (2010).
64. Karacan, I. *et al.* Mechanical testing of antimicrobial biocomposite coating on metallic medical implants as drug delivery system. *Mater. Sci. Eng. C* **104**, 109757 (2019).
65. Ren, L. *et al.* Effects of aspirin-loaded graphene oxide coating of a titanium surface on proliferation and osteogenic differentiation of MC3T3-E1 cells. *Sci. Rep.* **8**, 15143 (2018).
66. Tyler, B., Gullotti, D., Mangraviti, A., Utsuki, T. & Brem, H. Polylactic acid (PLA) controlled delivery carriers for biomedical applications. *Adv. Drug Deliv. Rev.* (2016). doi:10.1016/j.addr.2016.06.018
67. Casalini, T., Rossi, F., Castrovinci, A. & Perale, G. A Perspective on Polylactic Acid-Based Polymers Use for Nanoparticles Synthesis and Applications. *Frontiers in Bioengineering and Biotechnology* **7**, 259 (2019).
68. Sheikh, Z. *et al.* Biodegradable Materials for Bone Repair and Tissue Engineering Applications. *Materials (Basel).* **8**, 5744–5794 (2015).
69. Schmidmaier, G., Wildemann, B., Stemberger, A., Haas, N. P. & Raschke, M. Biodegradable poly(D,L-lactide) coating of implants for continuous release of growth factors. *J. Biomed. Mater. Res.* **58**, 449–455 (2001).
70. Miller, R. A., Brady, J. M. & Cutright, D. E. Degradation rates of oral resorbable implants (polylactates and polyglycolates): Rate modification with changes in PLA/PGA copolymer ratios. *J. Biomed. Mater. Res.* **11**, 711–719 (1977).
71. Cutright, D. E., Perez, B., Beasley, J. D., Larson, W. J. & Posey, W. R. Degradation rates of polymers and copolymers of polylactic and polyglycolic acids. *Oral Surgery, Oral Med. Oral Pathol.* **37**, 142–152 (1974).
72. JM, B., DE, C., RA, M. & GC, B. Resorption rate, route, route of elimination, and ultrastructure of the implant site of polylactic acid in the abdominal wall of the rat. *J. Biomed. Mater. Res.* **7**, 155–166 (1973).
73. Schmidmaier, G., Lucke, M., Wildemann, B., Haas, N. P. & Raschke, M. Prophylaxis and treatment of implant-related infections by antibiotic-coated implants: a review. *Injury* **37**, S105–S112 (2006).
74. Schwabe, P. *et al.* Effect of a novel nonviral gene delivery of BMP-2 on bone healing. *ScientificWorldJournal.* **2012**, 560142 (2012).
75. Deppe, H., Stemberger, A. & Hillemanns, M. Effects of osteopromotive and anti-infective membranes on bone regeneration: an experimental study in rat mandibular defects. *Int. J. Oral Maxillofac. Implants* **18**, 369–76 (2003).
76. G., S. *et al.* Bone morphogenetic protein-2 coating of titanium implants increases biomechanical strength and accelerates bone remodeling in fracture treatment: a biomechanical and histological

study in rats. *Bone* **30**, 816–822 (2002).
77. Kolk, A. *et al.* A novel nonviral gene delivery tool of BMP-2 for the reconstitution of critical-size bone defects in rats. *J. Biomed. Mater. Res. Part A* **104**, 2441–2455 (2016).
78. Haidari, S. *et al.* Functional analysis of bioactivated and antiinfective PDLLA-coated surfaces. *J. Biomed. Mater. Res. - Part A* **105**, 1672–1683 (2017).
79. Sartori, M. *et al.* Collagen type I coating stimulates bone regeneration and osteointegration of titanium implants in the osteopenic rat. *Int. Orthop.* **39**, 2041–2052 (2015).
80. Guo, Y. *et al.* Tightly adhered silk fibroin coatings on Ti6Al4V biometals for improved wettability and compatible mechanical properties. *Mater. Des.* **175**, 107825 (2019).
81. Van Vlierberghe, S., Vanderleyden, E., Boterberg, V. & Dubruel, P. Gelatin functionalization of biomaterial surfaces: Strategies for immobilization and visualization. *Polymers (Basel).* **3**, 114–130 (2011).
82. van der Stok, J. *et al.* Full regeneration of segmental bone defects using porous titanium implants loaded with BMP-2 containing fibrin gels. *Eur. Cells Mater.* **29**, 141–154 (2015).
83. Naskar, D., Nayak, S., Dey, T. & Kundu, S. C. Non-mulberry silk fibroin influence osteogenesis and osteoblast-macrophage cross talk on titanium based surface. *Sci. Rep.* **4**, 4745 (2015).
84. Noori, A., Ashrafi, S. J., Vaez-Ghaemi, R., Hatamian-Zaremi, A. & Webster, T. J. A review of fibrin and fibrin composites for bone tissue engineering. *Int. J. Nanomedicine* **Volume 12**, 4937–4961 (2017).
85. Undas, A. & Ariëns, R. A. S. Fibrin clot structure and function: A role in the pathophysiology of arterial and venous thromboembolic diseases. *Arterioscler. Thromb. Vasc. Biol.* **31**, (2011).
86. MOSESSON, M. W. Fibrinogen and fibrin structure and functions. *J. Thromb. Haemost.* **3**, 1894–1904 (2005).
87. Karfeld-Sulzer, L. S., Siegenthaler, B., Ghayor, C. & Weber, F. E. Fibrin hydrogel based bone substitute tethered with BMP-2 and BMP-2/7 heterodimers. *Materials (Basel).* **8**, 977–991 (2015).
88. Schillinger, U. *et al.* A fibrin glue composition as carrier for nucleic acid vectors. *Pharm. Res.* **25**, 2946–2962 (2008).
89. An, S. S. A. & Rajangam. Fibrinogen and fibrin based micro and nano scaffolds incorporated with drugs, proteins, cells and genes for therapeutic biomedical applications. *Int. J. Nanomedicine* **8**, 3641 (2013).
90. Linnes, M. P., Ratner, B. D. & Giachelli, C. M. A fibrinogen-based precision microporous scaffold for tissue engineering. *Biomaterials* **28**, 5298–5306 (2007).
91. Donaldson, D. J. & Mahan, J. T. Fibrinogen and fibronectin as substrates for epidermal cell migration during wound closure. *J. Cell Sci.* **62**, 117–127 (1983).
92. Oliveira, M. I. *et al.* Adsorbed Fibrinogen stimulates TLR-4 on monocytes and induces BMP-2 expression. *Acta Biomater.* **49**, 296–305 (2017).
93. Boukari, A., Francius, G. & Hemmerlé, J. AFM force spectroscopy of the fibrinogen adsorption process onto dental implants. *J. Biomed. Mater. Res. Part A* **78A**, 466–472 (2006).
94. Ben-David, D. *et al.* Low dose BMP-2 treatment for bone repair using a PEGylated fibrinogen hydrogel matrix. *Biomaterials* **34**, 2902–2910 (2013).
95. Kim, S. *et al.* Novel osteoinductive photo-cross-linkable chitosan-lactide-fibrinogen hydrogels enhance bone regeneration in critical size segmental bone defects. *Acta Biomater.* **10**, 5021–5033 (2014).
96. Lyris, V., Millen, C., Besi, E. & Pace-Balzan, A. Effect of leukocyte and platelet rich fibrin (L-PRF) on stability of dental implants. A systematic review and meta-analysis. *Br. J. Oral*

Maxillofac. Surg. (2021). doi:10.1016/J.BJOMS.2021.01.001
97. Serafini, G. *et al.* Platelet Rich Fibrin (PRF) and Its Related Products: Biomolecular Characterization of the Liquid Fibrinogen. *J. Clin. Med. 2020, Vol. 9, Page 1099* **9**, 1099 (2020).
98. Andrade, C. X., Quirynen, M., Rosenberg, D. R. & Pinto, N. R. Interaction between Different Implant Surfaces and Liquid Fibrinogen: A Pilot In Vitro Experiment. *Biomed Res. Int.* **2021**, 1–8 (2021).
99. Petrie, T. A., Reyes, C. D., Burns, K. L. & García, A. J. Simple application of fibronectin–mimetic coating enhances osseointegration of titanium implants. *J. Cell. Mol. Med.* **13**, 2602–2612 (2009).
100. Chen, W.-C. C. & Ko, C.-L. L. Roughened titanium surfaces with silane and further RGD peptide modification in vitro. *Mater. Sci. Eng. C* **33**, 2713–2722 (2013).
101. Oya, K. *et al.* Calcification by MC3T3-E1 cells on RGD peptide immobilized on titanium through electrodeposited PEG. *Biomaterials* **30**, 1281–1286 (2009).
102. Xiao, S. J. *et al.* Immobilization of the cell-adhesive peptide Arg-Gly-Asp-Cys (RGDC) on titanium surfaces by covalent chemical attachment. in *Journal of Materials Science: Materials in Medicine* **8**, 867–872 (Kluwer Academic Publishers, 1997).
103. Chen, X., Li, Y. & Aparicio, C. Biofunctional Coatings for Dental Implants. in *Thin Films and Coatings in Biology* 105–143 (Springer, Dordrecht, 2013). doi:10.1007/978-94-007-2592-8_4
104. Bagno, A. *et al.* Human osteoblast-like cell adhesion on titanium substrates covalently functionalized with synthetic peptides. *Bone* **40**, 693–699 (2007).
105. Keceli, H. G. *et al.* Dual delivery of platelet-derived growth factor and bone morphogenetic factor-6 on titanium surface to enhance the early period of implant osseointegration. *J. Periodontal Res.* **55**, 694–704 (2020).
106. Lynch, S. E. *et al.* Effects of the Platelet-Derived Growth Factor/Insulin-Like Growth Factor-I Combination on Bone Regeneration Around Titanium Dental Implants. Results of a Pilot Study in Beagle Dogs. *J. Periodontol.* **62**, 710–716 (1991).
107. Hall, J. *et al.* Bone formation at rhBMP-2-coated titanium implants in the rat ectopic model. *J. Clin. Periodontol.* **34**, 444–451 (2007).
108. Morra, M. Biochemical modification of titanium surfaces: Peptides and eCM proteins. *Eur. Cells Mater.* **12**, 1–15 (2006).
109. Puleo, D. A. & Nanci, A. Understanding and controlling the bone-implant interface. *Biomaterials* **20**, 2311–2321 (1999).
110. Jensen, E. D., Gopalakrishnan, R. & Westendorf, J. J. Bone morphogenic protein 2 activates protein kinase D to regulate histone deacetylase 7 localization and repression of Runx2. *J. Biol. Chem.* **284**, 2225–2233 (2009).
111. Yamaguchi, A., Komori, T. & Suda, T. Regulation of osteoblast differentiation mediated by bone morphogenetic proteins, hedgehogs, and Cbfa1. *Endocrine Reviews* **21**, 393–411 (2000).
112. Kashiwagi, K., Tsuji, T. & Shiba, K. Directional BMP-2 for functionalization of titanium surfaces. *Biomaterials* **30**, 1166–1175 (2009).
113. Barkaoui, A., Bettamer, A. & Ridha, H. A multi-scale bone study to estimate the risk of fracture related to osteoporosis. *Osteoporos. ...* **1**, (2011).
114. Michael, J. *et al.* Surface modification of titanium-based alloys with bioactive molecules using electrochemically fixed nucleic acids. *J. Biomed. Mater. Res. Part B Appl. Biomater.* **80B**, 146–155 (2007).
115. Faensen, B. *et al.* Local application of BMP-2 specific plasmids in fibrin glue does not promote implant fixation. *BMC Musculoskelet. Disord.* **12**, 163 (2011).

116. Smith, J. R. & Lamprou, D. A. Polymer coatings for biomedical applications: a review. *Trans. IMF* **92**, 9–19 (2014).
117. Prakasam, M. *et al.* Biodegradable Materials and Metallic Implants—A Review. *J. Funct. Biomater.* **8**, 44 (2017).
118. Rosen, V. BMP2 signaling in bone development and repair. *Cytokine Growth Factor Rev.* **20**, 475–480 (2009).
119. Stoeger, T. *et al.* In Situ Gene Expression Analysis During BMP2-induced Ectopic Bone Formation in Mice Shows Simultaneous Endochondral and Intramembranous Ossification. *Growth Factors* **20**, 197–210 (2003).
120. Tsuji, K. *et al.* BMP2 activity, although dispensable for bone formation, is required for the initiation of fracture healing. *Nat. Genet.* **38**, 1424–9 (2006).
121. Zhang, J. & Li, L. BMP signaling and stem cell regulation. *Dev. Biol.* **284**, 1–11 (2005).
122. Marie, P. J., Debiais, F. & Haÿ, E. Regulation of human cranial osteoblast phenotype by FGF-2, FGFR-2 and BMP-2 signaling. *Histology and Histopathology* **17**, 877–885 (2002).
123. Park, C. H. *et al.* Tissue engineering bone-ligament complexes using fiber-guiding scaffolds. *Biomaterials* **33**, 137–145 (2012).
124. Hunziker, E. B., Enggist, L., Küffer, A., Buser, D. & Liu, Y. Osseointegration: The slow delivery of BMP-2 enhances osteoinductivity. *Bone* **51**, 98–106 (2012).
125. Sachse, A. *et al.* Osteointegration of hydroxyapatite-titanium implants coated with nonglycosylated recombinant human bone morphogenetic protein-2 (BMP-2) in aged sheep. *Bone* **37**, 699–710 (2005).
126. Pimenta, L., Marchi, L., Oliveira, L., Coutinho, E. & Amaral, R. A Prospective, Randomized, Controlled Trial Comparing Radiographic and Clinical Outcomes between Stand-Alone Lateral Interbody Lumbar Fusion with either Silicate Calcium Phosphate or rh-BMP2. *J. Neurol. Surg. Part A Cent. Eur. Neurosurg.* **74**, 343–350 (2013).
127. Fischer, J. *et al.* Future of local bone regeneration - Protein versus gene therapy. *J. Craniomaxillofac. Surg.* **39**, 54–64 (2011).
128. Park, S.-Y., Kim, K.-H., Kim, S., Lee, Y.-M. & Seol, Y.-J. BMP-2 Gene Delivery-Based Bone Regeneration in Dentistry. *Pharmaceutics* **11**, 393 (2019).
129. Yamamoto, A., Kormann, M., Rosenecker, J. & Rudolph, C. Current prospects for mRNA gene delivery. *Eur. J. Pharm. Biopharm.* **71**, 484–9 (2009).
130. Elangovan, S., Kormann, M. S. D., Khorsand, B. & Salem, A. K. The oral and craniofacial relevance of chemically modified RNA therapeutics. *Discov. Med.* **21**, 35–9 (2016).
131. Leng, Q., Chen, L. & Lv, Y. RNA-based scaffolds for bone regeneration: Application and mechanisms of mRNA, miRNA and siRNA. *Theranostics* **10**, 3190–3205 (2020).
132. Balmayor, E. R. & van Griensven, M. Gene Therapy for Bone Engineering. *Front. Bioeng. Biotechnol.* **3**, 9 (2015).
133. Noguchi, P. Risks and Benefits of Gene Therapy. *N. Engl. J. Med.* **348**, 193–194 (2003).
134. Lv, H., Zhang, S., Wang, B., Cui, S. & Yan, J. Toxicity of cationic lipids and cationic polymers in gene delivery. *J. Control. Release* **114**, 100–109 (2006).
135. Sharma, D., Arora, S., Singh, J. & Layek, B. A review of the tortuous path of nonviral gene delivery and recent progress. *Int. J. Biol. Macromol.* **183**, 2055–2073 (2021).
136. Chen, W. *et al.* Functionalizing titanium surface with PAMAM dendrimer and human BMP2 gene via layer-by-layer assembly for enhanced osteogenesis. *J. Biomed. Mater. Res. Part A* **106**, 706–717 (2018).
137. Eawsakul, K., Tancharoen, S. & Nasongkla, N. Combination of dip coating of BMP-2 and spray

coating of PLGA on dental implants for osseointegration. *J. Drug Deliv. Sci. Technol.* **61**, 102296 (2021).
138. Evans, C. H. The vicissitudes of gene therapy. *Bone Joint Res.* **8**, 469–471 (2019).
139. Alberts, B. *et al. Essential cell biology*. (Garland Science, 2015).
140. Kormann, M. S. D. D. *et al.* Expression of therapeutic proteins after delivery of chemically modified mRNA in mice. *Nat. Biotechnol.* **29**, 154–157 (2011).
141. Lewis, J. D. & Izaurralde, E. The role of the cap structure in RNA processing and nuclear export. *Eur. J. Biochem.* **247**, 461–469 (1997).
142. Shatkin, A. J. Capping of eucaryotic mRNAs. *Cell* **9**, 645–653 (1976).
143. Burkard, K. T. D. & Butler, J. S. A Nuclear 3′-5′ Exonuclease Involved in mRNA Degradation Interacts with Poly(A) Polymerase and the hnRNA Protein Npl3p. *Mol. Cell. Biol.* **20**, 604–616 (2000).
144. Barrett, L. W., Fletcher, S. & Wilton, S. D. Untranslated Gene Regions and Other Non-coding Elements. in 1–56 (2013). doi:10.1007/978-3-0348-0679-4_1
145. Heine, A., Juranek, S. & Brossart, P. Clinical and immunological effects of mRNA vaccines in malignant diseases. *Mol. Cancer* **20**, 52 (2021).
146. Balmayor, E. R. Synthetic mRNA – emerging new class of drug for tissue regeneration. *Current Opinion in Biotechnology* **74**, 8–14 (2022).
147. Wikipedia. The structure of a mature eukaryotic mRNA. A fully processed mRNA includes a 5' cap, 5' UTR, coding region, 3' UTR, and poly(A) tail. Available at: https://en.wikipedia.org/wiki/Messenger_RNA#/media/File:MRNA_structure.svg.
148. Holtkamp, S. *et al.* Modification of antigen-encoding RNA increases stability, translational efficacy, and T-cell stimulatory capacity of dendritic cells. *Blood* **108**, 4009–17 (2006).
149. Schuberth-Wagner, C. *et al.* A Conserved Histidine in the RNA Sensor RIG-I Controls Immune Tolerance to N1-2'O-Methylated Self RNA. *Immunity* **43**, 41–51 (2015).
150. Hornung, V. *et al.* 5′-Triphosphate RNA is the ligand for RIG-I. *Science (80-.).* **314**, 994–997 (2006).
151. Muttach, F., Muthmann, N. & Rentmeister, A. Synthetic mRNA capping. *Beilstein J. Org. Chem.* **13**, 2819–2832 (2017).
152. Karikó, K., Buckstein, M., Ni, H. & Weissman, D. Suppression of RNA recognition by Toll-like receptors: The impact of nucleoside modification and the evolutionary origin of RNA. *Immunity* **23**, 165–175 (2005).
153. Pardi, N., Muramatsu, H., Weissman, D. & Karikó, K. In vitro transcription of long RNA containing modified nucleosides. in *Methods in Molecular Biology* **969**, 29–42 (Humana Press, Totowa, NJ, 2013).
154. RUDOLPH, C. & KORMANN, M. RNA WITH A COMBINATION OF UNMODIFIED AND MODIFIED NUCLEOTIDES FOR PROTEIN EXPRESSION. *WO Patent 2011/012316 A2* 47 (2011).
155. Campillo-Davo, D. *et al.* The Ins and Outs of Messenger RNA Electroporation for Physical Gene Delivery in Immune Cell-Based Therapy. *Pharm. 2021, Vol. 13, Page 396* **13**, 396 (2021).
156. Hashimoto, M. & Takemoto, T. Electroporation enables the efficient mRNA delivery into the mouse zygotes and facilitates CRISPR/Cas9-based genome editing. *Sci. Reports 2015 51* **5**, 1–8 (2015).
157. Qiu, P., Ziegelhoffer, P., Sun, J. & Yang, N. S. Gene gun delivery of mRNA in situ results in efficient transgene expression and genetic immunization. *Gene Ther.* **3**, 262–268 (1996).
158. Kowalski, P. S., Rudra, A., Miao, L. & Anderson, D. G. Delivering the Messenger: Advances

in Technologies for Therapeutic mRNA Delivery. *Mol. Ther.* **27**, 710–728 (2019).
159. Meng, Z. *et al.* A new developing class of gene delivery: messenger RNA-based therapeutics. *Biomater. Sci.* **5**, 2381–2392 (2017).
160. Phua, K. K. L., Leong, K. W. & Nair, S. K. Transfection efficiency and transgene expression kinetics of mRNA delivered in naked and nanoparticle format. *J. Control. Release* **166**, 227–233 (2013).
161. Khorsand, B. *et al.* A Comparative Study of the Bone Regenerative Effect of Chemically Modified RNA Encoding BMP-2 or BMP-9. *AAPS J.* **19**, 438–446 (2017).
162. Elangovan, S. *et al.* Chemically modified RNA activated matrices enhance bone regeneration. *J. Control. Release* **218**, 22–28 (2015).
163. Wadhwa, A., Aljabbari, A., Lokras, A., Foged, C. & Thakur, A. Opportunities and challenges in the delivery of mrna-based vaccines. *Pharmaceutics* **12**, 102 (2020).
164. Markov, O. O. *et al.* Novel cationic liposomes provide highly efficient delivery of DNA and RNA into dendritic cell progenitors and their immature offsets. *J. Control. Release* **160**, 200–10 (2012).
165. Malone, R. W., Felgner, P. L. & Verma, I. M. *Cationic liposome-mediated RNA transfection [cationic lipid vesicies/N-[1-(2,3-dioleyloxy)propyl]-NNN-timethylammonium chloride (DOTMA)/translationj*. *Proc. Natl. Acad. Sci. USA* **86**, (1989).
166. Rejman, J., Tavernier, G., Bavarsad, N., Demeester, J. & De Smedt, S. C. mRNA transfection of cervical carcinoma and mesenchymal stem cells mediated by cationic carriers. *J. Control. Release* **147**, 385–391 (2010).
167. Su, X., Fricke, J., Kavanagh, D. & Irvine, D. J. In vitro and in vivo mRNA delivery using lipid-enveloped pHresponsive polymer nanoparticles The MIT Faculty has made this article openly available . Please share Citation Accessed Citable Link Detailed Terms In vitro and in vivo mRNA delivery using lipid-. *Mol. Pharm.* **8**, 774–787 (2011).
168. Tavernier, G. *et al.* mRNA as gene therapeutic: How to control protein expression. *J. Control. Release* **150**, 238–247 (2011).
169. Zhang, W. *et al.* An Improved, Chemically Modified RNA Encoding BMP-2 Enhances Osteogenesis In Vitro and In Vivo. *Tissue Eng. Part A* **25**, 131–144 (2019).
170. Plank, C. *et al.* Enhancing and targeting nucleic acid delivery by magnetic force. *Expert Opin. Biol. Ther.* **3**, 745–758 (2003).
171. Badieyan, Z. S., Pasewald, T., Mykhaylyk, O., Rudolph, C. & Plank, C. Efficient ex vivo delivery of chemically modified messenger RNA using lipofection and magnetofection. *Biochem. Biophys. Res. Commun.* **482**, 796–801 (2017).
172. De La Vega, R. E. *et al.* Efficient healing of large osseous segmental defects using optimized chemically modified messenger RNA encoding BMP-2. *Sci. Adv.* **8**, eabl6242 (2022).
173. Xing, H. *et al.* Hierarchical assembly of nanostructured coating for siRNA-based dual therapy of bone regeneration and revascularization. *Biomaterials* **235**, 119784 (2020).
174. Grudzien-Nogalska, E. *et al.* Synthesis of Anti-Reverse Cap Analogs (ARCAs) and their Applications in mRNA Translation and Stability. *Methods in Enzymology* **431**, 203–227 (2007).
175. Jesorka, A. & Orwar, O. Liposomes: Technologies and Analytical Applications. *Annu. Rev. Anal. Chem.* **1**, 801–832 (2008).
176. Kuete, V., Karaosmanoğlu, O. & Sivas, H. Anticancer Activities of African Medicinal Spices and Vegetables. *Med. Spices Veg. from Africa Ther. Potential Against Metab. Inflammatory, Infect. Syst. Dis.* 271–297 (2017). doi:10.1016/B978-0-12-809286-6.00010-8
177. Katagiri, T. *et al.* Bone morphogenetic protein-2 converts the differentiation pathway of C2C12

myoblasts into the osteoblast lineage. *J. Cell Biol.* **127**, 1755–1766 (1994).
178. Saito, M. *et al.* Differentiation potential of osteoblast from cultured C2C12 cells on zirconia disk. *Dent. Mater. J.* **33**, 275–83 (2014).
179. Katagiri, T. Bone morphogenetic protein-2 converts the differentiation pathway of C2C12 myoblasts into the osteoblast lineage [published erratum appears in J Cell Biol 1995 Feb;128(4):following 713]. *J. Cell Biol.* **127**, 1755–1766 (1994).
180. Kopp, C. D. Branemark Osseointegration. *Dent. Clin. North Am.* **33**, 701–731 (1989).
181. Woo, E. J. Adverse Events Reported After the Use of Recombinant Human Bone Morphogenetic Protein 2. *J. Oral Maxillofac. Surg.* **70**, 765–767 (2012).
182. Lin, G.-H., Lim, G., Chan, H.-L., Giannobile, W. V. & Wang, H.-L. Recombinant human bone morphogenetic protein 2 outcomes for maxillary sinus floor augmentation: a systematic review and meta-analysis. *Clin. Oral Implants Res.* **27**, 1349–1359 (2016).
183. Youn, H. & Chung, J.-K. Modified mRNA as an alternative to plasmid DNA (pDNA) for transcript replacement and vaccination therapy. *Expert Opin. Biol. Ther.* **15**, 1337–1348 (2015).
184. Weissman, D. mRNA transcript therapy. *Expert Rev. Vaccines* **14**, 265–281 (2015).
185. Scott McIvor, R. Therapeutic Delivery of mRNA: The Medium Is the Message. *Mol. Ther.* **19**, 822–823 (2011).
186. Khorsand, B., Elangovan, S., Hong, L., Kormann, M. S. D. & Salem, A. K. A bioactive collagen membrane that enhances bone regeneration. *J. Biomed. Mater. Res. Part B Appl. Biomater.* **107**, 1824–1832 (2019).
187. Langenbach, F. & Handschel, J. Effects of dexamethasone, ascorbic acid and β-glycerophosphate on the osteogenic differentiation of stem cells in vitro. *Stem Cell Res. Ther.* **4**, 117 (2013).
188. Guan, S. & Rosenecker, J. Nanotechnologies in delivery of mRNA therapeutics using nonviral vector-based delivery systems. *Gene Ther.* **24**, 133–143 (2017).
189. Schott, J. W., Morgan, M., Galla, M. & Schambach, A. Viral and Synthetic RNA Vector Technologies and Applications. *Mol. Ther.* **24**, 1513–1527 (2016).
190. Zou, S., Scarfo, K., Nantz, M. H. & Hecker, J. G. Lipid-mediated delivery of RNA is more efficient than delivery of DNA in non-dividing cells. *Int. J. Pharm.* **389**, 232–243 (2010).
191. Hatakeyama, H. & Harashima, H. PEG dilemma- nucleic acids delivery to cancers by controlling biodistribution and intracellular trafficking. *Drug Deliv. Syst.* **31**, 293–299 (2016).
192. SHI, F. *et al.* Interference of poly(ethylene glycol)–lipid analogues with cationic-lipid-mediated delivery of oligonucleotides; role of lipid exchangeability and non-lamellar transitions. *Biochem. J.* **366**, 333–341 (2002).
193. Kannan, V., Balabathula, P., Thoma, L. A. & Wood, G. C. Effect of sucrose as a lyoprotectant on the integrity of paclitaxel-loaded liposomes during lyophilization. *J. Liposome Res.* **25**, 270–278 (2015).
194. Roy, A., Dutta, R., Kundu, N., Banik, D. & Sarkar, N. A Comparative Study of the Influence of Sugars Sucrose, Trehalose, and Maltose on the Hydration and Diffusion of DMPC Lipid Bilayer at Complete Hydration: Investigation of Structural and Spectroscopic Aspect of Lipid-Sugar Interaction. *Langmuir* **32**, 5124–5134 (2016).
195. Izutsu, K. I., Yomota, C. & Kawanishi, T. Stabilization of liposomes in frozen solutions through control of osmotic flow and internal solution freezing by trehalose. *J. Pharm. Sci.* **100**, 2935–2944 (2011).
196. Brus, C., Kleemann, E., Aigner, A., Czubayko, F. & Kissel, T. Stabilization of oligonucleotide-polyethylenimine complexes by freeze-drying: Physicochemical and biological

characterization. *J. Control. Release* **95**, 119–131 (2004).
197. Molina, M. D. C., Dean Allison, S. & Anchordoquy, T. J. Maintenance of nonviral vector particle size during the freezing step of the lyophilization process is insufficient for preservation of activity: Insight from other structural indicators. *J. Pharm. Sci.* **90**, 1445–1455 (2001).
198. Yadava, P., Gibbs, M., Castro, C. & Hughes, J. A. Effect of lyophilization and freeze-thawing on the stability of siRNA-liposome complexes. *AAPS PharmSciTech* **9**, 335–341 (2008).
199. Li, W., Ishida, T., Okada, Y., Oku, N. & Kiwada, H. Increased Gene Expression by Cationic Liposomes (TFL-3) in Lung Metastases Following Intravenous Injection. *Biol. Pharm. Bull.* **28**, 701–706 (2005).
200. Ma, B., Zhang, S., Jiang, H., Zhao, B. & Lv, H. Lipoplex morphologies and their influences on transfection efficiency in gene delivery. *J. Control. Release* **123**, 184–194 (2007).
201. Kneuer, G. *et al.* The influence of physicochemical parameters on the efficacy of non-viral DNA transfection complexes: A comparative study. *J. Nanosci. Nanotechnol.* **6**, 2776–2782 (2006).
202. Gulati, K. *et al.* Drug-releasing nano-engineered titanium implants: therapeutic efficacy in 3D cell culture model, controlled release and stability. *Mater. Sci. Eng. C* **69**, 831–840 (2016).
203. Jiang, Q.-H. *et al.* Bone response to the multilayer BMP-2 gene coated porous titanium implant surface. *Clin. Oral Implants Res.* **24**, 853–861 (2013).
204. Wu, K. *et al.* MicroRNA Functionalized Microporous Titanium Oxide Surface by Lyophilization with Enhanced Osteogenic Activity. *ACS Appl. Mater. Interfaces* **5**, 2733–2744 (2013).
205. Chen, C., Zhang, S.-M. & Lee, I.-S. Immobilizing bioactive molecules onto titanium implants to improve osseointegration. *Surf. Coatings Technol.* **228**, S312–S317 (2013).
206. da Silva, D. *et al.* Biocompatibility, biodegradation and excretion of polylactic acid (PLA) in medical implants and theranostic systems. *Chem. Eng. J.* **340**, 9–14 (2018).
207. Link, A. *et al.* Development of a Novel Polymer-Based mRNA Coating for Surgical Suture to Enhance Wound Healing. *Coatings* **9**, 374 (2019).
208. Lei, P., Padmashali, R. M. & Andreadis, S. T. Cell-controlled and spatially arrayed gene delivery from fibrin hydrogels. *Biomaterials* **30**, 3790–3799 (2009).
209. Ho, W., Tawil, B., Dunn, J. C. Y. & Wu, B. M. The Behavior of Human Mesenchymal Stem Cells in 3D Fibrin Clots: Dependence on Fibrinogen Concentration and Clot Structure. *Tissue Eng.* **12**, 1587–1595 (2006).
210. Jo, S. & Park, K. Surface modification using silanated poly(ethylene glycol)s. *Biomaterials* **21**, 605–616 (2000).
211. Kulkarni, M., Breen, A., Greiser, U., O'Brien, T. & Pandit, A. Fibrin−Lipoplex System for Controlled Topical Delivery of Multiple Genes. *Biomacromolecules* **10**, 1650–1654 (2009).
212. Janmey, P. A., Winer, J. P. & Weisel, J. W. Fibrin gels and their clinical and bioengineering applications. *J. R. Soc. Interface* **6**, 1–10 (2009).
213. Almeida Varela, H. *et al.* Platelet-rich fibrin to incorporate bioactive graft materials. in *Nanostructured Biomaterials for Cranio-Maxillofacial and Oral Applications* 119–142 (Elsevier, 2018). doi:10.1016/B978-0-12-814621-7.00007-X
214. Oju Jeon, Soo Hyun Ryu, Ji Hyung Chung & Kim, B.-S. Control of basic fibroblast growth factor release from fibrin gel with heparin and concentrations of fibrinogen and thrombin. *J. Control. Release* **105**, 249–259 (2005).
215. Koo, J. *et al.* Control of Anti-Thrombogenic Properties: Surface-Induced Self-Assembly of Fibrinogen Fibers. *Biomacromolecules* **13**, 1259–1268 (2012).
216. Ahmad, E., Fatima, M. T., Hoque, M., Owais, M. & Saleemuddin, M. Fibrin matrices: The

versatile therapeutic delivery systems. *Int. J. Biol. Macromol.* **81**, 121–136 (2015).
217. Horasawa, N., Yamashita, T., Uehara, S. & Udagawa, N. High-performance scaffolds on titanium surfaces: Osteoblast differentiation and mineralization promoted by a globular fibrinogen layer through cell-autonomous BMP signaling. *Mater. Sci. Eng. C* **46**, 86–96 (2015).
218. Gandhi, J. K. *et al.* Human Fibrinogen for Maintenance and Differentiation of Induced Pluripotent Stem Cells in Two Dimensions and Three Dimensions. *Stem Cells Transl. Med.* **8**, 512–521 (2019).
219. Bragdon, B. *et al.* Bone Morphogenetic Proteins: A critical review. *Cell. Signal.* **23**, 609–620 (2011).
220. Feichtinger, G. A. *et al.* Enhanced reporter gene assay for the detection of osteogenic differentiation. *Tissue Eng. Part C. Methods* **17**, 401–410 (2011).
221. Balmayor, E. R., Feichtinger, G. A., Azevedo, H. S., Van Griensven, M. & Reis, R. L. Starch-poly-ε-caprolactone microparticles reduce the needed amount of BMP-2. *Clin. Orthop. Relat. Res.* **467**, 3138–3148 (2009).
222. Liu, X. *et al.* Delivery of antagomiR204-conjugated gold nanoparticles from PLGA sheets and its implication in promoting osseointegration of titanium implant in type 2 diabetes mellitus. *Int. J. Nanomedicine* **Volume 12**, 7089–7101 (2017).
223. Andersson, T., Agholme, F., Aspenberg, P. & Tengvall, P. Surface immobilized zoledronate improves screw fixation in rat bone: A new method for the coating of metal implants. *J. Mater. Sci. Mater. Med.* **21**, 3029–3037 (2010).
224. Jakobsen, T. *et al.* Local delivery of zoledronate from a poly (D,L-lactide)-Coating increases fixation of press-fit implants. *J. Orthop. Res.* **34**, 65–71 (2016).

Chapter 7: Appendices

7.1. Appendix 1: Pilot experiment

7.1.1. Cell density optimization

Pilot Study: cell density optimization
Ordinary one-way ANOVA

ANOVA summary	
F	23.74
P value	0.0002
P value summary	***
Are differences among means statistically significant? (P < 0.05)	Yes
R square	0.8990

Brown-Forsythe test	
F (DFn, DFd)	1.366 (3, 8)
P value	0.3211
P value summary	ns
Significantly different standard deviations? (P < 0.05)	No

ANOVA table	**SS**	**DF**	**MS**	**F (DFn, DFd)**	**P value**
Treatment (between columns)	1.113e+011	3	3.709e+010	F (3, 8) = 23.74	P = 0.0002
Residual (within columns)	1.250e+010	8	1.563e+009		
Total	1.238e+011	11			

Multiple comparisons
Number of families: 1
Number of comparisons per family: 6
Alpha: 0.05

Tukey's multiple comparisons tests	**Mean Diff.**	**95% CI of diff.**	**Significant ?**	**Summary**		
3000 vs. 5000	-6789	-110147 to 96569	No	ns		A-B
3000 vs. 7000	-24510	-127868 to 78848	No	ns		A-C
3000 vs. 10000	-231853	-335211 to -128495	Yes	***		A-D
5000 vs. 7000	-17721	-121079 to 85637	No	ns		B-C
5000 vs. 10000	-225064	-328422 to -121706	Yes	***		B-D
7000 vs. 10000	-207343	-310701 to -103985	Yes	***		C-D

Test details	Mean 1	Mean 2	Mean Diff.	SE of diff.	n1	n2	q	DF
3000 vs. 5000	16521	23310	-6789	32276	3	3	0.2975	8
3000 vs. 7000	16521	41031	-24510	32276	3	3	1.074	8
3000 vs. 10000	16521	248374	-231853	32276	3	3	10.16	8
5000 vs. 7000	23310	41031	-17721	32276	3	3	0.7765	8
5000 vs. 10000	23310	248374	-225064	32276	3	3	9.862	8
7000 vs. 10000	41031	248374	-207343	32276	3	3	9.085	8

7.1.2. Dose/effect relationship (cmRNA concentration optimization)

Pilot Study: cmRNA conc.
Ordinary one-way ANOVA

ANOVA summary	
F	89.89
P value	< 0.0001
P value summary	****
Are differences among means statistically significant? (P < 0.05)	Yes
R square	0.9747

Brown-Forsythe test	
F (DFn, DFd)	0.7929 (6, 14)
P value	0.5905
P value summary	ns
Significantly different standard deviations? (P < 0.05)	No

ANOVA table	SS	DF	MS	F (DFn, DFd)	P value
Treatment (between columns)	1.202e+012	6	2.004e+011	F (6, 14) = 89.89	P < 0.0001
Residual (within columns)	3.121e+010	14	2.230e+009		
Total	1.234e+012	20			

Multiple comparisons
Number of families: 1
Number of comparisons per family: 21
Alpha: 0.05

Tukey's multiple comparisons tests	Mean Diff.	95% CI of diff.	Significant ?	Summary		
500.000 vs. 250.000	409880	278236 to 541524	Yes	****		A-B
500.000 vs. 125.000	647350	515706 to 778994	Yes	****		A-C
500.000 vs. 62.500	660672	529028 to 792316	Yes	****		A-D
500.000 vs. 31.250	681891	550247 to 813535	Yes	****		A-E
500.000 vs. 15.625	691054	559410 to 822698	Yes	****		A-F
500.000 vs. 7.800	692504	560860 to 824148	Yes	****		A-G
250.000 vs. 125.000	237470	105826 to 369114	Yes	***		B-C
250.000 vs. 62.500	250792	119148 to 382436	Yes	***		B-D
250.000 vs. 31.250	272011	140367 to 403655	Yes	****		B-E

250.000 vs. 15.625	281174	149530 to 412818	Yes	****		B-F
250.000 vs. 7.800	282624	150980 to 414268	Yes	****		B-G
125.000 vs. 62.500	13322	-118322 to 144966	No	ns		C-D
125.000 vs. 31.250	34541	-97103 to 166185	No	ns		C-E
125.000 vs. 15.625	43704	-87940 to 175348	No	ns		C-F
125.000 vs. 7.800	45154	-86490 to 176798	No	ns		C-G
62.500 vs. 31.250	21219	-110425 to 152863	No	ns		D-E
62.500 vs. 15.625	30382	-101262 to 162026	No	ns		D-F
62.500 vs. 7.800	31832	-99812 to 163476	No	ns		D-G
31.250 vs. 15.625	9163	-122481 to 140807	No	ns		E-F
31.250 vs. 7.800	10613	-121031 to 142257	No	ns		E-G
15.625 vs. 7.800	1450	-130194 to 133094	No	ns		F-G

Test details	Mean 1	Mean 2	Mean Diff.	SE of diff.	n1	n2	q	DF
500.000 vs. 250.000	701169	291289	409880	38553	3	3	15.04	14
500.000 vs. 125.000	701169	53819	647350	38553	3	3	23.75	14
500.000 vs. 62.500	701169	40497	660672	38553	3	3	24.23	14
500.000 vs. 31.250	701169	19278	681891	38553	3	3	25.01	14
500.000 vs. 15.625	701169	10115	691054	38553	3	3	25.35	14
500.000 vs. 7.800	701169	8665	692504	38553	3	3	25.40	14
250.000 vs. 125.000	291289	53819	237470	38553	3	3	8.711	14
250.000 vs. 62.500	291289	40497	250792	38553	3	3	9.200	14
250.000 vs. 31.250	291289	19278	272011	38553	3	3	9.978	14
250.000 vs. 15.625	291289	10115	281174	38553	3	3	10.31	14
250.000 vs. 7.800	291289	8665	282624	38553	3	3	10.37	14
125.000 vs. 62.500	53819	40497	13322	38553	3	3	0.4887	14
125.000 vs. 31.250	53819	19278	34541	38553	3	3	1.267	14
125.000 vs. 15.625	53819	10115	43704	38553	3	3	1.603	14
125.000 vs. 7.800	53819	8665	45154	38553	3	3	1.656	14
62.500 vs. 31.250	40497	19278	21219	38553	3	3	0.7784	14
62.500 vs. 15.625	40497	10115	30382	38553	3	3	1.114	14
62.500 vs. 7.800	40497	8665	31832	38553	3	3	1.168	14
31.250 vs. 15.625	19278	10115	9163	38553	3	3	0.3361	14
31.250 vs. 7.800	19278	8665	10613	38553	3	3	0.3893	14
15.625 vs. 7.800	10115	8665	1450	38553	3	3	0.05319	14

7.2. Appendix 2: Coating optimization via physical adsorption

7.2.1. Physical adsorption method optimization on 96 well plates

MetLuc lipoplexes drying methods.
Ordinary two-way ANOVA
Alpha: 0.05

Source of Variation	% Of total variation	P value	P value summary	Significant?
Interaction	0.05391	0.9708	ns	No
cmRNA concentration	88.84	< 0.0001	****	Yes
Lipoplexes drying method	0.2187	0.6323	ns	No

ANOVA table	SS	DF	MS	F (DFn, DFd)	P value
Interaction	3.353e+006	2	1.676e+006	F (2, 12) = 0.02971	P = 0.9708
cmRNA concentration	5.526e+009	2	2.763e+009	F (2, 12) = 48.96	P < 0.0001
Lipoplexes drying method	1.360e+007	1	1.360e+007	F (1, 12) = 0.2411	P = 0.6323
Residual	6.771e+008	12	5.642e+007		

Multiple comparisons between all the cmRNA concentrations and all drying methods
Number of families: 1
Number of comparisons per family: 15
Alpha: 0.05

Tukey's multiple comparisons tests	Mean Diff.	95% CI of diff.	Significant ?	Summary
500 ng/well: Dry RT vs. 500 ng/well: Dry\ice	-554.7	-21156 to 20046	No	ns
500 ng/well: Dry RT vs. 250 ng/well: Dry RT	26191	5590 to 46792	Yes	*
500 ng/well: Dry RT vs. 250 ng/well: Dry\ice	24118	3517 to 44719	Yes	*
500 ng/well: Dry RT vs. 125 ng/well: Dry RT	43671	23070 to 64272	Yes	***
500 ng/well: Dry RT vs. 125 ng/well: Dry\ice	41083	20482 to 61684	Yes	***
500 ng/well: Dry\ice vs. 250 ng/well: Dry RT	26745	6144 to 47346	Yes	**
500 ng/well: Dry\ice vs. 250 ng/well: Dry\ice	24673	4072 to 45274	Yes	*
500 ng/well: Dry\ice vs. 125 ng/well: Dry RT	44226	23625 to 64827	Yes	***
500 ng/well: Dry\ice vs. 125 ng/well: Dry\ice	41637	21036 to 62238	Yes	***
250 ng/well: Dry RT vs. 250 ng/well: Dry\ice	-2073	-22674 to 18528	No	ns
250 ng/well: Dry RT vs. 125 ng/well: Dry RT	17480	-3121 to 38081	No	ns
250 ng/well: Dry RT vs. 125 ng/well: Dry\ice	14892	-5709 to 35493	No	ns
250 ng/well: Dry\ice vs. 125 ng/well: Dry RT	19553	-1048 to 40154	No	ns
250 ng/well: Dry\ice vs. 125 ng/well: Dry\ice	16965	-3636 to 37566	No	ns
125 ng/well: Dry RT vs. 125 ng/well: Dry\ice	-2588	-23189 to 18013	No	ns

Test details	Mean 1	Mean 2	Mean Diff.	SE of diff.	N 1	N 2	q	D F
500 ng/well: Dry RT vs. 500 ng/well: Dry\ice	45493	46048	-554.7	6133	3	3	0.127 9	12
500 ng/well: Dry RT vs. 250 ng/well: Dry RT	45493	19303	26191	6133	3	3	6.039	12
500 ng/well: Dry RT vs. 250 ng/well: Dry\ice	45493	21375	24118	6133	3	3	5.561	12
500 ng/well: Dry RT vs. 125 ng/well: Dry RT	45493	1822	43671	6133	3	3	10.07	12
500 ng/well: Dry RT vs. 125 ng/well: Dry\ice	45493	4411	41083	6133	3	3	9.473	12
500 ng/well: Dry\ice vs. 250 ng/well: Dry RT	46048	19303	26745	6133	3	3	6.167	12
500 ng/well: Dry\ice vs. 250 ng/well: Dry\ice	46048	21375	24673	6133	3	3	5.689	12
500 ng/well: Dry\ice vs. 125 ng/well: Dry RT	46048	1822	44226	6133	3	3	10.20	12
500 ng/well: Dry\ice vs. 125 ng/well: Dry\ice	46048	4411	41637	6133	3	3	9.601	12
250 ng/well: Dry RT vs. 250 ng/well: Dry\ice	19303	21375	-2073	6133	3	3	0.477 9	12
250 ng/well: Dry RT vs. 125 ng/well: Dry RT	19303	1822	17480	6133	3	3	4.031	12
250 ng/well: Dry RT vs. 125 ng/well: Dry\ice	19303	4411	14892	6133	3	3	3.434	12
250 ng/well: Dry\ice vs. 125 ng/well: Dry RT	21375	1822	19553	6133	3	3	4.509	12
250 ng/well: Dry\ice vs. 125 ng/well: Dry\ice	21375	4411	16965	6133	3	3	3.912	12
125 ng/well: Dry RT vs. 125 ng/well: Dry\ice	1822	4411	-2588	6133	3	3	0.596 8	12

7.2.2. Coating via physical adsorption on Ti discs (MetLuc-Ti)

MetLuc coated Ti discs: MetLuc translation kinetics over time.
Two-way RM ANOVA
Matching: Stacked
Alpha: 0.05

Source of Variation	% Of total variation	P value	P value summary	Significant?
Interaction	15.25	0.0118	*	Yes
Time	42.84	< 0.0001	****	Yes
Column Factor	13.95	0.0245	*	Yes
Subjects (matching)	5.479	0.0576	ns	No

ANOVA table	SS	DF	MS	F (DFn, DFd)	P value
Interaction	7.671e+009	18	4.262e+008	F (18, 42) = 2.340	P = 0.0118
Time	2.154e+010	6	3.591e+009	F (6, 42) = 19.71	P < 0.0001

Column Factor	7.014e+009	3	2.338e+009	F (3, 7) = 5.938	P = 0.0245
Subjects (matching)	2.756e+009	7	3.937e+008	F (7, 42) = 2.161	P = 0.0576
Residual	7.650e+009	42	1.821e+008		

Multiple comparisons of different cmRNA concentrations within each timepoint

Number of families: 7
Number of comparisons per family: 6
Alpha: 0.05

Tukey's multiple comparisons test	Mean Diff.	95% CI of diff.	Significant?	Summary
1				
500 ng/well vs. 250 ng/well	47728	16085 to 79371	Yes	**
500 ng/well vs. 125 ng/well	62394	30751 to 94037	Yes	****
500 ng/well vs. 62.5 ng/well	88815	53437 to 124193	Yes	****
250 ng/well vs. 125 ng/well	14666	-16977 to 46309	No	ns
250 ng/well vs. 62.5 ng/well	41086	5708 to 76464	Yes	*
125 ng/well vs. 62.5 ng/well	26421	-8957 to 61799	No	ns
2				
500 ng/well vs. 250 ng/well	7179	-24464 to 38822	No	ns
500 ng/well vs. 125 ng/well	22613	-9030 to 54256	No	ns
500 ng/well vs. 62.5 ng/well	34640	-738.1 to 70018	No	ns
250 ng/well vs. 125 ng/well	15434	-16209 to 47077	No	ns
250 ng/well vs. 62.5 ng/well	27461	-7917 to 62839	No	ns
125 ng/well vs. 62.5 ng/well	12027	-23351 to 47405	No	ns
3				
500 ng/well vs. 250 ng/well	8611	-23032 to 40254	No	ns
500 ng/well vs. 125 ng/well	17139	-14504 to 48782	No	ns
500 ng/well vs. 62.5 ng/well	30130	-5248 to 65508	No	ns
250 ng/well vs. 125 ng/well	8528	-23115 to 40171	No	ns
250 ng/well vs. 62.5 ng/well	21518	-13860 to 56896	No	ns
125 ng/well vs. 62.5 ng/well	12991	-22387 to 48369	No	ns
4				
500 ng/well vs. 250 ng/well	3856	-27787 to 35499	No	ns
500 ng/well vs. 125 ng/well	13307	-18336 to 44950	No	ns
500 ng/well vs. 62.5 ng/well	21644	-13734 to 57022	No	ns
250 ng/well vs. 125 ng/well	9450	-22193 to 41093	No	ns
250 ng/well vs. 62.5 ng/well	17787	-17591 to 53166	No	ns
125 ng/well vs. 62.5 ng/well	8337	-27041 to 43715	No	ns
5				
500 ng/well vs. 250 ng/well	4132	-27511 to 35775	No	ns
500 ng/well vs. 125 ng/well	6801	-24842 to 38444	No	ns
500 ng/well vs. 62.5 ng/well	9789	-25589 to 45167	No	ns
250 ng/well vs. 125 ng/well	2669	-28974 to 34312	No	ns
250 ng/well vs. 62.5 ng/well	5657	-29721 to 41035	No	ns
125 ng/well vs. 62.5 ng/well	2988	-32390 to 38366	No	ns
6				
500 ng/well vs. 250 ng/well	339.0	-31304 to 31982	No	ns
500 ng/well vs. 125 ng/well	1443	-30200 to 33086	No	ns
500 ng/well vs. 62.5 ng/well	4013	-31365 to 39391	No	ns

250 ng/well vs. 125 ng/well	1104	-30539 to 32747	No	ns
250 ng/well vs. 62.5 ng/well	3674	-31704 to 39052	No	ns
125 ng/well vs. 62.5 ng/well	2570	-32808 to 37948	No	ns
7				
500 ng/well vs. 250 ng/well	334.3	-31309 to 31977	No	ns
500 ng/well vs. 125 ng/well	1115	-30528 to 32758	No	ns
500 ng/well vs. 62.5 ng/well	1557	-33821 to 36935	No	ns
250 ng/well vs. 125 ng/well	780.3	-30863 to 32423	No	ns
250 ng/well vs. 62.5 ng/well	1222	-34156 to 36600	No	ns
125 ng/well vs. 62.5 ng/well	442.0	-34936 to 35820	No	ns

Test details	Mean 1	Mean 2	Mean Diff.	SE of diff.	N1	N2	q	DF
1								
500 ng/well vs. 250 ng/well	102998	55270	47728	11898	3	3	5.673	49
500 ng/well vs. 125 ng/well	102998	40604	62394	11898	3	3	7.416	49
500 ng/well vs. 62.5 ng/well	102998	14184	88815	13303	3	2	9.442	49
250 ng/well vs. 125 ng/well	55270	40604	14666	11898	3	3	1.743	49
250 ng/well vs. 62.5 ng/well	55270	14184	41086	13303	3	2	4.368	49
125 ng/well vs. 62.5 ng/well	40604	14184	26421	13303	3	2	2.809	49
2								
500 ng/well vs. 250 ng/well	41303	34124	7179	11898	3	3	0.8533	49
500 ng/well vs. 125 ng/well	41303	18690	22613	11898	3	3	2.688	49
500 ng/well vs. 62.5 ng/well	41303	6663	34640	13303	3	2	3.683	49
250 ng/well vs. 125 ng/well	34124	18690	15434	11898	3	3	1.834	49
250 ng/well vs. 62.5 ng/well	34124	6663	27461	13303	3	2	2.919	49
125 ng/well vs. 62.5 ng/well	18690	6663	12027	13303	3	2	1.279	49
3								
500 ng/well vs. 250 ng/well	30765	22154	8611	11898	3	3	1.024	49
500 ng/well vs. 125 ng/well	30765	13626	17139	11898	3	3	2.037	49
500 ng/well vs. 62.5 ng/well	30765	635.3	30130	13303	3	2	3.203	49
250 ng/well vs. 125 ng/well	22154	13626	8528	11898	3	3	1.014	49
250 ng/well vs. 62.5 ng/well	22154	635.3	21518	13303	3	2	2.288	49
125 ng/well vs. 62.5 ng/well	13626	635.3	12991	13303	3	2	1.381	49
4								
500 ng/well vs. 250 ng/well	21804	17948	3856	11898	3	3	0.4584	49
500 ng/well vs. 125 ng/well	21804	8497	13307	11898	3	3	1.582	49
500 ng/well vs. 62.5 ng/well	21804	160.2	21644	13303	3	2	2.301	49
250 ng/well vs. 125 ng/well	17948	8497	9450	11898	3	3	1.123	49
250 ng/well vs. 62.5 ng/well	17948	160.2	17787	13303	3	2	1.891	49
125 ng/well vs. 62.5 ng/well	8497	160.2	8337	13303	3	2	0.8863	49
5								
500 ng/well vs. 250 ng/well	9822	5690	4132	11898	3	3	0.4911	49
500 ng/well vs. 125 ng/well	9822	3021	6801	11898	3	3	0.8083	49
500 ng/well vs. 62.5 ng/well	9822	32.70	9789	13303	3	2	1.041	49
250 ng/well vs. 125 ng/well	5690	3021	2669	11898	3	3	0.3172	49
250 ng/well vs. 62.5 ng/well	5690	32.70	5657	13303	3	2	0.6014	49
125 ng/well vs. 62.5 ng/well	3021	32.70	2988	13303	3	2	0.3176	49
6								

500 ng/well vs. 250 ng/well	4077	3738	339.0	11898	3	3	0.04029	49
500 ng/well vs. 125 ng/well	4077	2633	1443	11898	3	3	0.1716	49
500 ng/well vs. 62.5 ng/well	4077	63.35	4013	13303	3	2	0.4267	49
250 ng/well vs. 125 ng/well	3738	2633	1104	11898	3	3	0.1313	49
250 ng/well vs. 62.5 ng/well	3738	63.35	3674	13303	3	2	0.3906	49
125 ng/well vs. 62.5 ng/well	2633	63.35	2570	13303	3	2	0.2732	49
7								
500 ng/well vs. 250 ng/well	1757	1422	334.3	11898	3	3	0.03974	49
500 ng/well vs. 125 ng/well	1757	642.0	1115	11898	3	3	0.1325	49
500 ng/well vs. 62.5 ng/well	1757	200.0	1557	13303	3	2	0.1655	49
250 ng/well vs. 125 ng/well	1422	642.0	780.3	11898	3	3	0.09275	49
250 ng/well vs. 62.5 ng/well	1422	200.0	1222	13303	3	2	0.1299	49
125 ng/well vs. 62.5 ng/well	642.0	200.0	442.0	13303	3	2	0.04699	49

7.3. Appendix 3: Coating via physical entrapment on Ti discs

7.3.1. PDLLA coating on Ti

MetLuc-PDLLA coated Ti discs: MetLuc translation kinetics over time.
Two-way RM ANOVA
Matching: Stacked
Alpha: 0.05

Source of Variation	% Of total variation	P value	P value summary	Significant?
Interaction	20.52	< 0.0001	****	Yes
Time	50.21	< 0.0001	****	Yes
Column Factor	18.77	< 0.0001	****	Yes
Subjects (matching)	2.333	0.0818	ns	No

ANOVA table	SS	DF	MS	F (DFn, DFd)	P value
Interaction	1.214e+011	30	4.046e+009	F (30, 72) = 6.024	P < 0.0001
Time	2.970e+011	6	4.949e+010	F (6, 72) = 73.69	P < 0.0001
Column Factor	1.110e+011	5	2.220e+010	F (5, 12) = 19.30	P < 0.0001
Subjects (matching)	1.380e+010	12	1.150e+009	F (12, 72) = 1.712	P = 0.0818
Residual	4.836e+010	72	6.716e+008		

Multiple comparisons of the different groups within each timepoint

Number of families: 7
Number of comparisons per family: 15
Alpha: 0.05

Tukey's multiple comparisons test	Mean Diff.	95% CI of diff.	Significant?	Summary
1				
MetLuc-PDLLA 3 vs. MetLuc-PDLLA 2	-76661	-141439 to -11883	Yes	*
MetLuc-PDLLA 3 vs. MetLuc-PDLLA 1	-118581	-183359 to -53803	Yes	****
MetLuc-PDLLA 3 vs. MetLuc-PDLLA 0.5	-174174	-238952 to -109396	Yes	****
MetLuc-PDLLA 3 vs. MetLuc-PDLLA 0.25	-263929	-328707 to -199151	Yes	****
MetLuc-PDLLA 3 vs. MetLuc-Ti	-225159	-289937 to -160381	Yes	****
MetLuc-PDLLA 2 vs. MetLuc-PDLLA 1	-41921	-106699 to 22857	No	ns
MetLuc-PDLLA 2 vs. MetLuc-PDLLA 0.5	-97513	-162291 to -32735	Yes	***
MetLuc-PDLLA 2 vs. MetLuc-PDLLA 0.25	-187268	-252046 to -122490	Yes	****
MetLuc-PDLLA 2 vs. MetLuc-Ti	-148499	-213277 to -83721	Yes	****
MetLuc-PDLLA 1 vs. MetLuc-PDLLA 0.5	-55593	-120371 to 9185	No	ns
MetLuc-PDLLA 1 vs. MetLuc-PDLLA 0.25	-145347	-210125 to -80569	Yes	****
MetLuc-PDLLA 1 vs. MetLuc-Ti	-106578	-171356 to -41800	Yes	****
MetLuc-PDLLA 0.5 vs. MetLuc-PDLLA 0.25	-89755	-154533 to -24977	Yes	**

MetLuc-PDLLA 0.5 vs. MetLuc-Ti	-50985	-115763 to 13793	No	ns
MetLuc-PDLLA 0.25 vs. MetLuc-Ti	38769	-26009 to 103547	No	ns
2				
MetLuc-PDLLA 3 vs. MetLuc-PDLLA 2	-2543	-67321 to 62235	No	ns
MetLuc-PDLLA 3 vs. MetLuc-PDLLA 1	-5265	-70043 to 59513	No	ns
MetLuc-PDLLA 3 vs. MetLuc-PDLLA 0.5	-94841	-159619 to -30063	Yes	***
MetLuc-PDLLA 3 vs. MetLuc-PDLLA 0.25	-111222	-176000 to -46444	Yes	****
MetLuc-PDLLA 3 vs. MetLuc-Ti	-9703	-74481 to 55075	No	ns
MetLuc-PDLLA 2 vs. MetLuc-PDLLA 1	-2722	-67500 to 62056	No	ns
MetLuc-PDLLA 2 vs. MetLuc-PDLLA 0.5	-92297	-157075 to -27519	Yes	**
MetLuc-PDLLA 2 vs. MetLuc-PDLLA 0.25	-108679	-173457 to -43901	Yes	****
MetLuc-PDLLA 2 vs. MetLuc-Ti	-7159	-71937 to 57619	No	ns
MetLuc-PDLLA 1 vs. MetLuc-PDLLA 0.5	-89575	-154353 to -24797	Yes	**
MetLuc-PDLLA 1 vs. MetLuc-PDLLA 0.25	-105957	-170735 to -41179	Yes	***
MetLuc-PDLLA 1 vs. MetLuc-Ti	-4437	-69215 to 60341	No	ns
MetLuc-PDLLA 0.5 vs. MetLuc-PDLLA 0.25	-16381	-81159 to 48397	No	ns
MetLuc-PDLLA 0.5 vs. MetLuc-Ti	85138	20360 to 149916	Yes	**
MetLuc-PDLLA 0.25 vs. MetLuc-Ti	101519	36741 to 166297	Yes	***
3				
MetLuc-PDLLA 3 vs. MetLuc-PDLLA 2	-390.7	-65169 to 64387	No	ns
MetLuc-PDLLA 3 vs. MetLuc-PDLLA 1	-4985	-69763 to 59793	No	ns
MetLuc-PDLLA 3 vs. MetLuc-PDLLA 0.5	-64267	-129045 to 511.4	No	ns
MetLuc-PDLLA 3 vs. MetLuc-PDLLA 0.25	-95203	-159981 to -30425	Yes	***
MetLuc-PDLLA 3 vs. MetLuc-Ti	-86.07	-64864 to 64692	No	ns
MetLuc-PDLLA 2 vs. MetLuc-PDLLA 1	-4594	-69372 to 60184	No	ns
MetLuc-PDLLA 2 vs. MetLuc-PDLLA 0.5	-63876	-128654 to 902.1	No	ns
MetLuc-PDLLA 2 vs. MetLuc-PDLLA 0.25	-94812	-159590 to -30034	Yes	***
MetLuc-PDLLA 2 vs. MetLuc-Ti	304.6	-64473 to 65083	No	ns
MetLuc-PDLLA 1 vs. MetLuc-PDLLA 0.5	-59282	-124060 to 5496	No	ns
MetLuc-PDLLA 1 vs. MetLuc-PDLLA 0.25	-90218	-154996 to -25440	Yes	**
MetLuc-PDLLA 1 vs. MetLuc-Ti	4899	-59879 to 69677	No	ns
MetLuc-PDLLA 0.5 vs. MetLuc-PDLLA 0.25	-30936	-95714 to 33842	No	ns
MetLuc-PDLLA 0.5 vs. MetLuc-Ti	64181	-597.5 to 128959	No	ns
MetLuc-PDLLA 0.25 vs. MetLuc-Ti	95117	30339 to 159895	Yes	***
4				
MetLuc-PDLLA 3 vs. MetLuc-PDLLA 2	4485	-60293 to 69263	No	ns
MetLuc-PDLLA 3 vs. MetLuc-PDLLA 1	-844.7	-65623 to 63933	No	ns
MetLuc-PDLLA 3 vs. MetLuc-PDLLA 0.5	-68312	-133090 to -3534	Yes	*
MetLuc-PDLLA 3 vs. MetLuc-PDLLA 0.25	-72245	-137023 to -7467	Yes	*
MetLuc-PDLLA 3 vs. MetLuc-Ti	-10491	-75269 to 54287	No	ns

MetLuc-PDLLA 2 vs. MetLuc-PDLLA 1	-5330	-70108 to 59448	No	ns
MetLuc-PDLLA 2 vs. MetLuc-PDLLA 0.5	-72797	-137575 to -8019	Yes	*
MetLuc-PDLLA 2 vs. MetLuc-PDLLA 0.25	-76731	-141509 to -11953	Yes	*
MetLuc-PDLLA 2 vs. MetLuc-Ti	-14977	-79755 to 49801	No	ns
MetLuc-PDLLA 1 vs. MetLuc-PDLLA 0.5	-67467	-132245 to -2689	Yes	*
MetLuc-PDLLA 1 vs. MetLuc-PDLLA 0.25	-71401	-136179 to -6623	Yes	*
MetLuc-PDLLA 1 vs. MetLuc-Ti	-9647	-74425 to 55131	No	ns
MetLuc-PDLLA 0.5 vs. MetLuc-PDLLA 0.25	-3933	-68711 to 60845	No	ns
MetLuc-PDLLA 0.5 vs. MetLuc-Ti	57821	-6957 to 122599	No	ns
MetLuc-PDLLA 0.25 vs. MetLuc-Ti	61754	-3024 to 126532	No	ns
5				
MetLuc-PDLLA 3 vs. MetLuc-PDLLA 2	972.0	-63806 to 65750	No	ns
MetLuc-PDLLA 3 vs. MetLuc-PDLLA 1	-7451	-72229 to 57327	No	ns
MetLuc-PDLLA 3 vs. MetLuc-PDLLA 0.5	-18829	-83607 to 45949	No	ns
MetLuc-PDLLA 3 vs. MetLuc-PDLLA 0.25	-35380	-100158 to 29398	No	ns
MetLuc-PDLLA 3 vs. MetLuc-Ti	2600	-62178 to 67378	No	ns
MetLuc-PDLLA 2 vs. MetLuc-PDLLA 1	-8423	-73201 to 56355	No	ns
MetLuc-PDLLA 2 vs. MetLuc-PDLLA 0.5	-19801	-84579 to 44977	No	ns
MetLuc-PDLLA 2 vs. MetLuc-PDLLA 0.25	-36352	-101130 to 28426	No	ns
MetLuc-PDLLA 2 vs. MetLuc-Ti	1628	-63150 to 66406	No	ns
MetLuc-PDLLA 1 vs. MetLuc-PDLLA 0.5	-11379	-76157 to 53399	No	ns
MetLuc-PDLLA 1 vs. MetLuc-PDLLA 0.25	-27929	-92707 to 36849	No	ns
MetLuc-PDLLA 1 vs. MetLuc-Ti	10051	-54727 to 74829	No	ns
MetLuc-PDLLA 0.5 vs. MetLuc-PDLLA 0.25	-16551	-81329 to 48227	No	ns
MetLuc-PDLLA 0.5 vs. MetLuc-Ti	21429	-43349 to 86207	No	ns
MetLuc-PDLLA 0.25 vs. MetLuc-Ti	37980	-26798 to 102758	No	ns
6				
MetLuc-PDLLA 3 vs. MetLuc-PDLLA 2	-2641	-67419 to 62137	No	ns
MetLuc-PDLLA 3 vs. MetLuc-PDLLA 1	-8301	-73079 to 56477	No	ns
MetLuc-PDLLA 3 vs. MetLuc-PDLLA 0.5	-10867	-75645 to 53911	No	ns
MetLuc-PDLLA 3 vs. MetLuc-PDLLA 0.25	-16651	-81429 to 48127	No	ns
MetLuc-PDLLA 3 vs. MetLuc-Ti	3397	-61381 to 68175	No	ns
MetLuc-PDLLA 2 vs. MetLuc-PDLLA 1	-5660	-70438 to 59118	No	ns
MetLuc-PDLLA 2 vs. MetLuc-PDLLA 0.5	-8227	-73005 to 56551	No	ns
MetLuc-PDLLA 2 vs. MetLuc-PDLLA 0.25	-14011	-78789 to 50767	No	ns
MetLuc-PDLLA 2 vs. MetLuc-Ti	6037	-58741 to 70815	No	ns
MetLuc-PDLLA 1 vs. MetLuc-PDLLA 0.5	-2567	-67345 to 62211	No	ns
MetLuc-PDLLA 1 vs. MetLuc-PDLLA 0.25	-8351	-73129 to 56427	No	ns
MetLuc-PDLLA 1 vs. MetLuc-Ti	11697	-53081 to 76475	No	ns

MetLuc-PDLLA 0.5 vs. MetLuc-PDLLA 0.25	-5784	-70562 to 58994	No	ns
MetLuc-PDLLA 0.5 vs. MetLuc-Ti	14264	-50514 to 79042	No	ns
MetLuc-PDLLA 0.25 vs. MetLuc-Ti	20048	-44730 to 84826	No	ns
7				
MetLuc-PDLLA 3 vs. MetLuc-PDLLA 2	-1857	-66635 to 62921	No	ns
MetLuc-PDLLA 3 vs. MetLuc-PDLLA 1	-4351	-69129 to 60427	No	ns
MetLuc-PDLLA 3 vs. MetLuc-PDLLA 0.5	-4519	-69297 to 60259	No	ns
MetLuc-PDLLA 3 vs. MetLuc-PDLLA 0.25	-5253	-70031 to 59525	No	ns
MetLuc-PDLLA 3 vs. MetLuc-Ti	1014	-63764 to 65792	No	ns
MetLuc-PDLLA 2 vs. MetLuc-PDLLA 1	-2495	-67273 to 62283	No	ns
MetLuc-PDLLA 2 vs. MetLuc-PDLLA 0.5	-2663	-67441 to 62115	No	ns
MetLuc-PDLLA 2 vs. MetLuc-PDLLA 0.25	-3396	-68174 to 61382	No	ns
MetLuc-PDLLA 2 vs. MetLuc-Ti	2871	-61907 to 67649	No	ns
MetLuc-PDLLA 1 vs. MetLuc-PDLLA 0.5	-168.0	-64946 to 64610	No	ns
MetLuc-PDLLA 1 vs. MetLuc-PDLLA 0.25	-901.3	-65679 to 63877	No	ns
MetLuc-PDLLA 1 vs. MetLuc-Ti	5365	-59413 to 70143	No	ns
MetLuc-PDLLA 0.5 vs. MetLuc-PDLLA 0.25	-733.3	-65511 to 64045	No	ns
MetLuc-PDLLA 0.5 vs. MetLuc-Ti	5533	-59245 to 70311	No	ns
MetLuc-PDLLA 0.25 vs. MetLuc-Ti	6267	-58511 to 71045	No	ns

Test details	**Mean 1**	**Mean 2**	**Mean Diff.**	**SE of diff.**	**N 1**	**N 2**	**q**	**D F**
1								
MetLuc-PDLLA 3 vs. MetLuc-PDLLA 2	13559	90220	-76661	22211	3	3	4.881	84
MetLuc-PDLLA 3 vs. MetLuc-PDLLA 1	13559	132141	-118581	22211	3	3	7.550	84
MetLuc-PDLLA 3 vs. MetLuc-PDLLA 0.5	13559	187733	-174174	22211	3	3	11.09	84
MetLuc-PDLLA 3 vs. MetLuc-PDLLA 0.25	13559	277488	-263929	22211	3	3	16.81	84
MetLuc-PDLLA 3 vs. MetLuc-Ti	13559	238719	-225159	22211	3	3	14.34	84
MetLuc-PDLLA 2 vs. MetLuc-PDLLA 1	90220	132141	-41921	22211	3	3	2.669	84
MetLuc-PDLLA 2 vs. MetLuc-PDLLA 0.5	90220	187733	-97513	22211	3	3	6.209	84
MetLuc-PDLLA 2 vs. MetLuc-PDLLA 0.25	90220	277488	-187268	22211	3	3	11.92	84
MetLuc-PDLLA 2 vs. MetLuc-Ti	90220	238719	-148499	22211	3	3	9.455	84
MetLuc-PDLLA 1 vs. MetLuc-PDLLA 0.5	132141	187733	-55593	22211	3	3	3.540	84

MetLuc-PDLLA 1 vs. MetLuc-PDLLA 0.25	132141	277488	-145347	22211	3	3	9.255	84
MetLuc-PDLLA 1 vs. MetLuc-Ti	132141	238719	-106578	22211	3	3	6.786	84
MetLuc-PDLLA 0.5 vs. MetLuc-PDLLA 0.25	187733	277488	-89755	22211	3	3	5.715	84
MetLuc-PDLLA 0.5 vs. MetLuc-Ti	187733	238719	-50985	22211	3	3	3.246	84
MetLuc-PDLLA 0.25 vs. MetLuc-Ti	277488	238719	38769	22211	3	3	2.469	84
2								
MetLuc-PDLLA 3 vs. MetLuc-PDLLA 2	6657	9201	-2543	22211	3	3	0.1619	84
MetLuc-PDLLA 3 vs. MetLuc-PDLLA 1	6657	11923	-5265	22211	3	3	0.3353	84
MetLuc-PDLLA 3 vs. MetLuc-PDLLA 0.5	6657	101498	-94841	22211	3	3	6.039	84
MetLuc-PDLLA 3 vs. MetLuc-PDLLA 0.25	6657	117879	-111222	22211	3	3	7.082	84
MetLuc-PDLLA 3 vs. MetLuc-Ti	6657	16360	-9703	22211	3	3	0.6178	84
MetLuc-PDLLA 2 vs. MetLuc-PDLLA 1	9201	11923	-2722	22211	3	3	0.1733	84
MetLuc-PDLLA 2 vs. MetLuc-PDLLA 0.5	9201	101498	-92297	22211	3	3	5.877	84
MetLuc-PDLLA 2 vs. MetLuc-PDLLA 0.25	9201	117879	-108679	22211	3	3	6.920	84
MetLuc-PDLLA 2 vs. MetLuc-Ti	9201	16360	-7159	22211	3	3	0.4559	84
MetLuc-PDLLA 1 vs. MetLuc-PDLLA 0.5	11923	101498	-89575	22211	3	3	5.704	84
MetLuc-PDLLA 1 vs. MetLuc-PDLLA 0.25	11923	117879	-105957	22211	3	3	6.747	84
MetLuc-PDLLA 1 vs. MetLuc-Ti	11923	16360	-4437	22211	3	3	0.2825	84
MetLuc-PDLLA 0.5 vs. MetLuc-PDLLA 0.25	101498	117879	-16381	22211	3	3	1.043	84
MetLuc-PDLLA 0.5 vs. MetLuc-Ti	101498	16360	85138	22211	3	3	5.421	84
MetLuc-PDLLA 0.25 vs. MetLuc-Ti	117879	16360	101519	22211	3	3	6.464	84
3								
MetLuc-PDLLA 3 vs. MetLuc-PDLLA 2	7345	7736	-390.7	22211	3	3	0.02487	84
MetLuc-PDLLA 3 vs. MetLuc-PDLLA 1	7345	12330	-4985	22211	3	3	0.3174	84
MetLuc-PDLLA 3 vs. MetLuc-PDLLA 0.5	7345	71612	-64267	22211	3	3	4.092	84
MetLuc-PDLLA 3 vs. MetLuc-PDLLA 0.25	7345	102548	-95203	22211	3	3	6.062	84
MetLuc-PDLLA 3 vs. MetLuc-Ti	7345	7431	-86.07	22211	3	3	0.005480	84

MetLuc-PDLLA 2 vs. MetLuc-PDLLA 1	7736	12330	-4594	22211	3	3	0.2925	84
MetLuc-PDLLA 2 vs. MetLuc-PDLLA 0.5	7736	71612	-63876	22211	3	3	4.067	84
MetLuc-PDLLA 2 vs. MetLuc-PDLLA 0.25	7736	102548	-94812	22211	3	3	6.037	84
MetLuc-PDLLA 2 vs. MetLuc-Ti	7736	7431	304.6	22211	3	3	0.01939	84
MetLuc-PDLLA 1 vs. MetLuc-PDLLA 0.5	12330	71612	-59282	22211	3	3	3.775	84
MetLuc-PDLLA 1 vs. MetLuc-PDLLA 0.25	12330	102548	-90218	22211	3	3	5.744	84
MetLuc-PDLLA 1 vs. MetLuc-Ti	12330	7431	4899	22211	3	3	0.3119	84
MetLuc-PDLLA 0.5 vs. MetLuc-PDLLA 0.25	71612	102548	-30936	22211	3	3	1.970	84
MetLuc-PDLLA 0.5 vs. MetLuc-Ti	71612	7431	64181	22211	3	3	4.087	84
MetLuc-PDLLA 0.25 vs. MetLuc-Ti	102548	7431	95117	22211	3	3	6.056	84
4								
MetLuc-PDLLA 3 vs. MetLuc-PDLLA 2	7901	3415	4485	22211	3	3	0.2856	84
MetLuc-PDLLA 3 vs. MetLuc-PDLLA 1	7901	8745	-844.7	22211	3	3	0.05378	84
MetLuc-PDLLA 3 vs. MetLuc-PDLLA 0.5	7901	76213	-68312	22211	3	3	4.350	84
MetLuc-PDLLA 3 vs. MetLuc-PDLLA 0.25	7901	80146	-72245	22211	3	3	4.600	84
MetLuc-PDLLA 3 vs. MetLuc-Ti	7901	18392	-10491	22211	3	3	0.6680	84
MetLuc-PDLLA 2 vs. MetLuc-PDLLA 1	3415	8745	-5330	22211	3	3	0.3394	84
MetLuc-PDLLA 2 vs. MetLuc-PDLLA 0.5	3415	76213	-72797	22211	3	3	4.635	84
MetLuc-PDLLA 2 vs. MetLuc-PDLLA 0.25	3415	80146	-76731	22211	3	3	4.886	84
MetLuc-PDLLA 2 vs. MetLuc-Ti	3415	18392	-14977	22211	3	3	0.9536	84
MetLuc-PDLLA 1 vs. MetLuc-PDLLA 0.5	8745	76213	-67467	22211	3	3	4.296	84
MetLuc-PDLLA 1 vs. MetLuc-PDLLA 0.25	8745	80146	-71401	22211	3	3	4.546	84
MetLuc-PDLLA 1 vs. MetLuc-Ti	8745	18392	-9647	22211	3	3	0.6142	84
MetLuc-PDLLA 0.5 vs. MetLuc-PDLLA 0.25	76213	80146	-3933	22211	3	3	0.2504	84
MetLuc-PDLLA 0.5 vs. MetLuc-Ti	76213	18392	57821	22211	3	3	3.682	84
MetLuc-PDLLA 0.25 vs. MetLuc-Ti	80146	18392	61754	22211	3	3	3.932	84
5								
MetLuc-PDLLA 3 vs. MetLuc-PDLLA 2	3916	2944	972.0	22211	3	3	0.06189	84
MetLuc-PDLLA 3 vs. MetLuc-PDLLA 1	3916	11367	-7451	22211	3	3	0.4744	84

MetLuc-PDLLA 3 vs. MetLuc-PDLLA 0.5	3916	22745	-18829	22211	3	3	1.199	84
MetLuc-PDLLA 3 vs. MetLuc-PDLLA 0.25	3916	39296	-35380	22211	3	3	2.253	84
MetLuc-PDLLA 3 vs. MetLuc-Ti	3916	1316	2600	22211	3	3	0.1655	84
MetLuc-PDLLA 2 vs. MetLuc-PDLLA 1	2944	11367	-8423	22211	3	3	0.5363	84
MetLuc-PDLLA 2 vs. MetLuc-PDLLA 0.5	2944	22745	-19801	22211	3	3	1.261	84
MetLuc-PDLLA 2 vs. MetLuc-PDLLA 0.25	2944	39296	-36352	22211	3	3	2.315	84
MetLuc-PDLLA 2 vs. MetLuc-Ti	2944	1316	1628	22211	3	3	0.1037	84
MetLuc-PDLLA 1 vs. MetLuc-PDLLA 0.5	11367	22745	-11379	22211	3	3	0.7245	84
MetLuc-PDLLA 1 vs. MetLuc-PDLLA 0.25	11367	39296	-27929	22211	3	3	1.778	84
MetLuc-PDLLA 1 vs. MetLuc-Ti	11367	1316	10051	22211	3	3	0.6400	84
MetLuc-PDLLA 0.5 vs. MetLuc-PDLLA 0.25	22745	39296	-16551	22211	3	3	1.054	84
MetLuc-PDLLA 0.5 vs. MetLuc-Ti	22745	1316	21429	22211	3	3	1.364	84
MetLuc-PDLLA 0.25 vs. MetLuc-Ti	39296	1316	37980	22211	3	3	2.418	84
6								
MetLuc-PDLLA 3 vs. MetLuc-PDLLA 2	4341	6982	-2641	22211	3	3	0.1681	84
MetLuc-PDLLA 3 vs. MetLuc-PDLLA 1	4341	12642	-8301	22211	3	3	0.5285	84
MetLuc-PDLLA 3 vs. MetLuc-PDLLA 0.5	4341	15209	-10867	22211	3	3	0.6920	84
MetLuc-PDLLA 3 vs. MetLuc-PDLLA 0.25	4341	20993	-16651	22211	3	3	1.060	84
MetLuc-PDLLA 3 vs. MetLuc-Ti	4341	944.7	3397	22211	3	3	0.2163	84
MetLuc-PDLLA 2 vs. MetLuc-PDLLA 1	6982	12642	-5660	22211	3	3	0.3604	84
MetLuc-PDLLA 2 vs. MetLuc-PDLLA 0.5	6982	15209	-8227	22211	3	3	0.5238	84
MetLuc-PDLLA 2 vs. MetLuc-PDLLA 0.25	6982	20993	-14011	22211	3	3	0.8921	84
MetLuc-PDLLA 2 vs. MetLuc-Ti	6982	944.7	6037	22211	3	3	0.3844	84
MetLuc-PDLLA 1 vs. MetLuc-PDLLA 0.5	12642	15209	-2567	22211	3	3	0.1634	84
MetLuc-PDLLA 1 vs. MetLuc-PDLLA 0.25	12642	20993	-8351	22211	3	3	0.5317	84
MetLuc-PDLLA 1 vs. MetLuc-Ti	12642	944.7	11697	22211	3	3	0.7448	84
MetLuc-PDLLA 0.5 vs. MetLuc-PDLLA 0.25	15209	20993	-5784	22211	3	3	0.3683	84
MetLuc-PDLLA 0.5 vs. MetLuc-Ti	15209	944.7	14264	22211	3	3	0.9082	84
MetLuc-PDLLA 0.25 vs. MetLuc-Ti	20993	944.7	20048	22211	3	3	1.277	84
7								

MetLuc-PDLLA 3 vs. MetLuc-PDLLA 2	2211	4067	-1857	22211	3	3	0.1182	84
MetLuc-PDLLA 3 vs. MetLuc-PDLLA 1	2211	6562	-4351	22211	3	3	0.2771	84
MetLuc-PDLLA 3 vs. MetLuc-PDLLA 0.5	2211	6730	-4519	22211	3	3	0.2878	84
MetLuc-PDLLA 3 vs. MetLuc-PDLLA 0.25	2211	7463	-5253	22211	3	3	0.3345	84
MetLuc-PDLLA 3 vs. MetLuc-Ti	2211	1197	1014	22211	3	3	0.06456	84
MetLuc-PDLLA 2 vs. MetLuc-PDLLA 1	4067	6562	-2495	22211	3	3	0.1588	84
MetLuc-PDLLA 2 vs. MetLuc-PDLLA 0.5	4067	6730	-2663	22211	3	3	0.1695	84
MetLuc-PDLLA 2 vs. MetLuc-PDLLA 0.25	4067	7463	-3396	22211	3	3	0.2162	84
MetLuc-PDLLA 2 vs. MetLuc-Ti	4067	1197	2871	22211	3	3	0.1828	84
MetLuc-PDLLA 1 vs. MetLuc-PDLLA 0.5	6562	6730	-168.0	22211	3	3	0.01070	84
MetLuc-PDLLA 1 vs. MetLuc-PDLLA 0.25	6562	7463	-901.3	22211	3	3	0.05739	84
MetLuc-PDLLA 1 vs. MetLuc-Ti	6562	1197	5365	22211	3	3	0.3416	84
MetLuc-PDLLA 0.5 vs. MetLuc-PDLLA 0.25	6730	7463	-733.3	22211	3	3	0.04669	84
MetLuc-PDLLA 0.5 vs. MetLuc-Ti	6730	1197	5533	22211	3	3	0.3523	84
MetLuc-PDLLA 0.25 vs. MetLuc-Ti	7463	1197	6267	22211	3	3	0.3990	84

7.3.2. Fibrin/ogen coating on Ti

7.3.2.1. Optimizing fibrin formulation

Two-way RM ANOVA
Matching: Stacked
Alpha 0.05

Source of Variation	% Of total variation	P value	P value summary	Significant?
Interaction	8.262	0.0538	ns	No
Time	26.67	< 0.0001	****	Yes
thrombin concentrations	6.035	0.0013	**	Yes
Subjects (matching)	8.177	0.0737	ns	No

ANOVA table	SS	DF	MS	F (DFn, DFd)	P value
Interaction	1.330e+012	27	4.926e+010	F (27, 252) = 1.516	P = 0.0538
Time	4.293e+012	9	4.770e+011	F (9, 252) = 14.68	P < 0.0001
thrombin concentrations	9.715e+011	3	3.238e+011	F (3, 28) = 6.888	P = 0.0013
Subjects (matching)	1.316e+012	28	4.701e+010	F (28, 252) = 1.447	P = 0.0737
Residual	8.188e+012	252	3.249e+010		

Multiple comparisons of the different fibrin formulations within each timepoint
Number of families: 10
Number of comparisons per family: 6

Alpha: 0.05

Tukey's multiple comparisons test	Mean Diff.	95% CI of diff.	Significant?	Summary
1				
MetLuc-FT vs. MetLuc-F0.5T	-2655	-240741 to 235431	No	ns
MetLuc-FT vs. MetLuc-F0.25T	-4950	-243036 to 233136	No	ns
MetLuc-FT vs. MetLuc-F	-30359	-268445 to 207727	No	ns
MetLuc-F0.5T vs. MetLuc-F0.25T	-2295	-240381 to 235791	No	ns
MetLuc-F0.5T vs. MetLuc-F	-27704	-265790 to 210382	No	ns
MetLuc-F0.25T vs. MetLuc-F	-25409	-263495 to 212677	No	ns
2				
MetLuc-FT vs. MetLuc-F0.5T	-21096	-259182 to 216991	No	ns
MetLuc-FT vs. MetLuc-F0.25T	-78713	-316799 to 159373	No	ns
MetLuc-FT vs. MetLuc-F	-113016	-351102 to 125070	No	ns
MetLuc-F0.5T vs. MetLuc-F0.25T	-57617	-295703 to 180469	No	ns
MetLuc-F0.5T vs. MetLuc-F	-91920	-330006 to 146166	No	ns
MetLuc-F0.25T vs. MetLuc-F	-34303	-272389 to 203783	No	ns
3				
MetLuc-FT vs. MetLuc-F0.5T	-261348	-499435 to -23262	Yes	*
MetLuc-FT vs. MetLuc-F0.25T	-141065	-379151 to 97022	No	ns
MetLuc-FT vs. MetLuc-F	-134706	-372793 to 103380	No	ns
MetLuc-F0.5T vs. MetLuc-F0.25T	120284	-117802 to 358370	No	ns
MetLuc-F0.5T vs. MetLuc-F	126642	-111444 to 364729	No	ns
MetLuc-F0.25T vs. MetLuc-F	6358	-231728 to 244445	No	ns
4				
MetLuc-FT vs. MetLuc-F0.5T	-25236	-263322 to 212850	No	ns
MetLuc-FT vs. MetLuc-F0.25T	-346174	-584260 to -108088	Yes	**
MetLuc-FT vs. MetLuc-F	-185550	-423636 to 52536	No	ns
MetLuc-F0.5T vs. MetLuc-F0.25T	-320938	-559025 to -82852	Yes	**
MetLuc-F0.5T vs. MetLuc-F	-160314	-398400 to 77772	No	ns
MetLuc-F0.25T vs. MetLuc-F	160624	-77462 to 398711	No	ns
5				
MetLuc-FT vs. MetLuc-F0.5T	-88423	-326509 to 149664	No	ns
MetLuc-FT vs. MetLuc-F0.25T	-114941	-353027 to 123146	No	ns
MetLuc-FT vs. MetLuc-F	-379322	-617408 to -141236	Yes	***
MetLuc-F0.5T vs. MetLuc-F0.25T	-26518	-264604 to 211568	No	ns
MetLuc-F0.5T vs. MetLuc-F	-290899	-528986 to -52813	Yes	**
MetLuc-F0.25T vs. MetLuc-F	-264381	-502468 to -26295	Yes	*
6				
MetLuc-FT vs. MetLuc-F0.5T	-18022	-256108 to 220064	No	ns
MetLuc-FT vs. MetLuc-F0.25T	9904	-228182 to 247990	No	ns
MetLuc-FT vs. MetLuc-F	-174626	-412712 to 63461	No	ns
MetLuc-F0.5T vs. MetLuc-F0.25T	27926	-210160 to 266012	No	ns
MetLuc-F0.5T vs. MetLuc-F	-156604	-394690 to 81483	No	ns
MetLuc-F0.25T vs. MetLuc-F	-184530	-422616 to 53557	No	ns
7				
MetLuc-FT vs. MetLuc-F0.5T	-49201	-287288 to 188885	No	ns
MetLuc-FT vs. MetLuc-F0.25T	-24184	-262270 to 213902	No	ns

MetLuc-FT vs. MetLuc-F	-291108	-529194 to -53021	Yes	**
MetLuc-F0.5T vs. MetLuc-F0.25T	25017	-213069 to 263104	No	ns
MetLuc-F0.5T vs. MetLuc-F	-241907	-479993 to -3820	Yes	*
MetLuc-F0.25T vs. MetLuc-F	-266924	-505010 to -28837	Yes	*
8				
MetLuc-FT vs. MetLuc-F0.5T	-3575	-241661 to 234512	No	ns
MetLuc-FT vs. MetLuc-F0.25T	-26891	-264978 to 211195	No	ns
MetLuc-FT vs. MetLuc-F	-80076	-318163 to 158010	No	ns
MetLuc-F0.5T vs. MetLuc-F0.25T	-23317	-261403 to 214770	No	ns
MetLuc-F0.5T vs. MetLuc-F	-76502	-314588 to 161585	No	ns
MetLuc-F0.25T vs. MetLuc-F	-53185	-291271 to 184901	No	ns
9				
MetLuc-FT vs. MetLuc-F0.5T	18443	-219643 to 256530	No	ns
MetLuc-FT vs. MetLuc-F0.25T	-4408	-242494 to 233679	No	ns
MetLuc-FT vs. MetLuc-F	-64414	-302500 to 173673	No	ns
MetLuc-F0.5T vs. MetLuc-F0.25T	-22851	-260937 to 215235	No	ns
MetLuc-F0.5T vs. MetLuc-F	-82857	-320943 to 155229	No	ns
MetLuc-F0.25T vs. MetLuc-F	-60006	-298092 to 178080	No	ns
10				
MetLuc-FT vs. MetLuc-F0.5T	-3092	-241178 to 234995	No	ns
MetLuc-FT vs. MetLuc-F0.25T	-27419	-265505 to 210668	No	ns
MetLuc-FT vs. MetLuc-F	-60381	-298467 to 177705	No	ns
MetLuc-F0.5T vs. MetLuc-F0.25T	-24327	-262413 to 213759	No	ns
MetLuc-F0.5T vs. MetLuc-F	-57289	-295376 to 180797	No	ns
MetLuc-F0.25T vs. MetLuc-F	-32962	-271049 to 205124	No	ns

Test details	**Mean 1**	**Mean 2**	**Mean Diff.**	**SE of diff.**	**N 1**	**N 2**	**q**	**DF**
1								
MetLuc-FT vs. MetLuc-F0.5T	22531	25186	-2655	92120	8	8	0.04076	280
MetLuc-FT vs. MetLuc-F0.25T	22531	27481	-4950	92120	8	8	0.07599	280
MetLuc-FT vs. MetLuc-F	22531	52890	-30359	92120	8	8	0.4661	280
MetLuc-F0.5T vs. MetLuc-F0.25T	25186	27481	-2295	92120	8	8	0.03523	280
MetLuc-F0.5T vs. MetLuc-F	25186	52890	-27704	92120	8	8	0.4253	280
MetLuc-F0.25T vs. MetLuc-F	27481	52890	-25409	92120	8	8	0.3901	280
2								
MetLuc-FT vs. MetLuc-F0.5T	85245	106341	-21096	92120	8	8	0.3239	280
MetLuc-FT vs. MetLuc-F0.25T	85245	163958	-78713	92120	8	8	1.208	280
MetLuc-FT vs. MetLuc-F	85245	198261	-113016	92120	8	8	1.735	280

MetLuc-F0.5T vs. MetLuc-F0.25T	106341	163958	-57617	92120	8	8	0.8845	280
MetLuc-F0.5T vs. MetLuc-F	106341	198261	-91920	92120	8	8	1.411	280
MetLuc-F0.25T vs. MetLuc-F	163958	198261	-34303	92120	8	8	0.5266	280
3								
MetLuc-FT vs. MetLuc-F0.5T	155406	416755	-261348	92120	8	8	4.012	280
MetLuc-FT vs. MetLuc-F0.25T	155406	296471	-141065	92120	8	8	2.166	280
MetLuc-FT vs. MetLuc-F	155406	290113	-134706	92120	8	8	2.068	280
MetLuc-F0.5T vs. MetLuc-F0.25T	416755	296471	120284	92120	8	8	1.847	280
MetLuc-F0.5T vs. MetLuc-F	416755	290113	126642	92120	8	8	1.944	280
MetLuc-F0.25T vs. MetLuc-F	296471	290113	6358	92120	8	8	0.09761	280
4								
MetLuc-FT vs. MetLuc-F0.5T	229974	255210	-25236	92120	8	8	0.3874	280
MetLuc-FT vs. MetLuc-F0.25T	229974	576148	-346174	92120	8	8	5.314	280
MetLuc-FT vs. MetLuc-F	229974	415524	-185550	92120	8	8	2.849	280
MetLuc-F0.5T vs. MetLuc-F0.25T	255210	576148	-320938	92120	8	8	4.927	280
MetLuc-F0.5T vs. MetLuc-F	255210	415524	-160314	92120	8	8	2.461	280
MetLuc-F0.25T vs. MetLuc-F	576148	415524	160624	92120	8	8	2.466	280
5								
MetLuc-FT vs. MetLuc-F0.5T	177574	265997	-88423	92120	8	8	1.357	280
MetLuc-FT vs. MetLuc-F0.25T	177574	292515	-114941	92120	8	8	1.765	280
MetLuc-FT vs. MetLuc-F	177574	556897	-379322	92120	8	8	5.823	280
MetLuc-F0.5T vs. MetLuc-F0.25T	265997	292515	-26518	92120	8	8	0.4071	280
MetLuc-F0.5T vs. MetLuc-F	265997	556897	-290899	92120	8	8	4.466	280
MetLuc-F0.25T vs. MetLuc-F	292515	556897	-264381	92120	8	8	4.059	280
6								
MetLuc-FT vs. MetLuc-F0.5T	203802	221824	-18022	92120	8	8	0.2767	280

MetLuc-FT vs. MetLuc-F0.25T	203802	193898	9904	92120	8	8	0.1520	280
MetLuc-FT vs. MetLuc-F	203802	378428	-174626	92120	8	8	2.681	280
MetLuc-F0.5T vs. MetLuc-F0.25T	221824	193898	27926	92120	8	8	0.4287	280
MetLuc-F0.5T vs. MetLuc-F	221824	378428	-156604	92120	8	8	2.404	280
MetLuc-F0.25T vs. MetLuc-F	193898	378428	-184530	92120	8	8	2.833	280
7								
MetLuc-FT vs. MetLuc-F0.5T	154384	203585	-49201	92120	8	8	0.7553	280
MetLuc-FT vs. MetLuc-F0.25T	154384	178568	-24184	92120	8	8	0.3713	280
MetLuc-FT vs. MetLuc-F	154384	445492	-291108	92120	8	8	4.469	280
MetLuc-F0.5T vs. MetLuc-F0.25T	203585	178568	25017	92120	8	8	0.3841	280
MetLuc-F0.5T vs. MetLuc-F	203585	445492	-241907	92120	8	8	3.714	280
MetLuc-F0.25T vs. MetLuc-F	178568	445492	-266924	92120	8	8	4.098	280
8								
MetLuc-FT vs. MetLuc-F0.5T	53543	57117	-3575	92120	8	8	0.05488	280
MetLuc-FT vs. MetLuc-F0.25T	53543	80434	-26891	92120	8	8	0.4128	280
MetLuc-FT vs. MetLuc-F	53543	133619	-80076	92120	8	8	1.229	280
MetLuc-F0.5T vs. MetLuc-F0.25T	57117	80434	-23317	92120	8	8	0.3580	280
MetLuc-F0.5T vs. MetLuc-F	57117	133619	-76502	92120	8	8	1.174	280
MetLuc-F0.25T vs. MetLuc-F	80434	133619	-53185	92120	8	8	0.8165	280
9								
MetLuc-FT vs. MetLuc-F0.5T	83565	65122	18443	92120	8	8	0.2831	280
MetLuc-FT vs. MetLuc-F0.25T	83565	87973	-4408	92120	8	8	0.06767	280
MetLuc-FT vs. MetLuc-F	83565	147979	-64414	92120	8	8	0.9889	280
MetLuc-F0.5T vs. MetLuc-F0.25T	65122	87973	-22851	92120	8	8	0.3508	280
MetLuc-F0.5T vs. MetLuc-F	65122	147979	-82857	92120	8	8	1.272	280
MetLuc-F0.25T vs. MetLuc-F	87973	147979	-60006	92120	8	8	0.9212	280

10								
MetLuc-FT vs. MetLuc-F0.5T	27543	30635	-3092	92120	8	8	0.04746	280
MetLuc-FT vs. MetLuc-F0.25T	27543	54962	-27419	92120	8	8	0.4209	280
MetLuc-FT vs. MetLuc-F	27543	87924	-60381	92120	8	8	0.9270	280
MetLuc-F0.5T vs. MetLuc-F0.25T	30635	54962	-24327	92120	8	8	0.3735	280
MetLuc-F0.5T vs. MetLuc-F	30635	87924	-57289	92120	8	8	0.8795	280
MetLuc-F0.25T vs. MetLuc-F	54962	87924	-32962	92120	8	8	0.5060	280

7.3.2.2. Optimizing cmRNA concentration for fibrin coating

a. 500 ng/well MetLuc-F vs MetLuc-FT

Multiple t-test
Statistical significance determined using the Holm-Sidak method, with alpha=5.000%. Each row was analysed individually, without assuming a consistent SD.

days	**Significant?**	**P value**	**Mean1**	**Mean2**	**Difference**	**SE of difference**	**t ratio**	**df**
1	*	1.165708e-008	514102.0	79350.6	434752.0	18545.4	23.4425	8.0
2	*	2.975422e-005	1.508899e+006	403444.0	1.105455e+006	131046.0	8.43565	8.0
3	*	3.051470e-005	2.186257e+006	651521.0	1.534736e+006	182567.0	8.40641	8.0
4	*	1.445777e-005	1.635190e+006	462732.0	1.172458e+006	125959.0	9.30823	8.0
5	*	0.000154549	843594.0	297020.0	546574.0	81720.1	6.68837	8.0
6		0.0426227	205017.0	72506.4	132511.0	55023.1	2.40828	8.0
7	*	0.00020805	454770.0	151245.0	303525.0	47389.7	6.40487	8.0
8		0.346593	0.0	1993.7	-1993.7	1993.7	1.0	8.0
9		0.22418	32422.8	10795.2	21627.7	16416.8	1.31741	8.0
10		0.330486	32577.8	24155.5	8422.28	8129.36	1.03603	8.0

b. 250 ng/well MetLuc-F vs MetLuc-FT

Multiple t-test
Statistical significance determined using the Holm-Sidak method, with alpha=5.000%. Each row was analysed individually, without assuming a consistent SD.

days	Significant?	P value	Mean1	Mean2	Difference	SE of difference	t ratio	df
1	*	0.00435889	403402.0	65749.3	337653.0	85924.6	3.92964	8.0
2	*	0.000687381	982281.0	316931.0	665350.0	124408.0	5.34814	8.0
3	*	0.0013866	1.443981e+006	443240.0	1.000740e+006	209260.0	4.78229	8.0
4	*	3.981874e-006	941407.0	299348.0	642059.0	58052.5	11.06	8.0
5	*	0.000386241	514167.0	169262.0	344905.0	59038.2	5.84206	8.0
6	*	0.00105525	144324.0	42903.8	101420.0	20291.5	4.99816	8.0
7	*	0.000263507	290117.0	90959.2	199158.0	32196.5	6.18569	8.0
8		0.346593	0.0	582.1	-582.1	582.1	1.0	8.0
9		0.111481	18869.8	4963.48	13906.3	7775.05	1.78858	8.0
10		0.316525	20174.1	13758.9	6415.18	6004.6	1.06838	8.0

c. 125 ng/well MetLuc-F vs MetLuc-FT

Multiple t-test
Statistical significance determined using the Holm-Sidak method, with alpha=5.000%. Each row was analysed individually, without assuming a consistent SD.

days	Significant?	P value	Mean1	Mean2	Difference	SE of difference	t ratio	df
1	*	0.000638462	165812.0	35135.4	130677.0	24155.3	5.40986	8.0
2	*	0.00937921	365362.0	174473.0	190889.0	56166.2	3.39865	8.0
3	*	0.00128448	495934.0	214591.0	281343.0	58101.9	4.84223	8.0
4	*	0.000717141	297691.0	130485.0	167207.0	31471.8	5.3129	8.0
5	*	3.918600e-006	171141.0	65564.3	105577.0	9525.64	11.0834	8.0
6		0.0180751	42009.5	19619.6	22389.9	7557.59	2.96257	8.0
7	*	9.952460e-005	91808.0	39162.4	52645.6	7389.02	7.12484	8.0
8								
9		0.254463	5371.46	2623.74	2747.72	2238.14	1.22768	8.0
10		0.953227	7698.21	7816.69	-118.481	1957.75	0.0605187	8.0

d. 62.5 ng/well MetLuc-F vs MetLuc-FT

Multiple t-test
Statistical significance determined using the Holm-Sidak method, with alpha=5.000%. Each row was analysed individually, without assuming a consistent SD.

days	Significant?	P value	Mean1	Mean2	Difference	SE of difference	t ratio	df
1		0.0104618	72113.9	17627.8	54486.1	16386.8	3.32501	8.0
2		0.00896452	142585.0	53369.8	89215.0	26015.7	3.42927	8.0
3	*	0.0038859	200213.0	73355.6	126858.0	31622.0	4.01169	8.0
4	*	0.000242911	92422.4	48871.7	43550.7	6956.34	6.26058	8.0
5		0.00963609	49589.7	23301.1	26288.6	7776.78	3.38039	8.0
6		0.834781	9375.54	8633.57	741.967	3443.23	0.215486	8.0
7		0.0332663	25744.6	15172.7	10571.9	4117.88	2.56731	8.0
8		0.315617	0.0	157.8	-157.8	147.405	1.07052	8.0
9		0.282588	2530.58	1215.9	1314.68	1141.23	1.15198	8.0
10		0.18769	2282.23	3743.05	-1460.82	1014.1	1.4405	8.0

e. MetLuc-F cmRNA concentration

Two-way RM ANOVA
Matching: Stacked
Alpha: 0.05

Source of Variation	% Of total variation	P value	P value summary	Significant?
Interaction	25.14	< 0.0001	****	Yes
Time	45.12	< 0.0001	****	Yes
cmRNA conc.	25.32	< 0.0001	****	Yes
Subjects (matching)	1.461	< 0.0001	****	Yes

ANOVA table	SS	DF	MS	F (DFn, DFd)	P value
Interaction	1.426e+013	27	5.283e+011	F (27, 144) = 45.26	P < 0.0001
Time	2.560e+013	9	2.845e+012	F (9, 144) = 243.8	P < 0.0001
cmRNA conc.	1.436e+013	3	4.788e+012	F (3, 16) = 92.40	P < 0.0001
Subjects (matching)	8.291e+011	16	5.182e+010	F (16, 144) = 4.440	P < 0.0001
Residual	1.681e+012	144	1.167e+010		

Multiple comparison of the different groups within each timepoint
Number of families: 10
Number of comparisons per family: 6
Alpha: 0.05

Tukey's multiple comparisons test	Mean Diff.	95% CI of diff.	Significant?	Summary
1				
MetLuc-F (500 ng/well) vs. MetLuc-F (250 ng/well)	110700	-94951 to 316351	No	ns
MetLuc-F (500 ng/well) vs. MetLuc-F (125 ng/well)	348290	142639 to 553941	Yes	***
MetLuc-F (500 ng/well) vs. MetLuc-F (62.5 ng/well)	441988	236337 to 647639	Yes	****
MetLuc-F (250 ng/well) vs. MetLuc-F (125 ng/well)	237590	31939 to 443241	Yes	*

MetLuc-F (250 ng/well) vs. MetLuc-F (62.5 ng/well)	331288	125637 to 536939	Yes	***
MetLuc-F (125 ng/well) vs. MetLuc-F (62.5 ng/well)	93698	-111953 to 299349	No	ns
2				
MetLuc-F (500 ng/well) vs. MetLuc-F (250 ng/well)	526618	320967 to 732269	Yes	****
MetLuc-F (500 ng/well) vs. MetLuc-F (125 ng/well)	1.144e+006	937886 to 1.349e+006	Yes	****
MetLuc-F (500 ng/well) vs. MetLuc-F (62.5 ng/well)	1.366e+006	1.161e+006 to 1.572e+006	Yes	****
MetLuc-F (250 ng/well) vs. MetLuc-F (125 ng/well)	616919	411268 to 822570	Yes	****
MetLuc-F (250 ng/well) vs. MetLuc-F (62.5 ng/well)	839697	634046 to 1.045e+006	Yes	****
MetLuc-F (125 ng/well) vs. MetLuc-F (62.5 ng/well)	222777	17126 to 428428	Yes	*
3				
MetLuc-F (500 ng/well) vs. MetLuc-F (250 ng/well)	742276	536625 to 947927	Yes	****
MetLuc-F (500 ng/well) vs. MetLuc-F (125 ng/well)	1.690e+006	1.485e+006 to 1.896e+006	Yes	****
MetLuc-F (500 ng/well) vs. MetLuc-F (62.5 ng/well)	1.986e+006	1.780e+006 to 2.192e+006	Yes	****
MetLuc-F (250 ng/well) vs. MetLuc-F (125 ng/well)	948046	742395 to 1.154e+006	Yes	****
MetLuc-F (250 ng/well) vs. MetLuc-F (62.5 ng/well)	1.244e+006	1.038e+006 to 1.449e+006	Yes	****
MetLuc-F (125 ng/well) vs. MetLuc-F (62.5 ng/well)	295721	90070 to 501372	Yes	**
4				
MetLuc-F (500 ng/well) vs. MetLuc-F (250 ng/well)	693783	488132 to 899434	Yes	****
MetLuc-F (500 ng/well) vs. MetLuc-F (125 ng/well)	1.337e+006	1.132e+006 to 1.543e+006	Yes	****
MetLuc-F (500 ng/well) vs. MetLuc-F (62.5 ng/well)	1.543e+006	1.337e+006 to 1.748e+006	Yes	****
MetLuc-F (250 ng/well) vs. MetLuc-F (125 ng/well)	643715	438064 to 849366	Yes	****
MetLuc-F (250 ng/well) vs. MetLuc-F (62.5 ng/well)	848984	643333 to 1.055e+006	Yes	****
MetLuc-F (125 ng/well) vs. MetLuc-F (62.5 ng/well)	205269	-381.9 to 410920	No	ns
5				
MetLuc-F (500 ng/well) vs. MetLuc-F (250 ng/well)	329427	123776 to 535078	Yes	***
MetLuc-F (500 ng/well) vs. MetLuc-F (125 ng/well)	672453	466802 to 878104	Yes	****

MetLuc-F (500 ng/well) vs. MetLuc-F (62.5 ng/well)	794004	588353 to 999655	Yes	****
MetLuc-F (250 ng/well) vs. MetLuc-F (125 ng/well)	343026	137375 to 548677	Yes	***
MetLuc-F (250 ng/well) vs. MetLuc-F (62.5 ng/well)	464577	258926 to 670228	Yes	****
MetLuc-F (125 ng/well) vs. MetLuc-F (62.5 ng/well)	121551	-84100 to 327202	No	ns
6				
MetLuc-F (500 ng/well) vs. MetLuc-F (250 ng/well)	60693	-144958 to 266344	No	ns
MetLuc-F (500 ng/well) vs. MetLuc-F (125 ng/well)	163008	-42643 to 368659	No	ns
MetLuc-F (500 ng/well) vs. MetLuc-F (62.5 ng/well)	195642	-10009 to 401293	No	ns
MetLuc-F (250 ng/well) vs. MetLuc-F (125 ng/well)	102314	-103337 to 307965	No	ns
MetLuc-F (250 ng/well) vs. MetLuc-F (62.5 ng/well)	134948	-70703 to 340599	No	ns
MetLuc-F (125 ng/well) vs. MetLuc-F (62.5 ng/well)	32634	-173017 to 238285	No	ns
7				
MetLuc-F (500 ng/well) vs. MetLuc-F (250 ng/well)	164653	-40998 to 370304	No	ns
MetLuc-F (500 ng/well) vs. MetLuc-F (125 ng/well)	362962	157311 to 568613	Yes	****
MetLuc-F (500 ng/well) vs. MetLuc-F (62.5 ng/well)	429025	223374 to 634676	Yes	****
MetLuc-F (250 ng/well) vs. MetLuc-F (125 ng/well)	198309	-7342 to 403960	No	ns
MetLuc-F (250 ng/well) vs. MetLuc-F (62.5 ng/well)	264372	58721 to 470023	Yes	**
MetLuc-F (125 ng/well) vs. MetLuc-F (62.5 ng/well)	66063	-139588 to 271714	No	ns
8				
MetLuc-F (500 ng/well) vs. MetLuc-F (250 ng/well)	0.0	-205651 to 205651	No	ns
MetLuc-F (500 ng/well) vs. MetLuc-F (125 ng/well)	0.0	-205651 to 205651	No	ns
MetLuc-F (500 ng/well) vs. MetLuc-F (62.5 ng/well)	0.0	-205651 to 205651	No	ns
MetLuc-F (250 ng/well) vs. MetLuc-F (125 ng/well)	0.0	-205651 to 205651	No	ns
MetLuc-F (250 ng/well) vs. MetLuc-F (62.5 ng/well)	0.0	-205651 to 205651	No	ns
MetLuc-F (125 ng/well) vs. MetLuc-F (62.5 ng/well)	0.0	-205651 to 205651	No	ns
9				

MetLuc-F (500 ng/well) vs. MetLuc-F (250 ng/well)	13553	-192098 to 219204	No	ns
MetLuc-F (500 ng/well) vs. MetLuc-F (125 ng/well)	27051	-178600 to 232702	No	ns
MetLuc-F (500 ng/well) vs. MetLuc-F (62.5 ng/well)	29892	-175759 to 235543	No	ns
MetLuc-F (250 ng/well) vs. MetLuc-F (125 ng/well)	13498	-192153 to 219149	No	ns
MetLuc-F (250 ng/well) vs. MetLuc-F (62.5 ng/well)	16339	-189312 to 221990	No	ns
MetLuc-F (125 ng/well) vs. MetLuc-F (62.5 ng/well)	2841	-202810 to 208492	No	ns
10				
MetLuc-F (500 ng/well) vs. MetLuc-F (250 ng/well)	12404	-193247 to 218055	No	ns
MetLuc-F (500 ng/well) vs. MetLuc-F (125 ng/well)	24880	-180771 to 230531	No	ns
MetLuc-F (500 ng/well) vs. MetLuc-F (62.5 ng/well)	30296	-175355 to 235947	No	ns
MetLuc-F (250 ng/well) vs. MetLuc-F (125 ng/well)	12476	-193175 to 218127	No	ns
MetLuc-F (250 ng/well) vs. MetLuc-F (62.5 ng/well)	17892	-187759 to 223543	No	ns
MetLuc-F (125 ng/well) vs. MetLuc-F (62.5 ng/well)	5416	-200235 to 211067	No	ns

Test details	**Mean 1**	**Mean 2**	**Mean Diff.**	**SE of diff.**	**N 1**	**N 2**	**q**	**D F**
1								
MetLuc-F (500 ng/well) vs. MetLuc-F (250 ng/well)	514102	403402	110700	79211	5	5	1.976	16 0
MetLuc-F (500 ng/well) vs. MetLuc-F (125 ng/well)	514102	165812	348290	79211	5	5	6.218	16 0
MetLuc-F (500 ng/well) vs. MetLuc-F (62.5 ng/well)	514102	72114	441988	79211	5	5	7.891	16 0
MetLuc-F (250 ng/well) vs. MetLuc-F (125 ng/well)	403402	165812	237590	79211	5	5	4.242	16 0
MetLuc-F (250 ng/well) vs. MetLuc-F (62.5 ng/well)	403402	72114	331288	79211	5	5	5.915	16 0
MetLuc-F (125 ng/well) vs. MetLuc-F (62.5 ng/well)	165812	72114	93698	79211	5	5	1.673	16 0
2								
MetLuc-F (500 ng/well) vs. MetLuc-F (250 ng/well)	1.509e+ 006	982281	526618	79211	5	5	9.402	16 0
MetLuc-F (500 ng/well) vs. MetLuc-F (125 ng/well)	1.509e+ 006	365362	1.144e+ 006	79211	5	5	20.42	16 0
MetLuc-F (500 ng/well) vs. MetLuc-F (62.5 ng/well)	1.509e+ 006	142585	1.366e+ 006	79211	5	5	24.39	16 0

MetLuc-F (250 ng/well) vs. MetLuc-F (125 ng/well)	982281	365362	616919	79211	5	5	11.01	160
MetLuc-F (250 ng/well) vs. MetLuc-F (62.5 ng/well)	982281	142585	839697	79211	5	5	14.99	160
MetLuc-F (125 ng/well) vs. MetLuc-F (62.5 ng/well)	365362	142585	222777	79211	5	5	3.977	160
3								
MetLuc-F (500 ng/well) vs. MetLuc-F (250 ng/well)	2.186e+006	1.444e+006	742276	79211	5	5	13.25	160
MetLuc-F (500 ng/well) vs. MetLuc-F (125 ng/well)	2.186e+006	495934	1.690e+006	79211	5	5	30.18	160
MetLuc-F (500 ng/well) vs. MetLuc-F (62.5 ng/well)	2.186e+006	200213	1.986e+006	79211	5	5	35.46	160
MetLuc-F (250 ng/well) vs. MetLuc-F (125 ng/well)	1.444e+006	495934	948046	79211	5	5	16.93	160
MetLuc-F (250 ng/well) vs. MetLuc-F (62.5 ng/well)	1.444e+006	200213	1.244e+006	79211	5	5	22.21	160
MetLuc-F (125 ng/well) vs. MetLuc-F (62.5 ng/well)	495934	200213	295721	79211	5	5	5.280	160
4								
MetLuc-F (500 ng/well) vs. MetLuc-F (250 ng/well)	1.635e+006	941407	693783	79211	5	5	12.39	160
MetLuc-F (500 ng/well) vs. MetLuc-F (125 ng/well)	1.635e+006	297691	1.337e+006	79211	5	5	23.88	160
MetLuc-F (500 ng/well) vs. MetLuc-F (62.5 ng/well)	1.635e+006	92422	1.543e+006	79211	5	5	27.54	160
MetLuc-F (250 ng/well) vs. MetLuc-F (125 ng/well)	941407	297691	643715	79211	5	5	11.49	160
MetLuc-F (250 ng/well) vs. MetLuc-F (62.5 ng/well)	941407	92422	848984	79211	5	5	15.16	160
MetLuc-F (125 ng/well) vs. MetLuc-F (62.5 ng/well)	297691	92422	205269	79211	5	5	3.665	160
5								
MetLuc-F (500 ng/well) vs. MetLuc-F (250 ng/well)	843594	514167	329427	79211	5	5	5.881	160
MetLuc-F (500 ng/well) vs. MetLuc-F (125 ng/well)	843594	171141	672453	79211	5	5	12.01	160
MetLuc-F (500 ng/well) vs. MetLuc-F (62.5 ng/well)	843594	49590	794004	79211	5	5	14.18	160
MetLuc-F (250 ng/well) vs. MetLuc-F (125 ng/well)	514167	171141	343026	79211	5	5	6.124	160
MetLuc-F (250 ng/well) vs. MetLuc-F (62.5 ng/well)	514167	49590	464577	79211	5	5	8.294	160
MetLuc-F (125 ng/well) vs. MetLuc-F (62.5 ng/well)	171141	49590	121551	79211	5	5	2.170	160
6								
MetLuc-F (500 ng/well) vs. MetLuc-F (250 ng/well)	205017	144324	60693	79211	5	5	1.084	160

MetLuc-F (500 ng/well) vs. MetLuc-F (125 ng/well)	205017	42009	163008	79211	5	5	2.910	160
MetLuc-F (500 ng/well) vs. MetLuc-F (62.5 ng/well)	205017	9376	195642	79211	5	5	3.493	160
MetLuc-F (250 ng/well) vs. MetLuc-F (125 ng/well)	144324	42009	102314	79211	5	5	1.827	160
MetLuc-F (250 ng/well) vs. MetLuc-F (62.5 ng/well)	144324	9376	134948	79211	5	5	2.409	160
MetLuc-F (125 ng/well) vs. MetLuc-F (62.5 ng/well)	42009	9376	32634	79211	5	5	0.5826	160
7								
MetLuc-F (500 ng/well) vs. MetLuc-F (250 ng/well)	454770	290117	164653	79211	5	5	2.940	160
MetLuc-F (500 ng/well) vs. MetLuc-F (125 ng/well)	454770	91808	362962	79211	5	5	6.480	160
MetLuc-F (500 ng/well) vs. MetLuc-F (62.5 ng/well)	454770	25745	429025	79211	5	5	7.660	160
MetLuc-F (250 ng/well) vs. MetLuc-F (125 ng/well)	290117	91808	198309	79211	5	5	3.541	160
MetLuc-F (250 ng/well) vs. MetLuc-F (62.5 ng/well)	290117	25745	264372	79211	5	5	4.720	160
MetLuc-F (125 ng/well) vs. MetLuc-F (62.5 ng/well)	91808	25745	66063	79211	5	5	1.179	160
8								
MetLuc-F (500 ng/well) vs. MetLuc-F (250 ng/well)	0.0	0.0	0.0	79211	5	5	0.0	160
MetLuc-F (500 ng/well) vs. MetLuc-F (125 ng/well)	0.0	0.0	0.0	79211	5	5	0.0	160
MetLuc-F (500 ng/well) vs. MetLuc-F (62.5 ng/well)	0.0	0.0	0.0	79211	5	5	0.0	160
MetLuc-F (250 ng/well) vs. MetLuc-F (125 ng/well)	0.0	0.0	0.0	79211	5	5	0.0	160
MetLuc-F (250 ng/well) vs. MetLuc-F (62.5 ng/well)	0.0	0.0	0.0	79211	5	5	0.0	160
MetLuc-F (125 ng/well) vs. MetLuc-F (62.5 ng/well)	0.0	0.0	0.0	79211	5	5	0.0	160
9								
MetLuc-F (500 ng/well) vs. MetLuc-F (250 ng/well)	32423	18870	13553	79211	5	5	0.2420	160
MetLuc-F (500 ng/well) vs. MetLuc-F (125 ng/well)	32423	5371	27051	79211	5	5	0.4830	160
MetLuc-F (500 ng/well) vs. MetLuc-F (62.5 ng/well)	32423	2531	29892	79211	5	5	0.5337	160
MetLuc-F (250 ng/well) vs. MetLuc-F (125 ng/well)	18870	5371	13498	79211	5	5	0.2410	160
MetLuc-F (250 ng/well) vs. MetLuc-F (62.5 ng/well)	18870	2531	16339	79211	5	5	0.2917	160
MetLuc-F (125 ng/well) vs. MetLuc-F (62.5 ng/well)	5371	2531	2841	79211	5	5	0.05072	160

10								
MetLuc-F (500 ng/well) vs. MetLuc-F (250 ng/well)	32578	20174	12404	79211	5	5	0.2215	160
MetLuc-F (500 ng/well) vs. MetLuc-F (125 ng/well)	32578	7698	24880	79211	5	5	0.4442	160
MetLuc-F (500 ng/well) vs. MetLuc-F (62.5 ng/well)	32578	2282	30296	79211	5	5	0.5409	160
MetLuc-F (250 ng/well) vs. MetLuc-F (125 ng/well)	20174	7698	12476	79211	5	5	0.2227	160
MetLuc-F (250 ng/well) vs. MetLuc-F (62.5 ng/well)	20174	2282	17892	79211	5	5	0.3194	160
MetLuc-F (125 ng/well) vs. MetLuc-F (62.5 ng/well)	7698	2282	5416	79211	5	5	0.09670	160

f. MetLuc-F cmRNA concentration day 3 peak

One-way ANOVA analysis

Repeated measures ANOVA summary	
Assume sphericity?	No
F	45.76
P value	0.0009
P value summary	***
Statistically significant (P < 0.05)?	Yes
Geisser-Greenhouse's epsilon	0.4179
R square	0.9196
Was the matching effective?	
F	0.3054
P value	0.8689
P value summary	ns
Is there significant matching (P < 0.05)?	No
R square	0.008116

ANOVA table	**SS**	**DF**	**MS**	**F (DFn, DFd)**	**P value**
Treatment (between columns)	1.236e+013	3	4.119e+012	F (1.254, 5.015) = 45.76	P = 0.0009
Individual (between rows)	1.100e+011	4	2.749e+010	F (4, 12) = 0.3054	P = 0.8689
Residual (random)	1.080e+012	12	9.002e+010		
Total	1.355e+013	19			

Multiple comparisons
Number of families: 1
Number of comparisons per family: 6
Alpha: 0.05

Tukey's multiple comparisons test	**Mean Diff.**	**95% CI of diff.**	**Significant ?**	**Summary**		
500 vs. 250	742276	-510939 to 1.995e+006	No	ns		A-B
500 vs. 125	1.690e+006	974581 to 2.406e+006	Yes	**		A-C
500 vs. 62.5	1.986e+006	1.389e+006 to 2.583e+006	Yes	***		A-D

250 vs. 125	948046	232446 to 1.664e+006	Yes	*		B-C
250 vs. 62.5	1.244e+006	462812 to 2.025e+006	Yes	*		B-D
125 vs. 62.5	295721	156948 to 434495	Yes	**		C-D

Test details	Mean 1	Mean 2	Mean Diff.	SE of diff.	n1	n2	q	DF
500 vs. 250	2.186e+006	1.444e+006	742276	307851	5	5	3.410	4
500 vs. 125	2.186e+006	495934	1.690e+006	175821	5	5	13.60	4
500 vs. 62.5	2.186e+006	200213	1.986e+006	146632	5	5	19.15	4
250 vs. 125	1.444e+006	495934	948046	175786	5	5	7.627	4
250 vs. 62.5	1.444e+006	200213	1.244e+006	191841	5	5	9.169	4
125 vs. 62.5	495934	200213	295721	34090	5	5	12.27	4

7.3.3. Cell viability

7.3.3.1. Alamar blue test

Alamar blue data were normalized to material control.
Ordinary Two-way ANOVA
Alpha: 0.05

Source of Variation	% Of total variation	P value	P value summary	Significant?
Interaction	21.18	0.3202	ns	No
Time	2.312	0.7553	ns	No
Coating type	14.56	0.0767	ns	No

ANOVA table	SS	DF	MS	F (DFn, DFd)	P value
Interaction	0.6643	9	0.07381	F (9, 32) = 1.215	P = 0.3202
Time	0.07252	3	0.02417	F (3, 32) = 0.3980	P = 0.7553
Coating type	0.4566	3	0.1522	F (3, 32) = 2.506	P = 0.0767
Residual	1.944	32	0.06074		

Multiple comparisons within each timepoint, comparing types of Ti coatings (simple effects within rows)
Number of families: 4
Number of comparisons per family:6

Tukey's multiple comparisons test	Mean Diff.	95% CI of diff.	Significant?	Summary
1				
MetLuc-Ti vs. MetLuc-PDLLA 0.25	-0.3868	-0.9320 to 0.1584	No	ns
MetLuc-Ti vs. MetLuc-FT	0.1247	-0.4205 to 0.6699	No	ns
MetLuc-Ti vs. MetLuc-F	-0.05073	-0.5959 to 0.4945	No	ns
MetLuc-PDLLA 0.25 vs. MetLuc-FT	0.5114	-0.03375 to 1.057	No	ns
MetLuc-PDLLA 0.25 vs. MetLuc-F	0.3360	-0.2091 to 0.8812	No	ns
MetLuc-FT vs. MetLuc-F	-0.1754	-0.7206 to 0.3698	No	ns
3				
MetLuc-Ti vs. MetLuc-PDLLA 0.25	0.01389	-0.5313 to 0.5591	No	ns
MetLuc-Ti vs. MetLuc-FT	0.3563	-0.1889 to 0.9015	No	ns
MetLuc-Ti vs. MetLuc-F	0.1214	-0.4238 to 0.6665	No	ns
MetLuc-PDLLA 0.25 vs. MetLuc-FT	0.3424	-0.2028 to 0.8876	No	ns
MetLuc-PDLLA 0.25 vs. MetLuc-F	0.1075	-0.4377 to 0.6527	No	ns

MetLuc-FT vs. MetLuc-F	-0.2349	-0.7801 to 0.3103	No	ns
7				
MetLuc-Ti vs. MetLuc-PDLLA 0.25	-0.2469	-0.7920 to 0.2983	No	ns
MetLuc-Ti vs. MetLuc-FT	-0.1515	-0.6967 to 0.3937	No	ns
MetLuc-Ti vs. MetLuc-F	-0.09442	-0.6396 to 0.4508	No	ns
MetLuc-PDLLA 0.25 vs. MetLuc-FT	0.09535	-0.4498 to 0.6405	No	ns
MetLuc-PDLLA 0.25 vs. MetLuc-F	0.1524	-0.3927 to 0.6976	No	ns
MetLuc-FT vs. MetLuc-F	0.05709	-0.4881 to 0.6023	No	ns
14				
MetLuc-Ti vs. MetLuc-PDLLA 0.25	-0.3318	-0.8769 to 0.2134	No	ns
MetLuc-Ti vs. MetLuc-FT	-0.3502	-0.8954 to 0.1950	No	ns
MetLuc-Ti vs. MetLuc-F	-0.4558	-1.001 to 0.08937	No	ns
MetLuc-PDLLA 0.25 vs. MetLuc-FT	-0.01846	-0.5637 to 0.5267	No	ns
MetLuc-PDLLA 0.25 vs. MetLuc-F	-0.1241	-0.6693 to 0.4211	No	ns
MetLuc-FT vs. MetLuc-F	-0.1056	-0.6508 to 0.4396	No	ns

Test details	**Mean 1**	**Mean 2**	**Mean Diff.**	**SE of diff.**	**N 1**	**N 2**	**q**	**D F**
1								
MetLuc-Ti vs. MetLuc-PDLLA 0.25	0.5344	0.9211	-0.3868	0.2012	3	3	2.718	32
MetLuc-Ti vs. MetLuc-FT	0.5344	0.4097	0.1247	0.2012	3	3	0.8761	32
MetLuc-Ti vs. MetLuc-F	0.5344	0.5851	-0.05073	0.2012	3	3	0.3566	32
MetLuc-PDLLA 0.25 vs. MetLuc-FT	0.9211	0.4097	0.5114	0.2012	3	3	3.594	32
MetLuc-PDLLA 0.25 vs. MetLuc-F	0.9211	0.5851	0.3360	0.2012	3	3	2.362	32
MetLuc-FT vs. MetLuc-F	0.4097	0.5851	-0.1754	0.2012	3	3	1.233	32
3								
MetLuc-Ti vs. MetLuc-PDLLA 0.25	0.7833	0.7694	0.01389	0.2012	3	3	0.0976 0	32
MetLuc-Ti vs. MetLuc-FT	0.7833	0.4270	0.3563	0.2012	3	3	2.504	32
MetLuc-Ti vs. MetLuc-F	0.7833	0.6620	0.1214	0.2012	3	3	0.8529	32
MetLuc-PDLLA 0.25 vs. MetLuc-FT	0.7694	0.4270	0.3424	0.2012	3	3	2.406	32
MetLuc-PDLLA 0.25 vs. MetLuc-F	0.7694	0.6620	0.1075	0.2012	3	3	0.7553	32
MetLuc-FT vs. MetLuc-F	0.4270	0.6620	-0.2349	0.2012	3	3	1.651	32
7								
MetLuc-Ti vs. MetLuc-PDLLA 0.25	0.4414	0.6883	-0.2469	0.2012	3	3	1.735	32
MetLuc-Ti vs. MetLuc-FT	0.4414	0.5929	-0.1515	0.2012	3	3	1.065	32
MetLuc-Ti vs. MetLuc-F	0.4414	0.5358	-0.09442	0.2012	3	3	0.6636	32
MetLuc-PDLLA 0.25 vs. MetLuc-FT	0.6883	0.5929	0.09535	0.2012	3	3	0.6701	32
MetLuc-PDLLA 0.25 vs. MetLuc-F	0.6883	0.5358	0.1524	0.2012	3	3	1.071	32
MetLuc-FT vs. MetLuc-F	0.5929	0.5358	0.05709	0.2012	3	3	0.4012	32
14								

MetLuc-Ti vs. MetLuc-PDLLA 0.25	0.3721	0.7038	-0.3318	0.2012	3	3	2.332	32
MetLuc-Ti vs. MetLuc-FT	0.3721	0.7223	-0.3502	0.2012	3	3	2.461	32
MetLuc-Ti vs. MetLuc-F	0.3721	0.8279	-0.4558	0.2012	3	3	3.204	32
MetLuc-PDLLA 0.25 vs. MetLuc-FT	0.7038	0.7223	-0.01846	0.2012	3	3	0.1298	32
MetLuc-PDLLA 0.25 vs. MetLuc-F	0.7038	0.8279	-0.1241	0.2012	3	3	0.8719	32
MetLuc-FT vs. MetLuc-F	0.7223	0.8279	-0.1056	0.2012	3	3	0.7422	32

7.3.3.2. Picogreen assay

Picogreen assay data normalized to material control.
Ordinary Two-way ANOVA
Alpha: 0.05

Source of Variation	% Of total variation	P value	P value summary	Significant?
Interaction	32.92	< 0.0001	****	Yes
time	8.078	0.0044	**	Yes
coating type	42.76	< 0.0001	****	Yes

ANOVA table	SS	DF	MS	F (DFn, DFd)	P value
Interaction	1.355	9	0.1505	F (9, 32) = 7.204	P < 0.0001
time	0.3325	3	0.1108	F (3, 32) = 5.304	P = 0.0044
coating type	1.760	3	0.5866	F (3, 32) = 28.08	P < 0.0001
Residual	0.6686	32	0.02089		

Multiple comparisons within each timepoint, compare different coating types (simple effects within rows)
Number of families: 4
Number of comparisons per family: 6

Tukey's multiple comparisons test	Mean Diff.	95% CI of diff.	Significant?	Summary
1				
MetLuc-Ti vs. MetLuc-PDLLA 0.25	-0.06620	-0.3860 to 0.2536	No	ns
MetLuc-Ti vs. MetLuc-FT	-0.7261	-1.046 to -0.4064	Yes	****
MetLuc-Ti vs. MetLuc-F	-0.6827	-1.002 to -0.3629	Yes	****
MetLuc-PDLLA 0.25 vs. MetLuc-FT	-0.6599	-0.9797 to -0.3402	Yes	****
MetLuc-PDLLA 0.25 vs. MetLuc-F	-0.6165	-0.9362 to -0.2967	Yes	****
MetLuc-FT vs. MetLuc-F	0.04347	-0.2763 to 0.3632	No	ns
3				
MetLuc-Ti vs. MetLuc-PDLLA 0.25	-0.2988	-0.6185 to 0.02098	No	ns
MetLuc-Ti vs. MetLuc-FT	-0.5193	-0.8391 to -0.1996	Yes	***
MetLuc-Ti vs. MetLuc-F	-0.6940	-1.014 to -0.3743	Yes	****
MetLuc-PDLLA 0.25 vs. MetLuc-FT	-0.2206	-0.5403 to 0.09921	No	ns
MetLuc-PDLLA 0.25 vs. MetLuc-F	-0.3953	-0.7150 to -0.07549	Yes	*
MetLuc-FT vs. MetLuc-F	-0.1747	-0.4945 to 0.1451	No	ns
7				
MetLuc-Ti vs. MetLuc-PDLLA 0.25	-0.1088	-0.4286 to 0.2109	No	ns
MetLuc-Ti vs. MetLuc-FT	0.04132	-0.2784 to 0.3611	No	ns
MetLuc-Ti vs. MetLuc-F	-0.2716	-0.5913 to 0.04820	No	ns
MetLuc-PDLLA 0.25 vs. MetLuc-FT	0.1501	-0.1696 to 0.4699	No	ns
MetLuc-PDLLA 0.25 vs. MetLuc-F	-0.1627	-0.4825 to 0.1570	No	ns

MetLuc-FT vs. MetLuc-F	-0.3129	-0.6326 to 0.006881	No	ns
14				
MetLuc-Ti vs. MetLuc-PDLLA 0.25	-0.6593	-0.9790 to -0.3395	Yes	****
MetLuc-Ti vs. MetLuc-FT	-0.5556	-0.8754 to -0.2358	Yes	***
MetLuc-Ti vs. MetLuc-F	-0.3196	-0.6393 to 0.0001963	No	ns
MetLuc-PDLLA 0.25 vs. MetLuc-FT	0.1037	-0.2161 to 0.4234	No	ns
MetLuc-PDLLA 0.25 vs. MetLuc-F	0.3397	0.01994 to 0.6595	Yes	*
MetLuc-FT vs. MetLuc-F	0.2360	-0.08373 to 0.5558	No	ns

Test details	**Mean 1**	**Mean 2**	**Mean Diff.**	**SE of diff.**	**N 1**	**N 2**	**q**	**D F**
1								
MetLuc-Ti vs. MetLuc-PDLLA 0.25	0.002584	0.06879	-0.06620	0.1180	3	3	0.7933	32
MetLuc-Ti vs. MetLuc-FT	0.002584	0.7287	-0.7261	0.1180	3	3	8.701	32
MetLuc-Ti vs. MetLuc-F	0.002584	0.6853	-0.6827	0.1180	3	3	8.180	32
MetLuc-PDLLA 0.25 vs. MetLuc-FT	0.06879	0.7287	-0.6599	0.1180	3	3	7.908	32
MetLuc-PDLLA 0.25 vs. MetLuc-F	0.06879	0.6853	-0.6165	0.1180	3	3	7.387	32
MetLuc-FT vs. MetLuc-F	0.7287	0.6853	0.04347	0.1180	3	3	0.5209	32
3								
MetLuc-Ti vs. MetLuc-PDLLA 0.25	0.06506	0.3638	-0.2988	0.1180	3	3	3.580	32
MetLuc-Ti vs. MetLuc-FT	0.06506	0.5844	-0.5193	0.1180	3	3	6.223	32
MetLuc-Ti vs. MetLuc-F	0.06506	0.7591	-0.6940	0.1180	3	3	8.316	32
MetLuc-PDLLA 0.25 vs. MetLuc-FT	0.3638	0.5844	-0.2206	0.1180	3	3	2.643	32
MetLuc-PDLLA 0.25 vs. MetLuc-F	0.3638	0.7591	-0.3953	0.1180	3	3	4.736	32
MetLuc-FT vs. MetLuc-F	0.5844	0.7591	-0.1747	0.1180	3	3	2.093	32
7								
MetLuc-Ti vs. MetLuc-PDLLA 0.25	0.4166	0.5254	-0.1088	0.1180	3	3	1.304	32
MetLuc-Ti vs. MetLuc-FT	0.4166	0.3752	0.04132	0.1180	3	3	0.4952	32
MetLuc-Ti vs. MetLuc-F	0.4166	0.6881	-0.2716	0.1180	3	3	3.254	32
MetLuc-PDLLA 0.25 vs. MetLuc-FT	0.5254	0.3752	0.1501	0.1180	3	3	1.799	32
MetLuc-PDLLA 0.25 vs. MetLuc-F	0.5254	0.6881	-0.1627	0.1180	3	3	1.950	32
MetLuc-FT vs. MetLuc-F	0.3752	0.6881	-0.3129	0.1180	3	3	3.749	32
14								
MetLuc-Ti vs. MetLuc-PDLLA 0.25	0.2151	0.8744	-0.6593	0.1180	3	3	7.900	32
MetLuc-Ti vs. MetLuc-FT	0.2151	0.7707	-0.5556	0.1180	3	3	6.658	32

MetLuc-Ti vs. MetLuc-F	0.2151	0.5347	-0.3196	0.1180	3	3	3.829	32
MetLuc-PDLLA 0.25 vs. MetLuc-FT	0.8744	0.7707	0.1037	0.1180	3	3	1.242	32
MetLuc-PDLLA 0.25 vs. MetLuc-F	0.8744	0.5347	0.3397	0.1180	3	3	4.071	32
MetLuc-FT vs. MetLuc-F	0.7707	0.5347	0.2360	0.1180	3	3	2.828	32

7.3.4. Lipoplexes release

Release of BMP2 cmRNA from fibrin and fibrinogen Ti coatings
Ordinary Two-way ANOVA
Alpha: 0.05

Source of Variation	% Of total variation	P value	P value summary	Significant?
Interaction	32.24	< 0.0001	****	Yes
Time	51.65	< 0.0001	****	Yes
coating type	0.006311	0.8849	ns	No

ANOVA table	SS	DF	MS	F (DFn, DFd)	P value
Interaction	4537	8	567.2	F (8, 54) = 13.51	P < 0.0001
Time	7270	8	908.7	F (8, 54) = 21.64	P < 0.0001
coating type	0.8882	1	0.8882	F (1, 54) = 0.02116	P = 0.8849
Residual	2267	54	41.99		

Multiple comparisons within each timepoint comparing fibrin (FT) vs fibrinogen (F)
Number of families: 1
Number of comparisons per family: 9

Sidak's multiple comparisons test	Mean Diff.	95% CI of diff.	Significant?	Summary
BMP2-F - BMP2-FT				
2 hrs	18.46	5.262 to 31.66	Yes	**
day 1	-5.291	-18.49 to 7.907	No	ns
day 2	-3.687	-16.88 to 9.511	No	ns
day 3	32.37	19.17 to 45.56	Yes	****
day 4	-20.28	-33.48 to -7.085	Yes	***
day 5	-20.67	-33.87 to -7.475	Yes	***
day 6	0.5029	-12.70 to 13.70	No	ns
day 7	0.3531	-12.84 to 13.55	No	ns
Digest	0.2503	-12.95 to 13.45	No	ns

Test details	Mean 1	Mean 2	Mean Diff.	SE of diff.	N1	N2	t	DF
BMP2-F - BMP2-FT								
2 hrs	20.28	1.819	18.46	4.582	4	4	4.029	54
day 1	1.229	6.520	-5.291	4.582	4	4	1.155	54
day 2	0.0	3.687	-3.687	4.582	4	4	0.8046	54
day 3	32.37	0.0	32.37	4.582	4	4	7.064	54
day 4	22.09	42.37	-20.28	4.582	4	4	4.427	54
day 5	5.008	25.68	-20.67	4.582	4	4	4.512	54
day 6	0.5029	0.0	0.5029	4.582	4	4	0.1098	54
day 7	0.6772	0.3241	0.3531	4.582	4	4	0.07707	54
Digest	2.251	2.001	0.2503	4.582	4	4	0.05463	54

7.3.5. BMP2 expression

BMP2 expression measured via ELISA.
Ordinary Two-way ANOVA
Alpha: 0.05

Source of Variation	% Of total variation	P value	P value summary	Significant?
Interaction	26.96	< 0.0001	****	Yes
Time	23.41	< 0.0001	****	Yes
mRNA conc.	38.01	< 0.0001	****	Yes

ANOVA table	SS	DF	MS	F (DFn, DFd)	P value
Interaction	1.212e+006	9	134718	F (9, 32) = 8.254	P < 0.0001
Time	1.053e+006	3	350850	F (3, 32) = 21.50	P < 0.0001
mRNA conc.	1.709e+006	3	569741	F (3, 32) = 34.91	P < 0.0001
Residual	522317	32	16322		

Multiple comparisons within each timepoint, comparing the different coating types and cmRNA concentrations (simple effects within rows)
Number of families: 4
Number of comparisons per family: 6

Tukey's multiple comparisons test	Mean Diff.	95% CI of diff.	Significant?	Summary
1				
BMP2-F (500 ng/well) vs. BMP2-F (250 ng/well)	353.5	70.85 to 636.1	Yes	**
BMP2-F (500 ng/well) vs. BMP2-FT (500 ng/well)	785.0	502.4 to 1068	Yes	****
BMP2-F (500 ng/well) vs. BMP2-FT (250 ng/well)	785.0	502.4 to 1068	Yes	****
BMP2-F (250 ng/well) vs. BMP2-FT (500 ng/well)	431.5	148.9 to 714.1	Yes	**
BMP2-F (250 ng/well) vs. BMP2-FT (250 ng/well)	431.5	148.9 to 714.1	Yes	**
BMP2-FT (500 ng/well) vs. BMP2-FT (250 ng/well)	0.0	-282.6 to 282.6	No	ns
2				
BMP2-F (500 ng/well) vs. BMP2-F (250 ng/well)	414.9	132.3 to 697.5	Yes	**
BMP2-F (500 ng/well) vs. BMP2-FT (500 ng/well)	865.9	583.3 to 1149	Yes	****
BMP2-F (500 ng/well) vs. BMP2-FT (250 ng/well)	865.9	583.3 to 1149	Yes	****
BMP2-F (250 ng/well) vs. BMP2-FT (500 ng/well)	451.0	168.4 to 733.6	Yes	***
BMP2-F (250 ng/well) vs. BMP2-FT (250 ng/well)	451.0	168.4 to 733.6	Yes	***
BMP2-FT (500 ng/well) vs. BMP2-FT (250 ng/well)	0.0	-282.6 to 282.6	No	ns
3				

BMP2-F (500 ng/well) vs. BMP2-F (250 ng/well)	164.3	-118.3 to 447.0	No	ns
BMP2-F (500 ng/well) vs. BMP2-FT (500 ng/well)	173.4	-109.2 to 456.0	No	ns
BMP2-F (500 ng/well) vs. BMP2-FT (250 ng/well)	173.4	-109.2 to 456.0	No	ns
BMP2-F (250 ng/well) vs. BMP2-FT (500 ng/well)	9.062	-273.6 to 291.7	No	ns
BMP2-F (250 ng/well) vs. BMP2-FT (250 ng/well)	9.062	-273.6 to 291.7	No	ns
BMP2-FT (500 ng/well) vs. BMP2-FT (250 ng/well)	0.0	-282.6 to 282.6	No	ns
4				
BMP2-F (500 ng/well) vs. BMP2-F (250 ng/well)	0.0	-282.6 to 282.6	No	ns
BMP2-F (500 ng/well) vs. BMP2-FT (500 ng/well)	0.0	-282.6 to 282.6	No	ns
BMP2-F (500 ng/well) vs. BMP2-FT (250 ng/well)	0.0	-282.6 to 282.6	No	ns
BMP2-F (250 ng/well) vs. BMP2-FT (500 ng/well)	0.0	-282.6 to 282.6	No	ns
BMP2-F (250 ng/well) vs. BMP2-FT (250 ng/well)	0.0	-282.6 to 282.6	No	ns
BMP2-FT (500 ng/well) vs. BMP2-FT (250 ng/well)	0.0	-282.6 to 282.6	No	ns

Test details	**Mean 1**	**Mean 2**	**Mean Diff.**	**SE of diff.**	**N 1**	**N 2**	**q**	**D F**
1								
BMP2-F (500 ng/well) vs. BMP2-F (250 ng/well)	785.0	431.5	353.5	104.3	3	3	4.792	32
BMP2-F (500 ng/well) vs. BMP2-FT (500 ng/well)	785.0	0.0	785.0	104.3	3	3	10.64	32
BMP2-F (500 ng/well) vs. BMP2-FT (250 ng/well)	785.0	0.0	785.0	104.3	3	3	10.64	32
BMP2-F (250 ng/well) vs. BMP2-FT (500 ng/well)	431.5	0.0	431.5	104.3	3	3	5.850	32
BMP2-F (250 ng/well) vs. BMP2-FT (250 ng/well)	431.5	0.0	431.5	104.3	3	3	5.850	32
BMP2-FT (500 ng/well) vs. BMP2-FT (250 ng/well)	0.0	0.0	0.0	104.3	3	3	0.0	32
2								
BMP2-F (500 ng/well) vs. BMP2-F (250 ng/well)	865.9	451.0	414.9	104.3	3	3	5.625	32
BMP2-F (500 ng/well) vs. BMP2-FT (500 ng/well)	865.9	0.0	865.9	104.3	3	3	11.74	32
BMP2-F (500 ng/well) vs. BMP2-FT (250 ng/well)	865.9	0.0	865.9	104.3	3	3	11.74	32

BMP2-F (250 ng/well) vs. BMP2-FT (500 ng/well)	451.0	0.0	451.0	104.3	3	3	6.114	32
BMP2-F (250 ng/well) vs. BMP2-FT (250 ng/well)	451.0	0.0	451.0	104.3	3	3	6.114	32
BMP2-FT (500 ng/well) vs. BMP2-FT (250 ng/well)	0.0	0.0	0.0	104.3	3	3	0.0	32
3								
BMP2-F (500 ng/well) vs. BMP2-F (250 ng/well)	173.4	9.062	164.3	104.3	3	3	2.228	32
BMP2-F (500 ng/well) vs. BMP2-FT (500 ng/well)	173.4	0.0	173.4	104.3	3	3	2.351	32
BMP2-F (500 ng/well) vs. BMP2-FT (250 ng/well)	173.4	0.0	173.4	104.3	3	3	2.351	32
BMP2-F (250 ng/well) vs. BMP2-FT (500 ng/well)	9.062	0.0	9.062	104.3	3	3	0.1228	32
BMP2-F (250 ng/well) vs. BMP2-FT (250 ng/well)	9.062	0.0	9.062	104.3	3	3	0.1228	32
BMP2-FT (500 ng/well) vs. BMP2-FT (250 ng/well)	0.0	0.0	0.0	104.3	3	3	0.0	32
4								
BMP2-F (500 ng/well) vs. BMP2-F (250 ng/well)	0.0	0.0	0.0	104.3	3	3	0.0	32
BMP2-F (500 ng/well) vs. BMP2-FT (500 ng/well)	0.0	0.0	0.0	104.3	3	3	0.0	32
BMP2-F (500 ng/well) vs. BMP2-FT (250 ng/well)	0.0	0.0	0.0	104.3	3	3	0.0	32
BMP2-F (250 ng/well) vs. BMP2-FT (500 ng/well)	0.0	0.0	0.0	104.3	3	3	0.0	32
BMP2-F (250 ng/well) vs. BMP2-FT (250 ng/well)	0.0	0.0	0.0	104.3	3	3	0.0	32
BMP2-FT (500 ng/well) vs. BMP2-FT (250 ng/well)	0.0	0.0	0.0	104.3	3	3	0.0	32

Comparing the different timepoints - effect of time (main row effect)
Number of families: 1
Number of comparisons per family: 6

Tukey's multiple comparisons test	Mean Diff.	95% CI of diff.	Significant?	Summary
1 vs. 2	-25.10	-166.4 to 116.2	No	ns
1 vs. 3	258.5	117.2 to 399.8	Yes	***
1 vs. 4	304.1	162.8 to 445.4	Yes	****
2 vs. 3	283.6	142.3 to 424.9	Yes	****
2 vs. 4	329.2	187.9 to 470.5	Yes	****
3 vs. 4	45.62	-95.70 to 186.9	No	ns

Test details	Mean 1	Mean 2	Mean Diff.	SE of diff.	N1	N2	q	DF
1 vs. 2	304.1	329.2	-25.10	52.16	12	12	0.6806	32
1 vs. 3	304.1	45.62	258.5	52.16	12	12	7.009	32
1 vs. 4	304.1	0.0	304.1	52.16	12	12	8.246	32
2 vs. 3	329.2	45.62	283.6	52.16	12	12	7.690	32
2 vs. 4	329.2	0.0	329.2	52.16	12	12	8.927	32

3 vs. 4	45.62	0.0	45.62	52.16	12	12	1.237	32

7.3.6. Osteogenic activity

7.3.6.1. ALP activity

ALP activity of C2C12 cells seeded on Ti coated with fibrin and fibrinogen loaded with BMP2 lipoplexes.
Ordinary Two-way ANOVA
Alpha 0.05

Source of Variation	% Of total variation	P value	P value summary	Significant?
Interaction	13.98	0.0820	ns	No
Time	1.185	0.3676	ns	No
coating type and cmRNA conc	57.01	< 0.0001	****	Yes

ANOVA table	SS	DF	MS	F (DFn, DFd)	P value
Interaction	37.45	14	2.675	F (14, 48) = 1.722	P = 0.0820
Time	3.174	2	1.587	F (2, 48) = 1.022	P = 0.3676
coating type and cmRNA conc	152.7	7	21.82	F (7, 48) = 14.05	P < 0.0001
Residual	74.54	48	1.553		

Multiple comparisons within each timepoint, comparing the different coating and cmRNA concentrations (simple effects within rows)
Number of families: 3
Number of comparisons per family: 28

Tukey's multiple comparisons test	Mean Diff.	95% CI of diff.	Significant ?	Summary
5				
BMP2-F (500ng/well) vs. BMP2-F (250ng/well)	1.640	-1.584 to 4.863	No	ns
BMP2-F (500ng/well) vs. BMP2-F (125 ng/well)	3.545	0.3214 to 6.769	Yes	*
BMP2-F (500ng/well) vs. BMP2-F (62.5 ng/well)	4.446	1.222 to 7.669	Yes	**
BMP2-F (500ng/well) vs. BMP2-FT (500 ng/well)	3.974	0.7502 to 7.198	Yes	**
BMP2-F (500ng/well) vs. BMP2-FT (250 ng/well)	3.342	0.1187 to 6.566	Yes	*
BMP2-F (500ng/well) vs. BMP2-FT (125 ng/well)	4.237	1.013 to 7.461	Yes	**
BMP2-F (500ng/well) vs. BMP2-FT (62.5 ng/well)	4.437	1.213 to 7.661	Yes	**
BMP2-F (250ng/well) vs. BMP2-F (125 ng/well)	1.905	-1.318 to 5.129	No	ns
BMP2-F (250ng/well) vs. BMP2-F (62.5 ng/well)	2.806	-0.4180 to 6.029	No	ns
BMP2-F (250ng/well) vs. BMP2-FT (500 ng/well)	2.334	-0.8896 to 5.558	No	ns
BMP2-F (250ng/well) vs. BMP2-FT (250 ng/well)	1.703	-1.521 to 4.926	No	ns
BMP2-F (250ng/well) vs. BMP2-FT (125 ng/well)	2.597	-0.6264 to 5.821	No	ns

BMP2-F (250ng/well) vs. BMP2-FT (62.5 ng/well)	2.797	-0.4264 to 6.021	No	ns
BMP2-F (125 ng/well) vs. BMP2-F (62.5 ng/well)	0.9005	-2.323 to 4.124	No	ns
BMP2-F (125 ng/well) vs. BMP2-FT (500 ng/well)	0.4289	-2.795 to 3.653	No	ns
BMP2-F (125 ng/well) vs. BMP2-FT (250 ng/well)	-0.2027	-3.426 to 3.021	No	ns
BMP2-F (125 ng/well) vs. BMP2-FT (125 ng/well)	0.6920	-2.532 to 3.916	No	ns
BMP2-F (125 ng/well) vs. BMP2-FT (62.5 ng/well)	0.8920	-2.332 to 4.116	No	ns
BMP2-F (62.5 ng/well) vs. BMP2-FT (500 ng/well)	-0.4716	-3.695 to 2.752	No	ns
BMP2-F (62.5 ng/well) vs. BMP2-FT (250 ng/well)	-1.103	-4.327 to 2.120	No	ns
BMP2-F (62.5 ng/well) vs. BMP2-FT (125 ng/well)	-0.2084	-3.432 to 3.015	No	ns
BMP2-F (62.5 ng/well) vs. BMP2-FT (62.5 ng/well)	-0.008430	-3.232 to 3.215	No	ns
BMP2-FT (500 ng/well) vs. BMP2-FT (250 ng/well)	-0.6316	-3.855 to 2.592	No	ns
BMP2-FT (500 ng/well) vs. BMP2-FT (125 ng/well)	0.2632	-2.961 to 3.487	No	ns
BMP2-FT (500 ng/well) vs. BMP2-FT (62.5 ng/well)	0.4632	-2.761 to 3.687	No	ns
BMP2-FT (250 ng/well) vs. BMP2-FT (125 ng/well)	0.8947	-2.329 to 4.118	No	ns
BMP2-FT (250 ng/well) vs. BMP2-FT (62.5 ng/well)	1.095	-2.129 to 4.318	No	ns
BMP2-FT (125 ng/well) vs. BMP2-FT (62.5 ng/well)	0.2000	-3.024 to 3.424	No	ns
7				
BMP2-F (500ng/well) vs. BMP2-F (250ng/well)	0.1381	-3.086 to 3.362	No	ns
BMP2-F (500ng/well) vs. BMP2-F (125 ng/well)	4.511	1.287 to 7.734	Yes	**
BMP2-F (500ng/well) vs. BMP2-F (62.5 ng/well)	4.817	1.593 to 8.040	Yes	***
BMP2-F (500ng/well) vs. BMP2-FT (500 ng/well)	5.089	1.865 to 8.312	Yes	***
BMP2-F (500ng/well) vs. BMP2-FT (250 ng/well)	5.070	1.846 to 8.294	Yes	***
BMP2-F (500ng/well) vs. BMP2-FT (125 ng/well)	5.340	2.116 to 8.564	Yes	****
BMP2-F (500ng/well) vs. BMP2-FT (62.5 ng/well)	5.414	2.191 to 8.638	Yes	****
BMP2-F (250ng/well) vs. BMP2-F (125 ng/well)	4.372	1.149 to 7.596	Yes	**
BMP2-F (250ng/well) vs. BMP2-F (62.5 ng/well)	4.679	1.455 to 7.902	Yes	***

BMP2-F (250ng/well) vs. BMP2-FT (500 ng/well)	4.951	1.727 to 8.174	Yes	***
BMP2-F (250ng/well) vs. BMP2-FT (250 ng/well)	4.932	1.708 to 8.156	Yes	***
BMP2-F (250ng/well) vs. BMP2-FT (125 ng/well)	5.202	1.978 to 8.425	Yes	***
BMP2-F (250ng/well) vs. BMP2-FT (62.5 ng/well)	5.276	2.053 to 8.500	Yes	***
BMP2-F (125 ng/well) vs. BMP2-F (62.5 ng/well)	0.3063	-2.917 to 3.530	No	ns
BMP2-F (125 ng/well) vs. BMP2-FT (500 ng/well)	0.5783	-2.645 to 3.802	No	ns
BMP2-F (125 ng/well) vs. BMP2-FT (250 ng/well)	0.5596	-2.664 to 3.783	No	ns
BMP2-F (125 ng/well) vs. BMP2-FT (125 ng/well)	0.8294	-2.394 to 4.053	No	ns
BMP2-F (125 ng/well) vs. BMP2-FT (62.5 ng/well)	0.9038	-2.320 to 4.127	No	ns
BMP2-F (62.5 ng/well) vs. BMP2-FT (500 ng/well)	0.2719	-2.952 to 3.496	No	ns
BMP2-F (62.5 ng/well) vs. BMP2-FT (250 ng/well)	0.2533	-2.970 to 3.477	No	ns
BMP2-F (62.5 ng/well) vs. BMP2-FT (125 ng/well)	0.5231	-2.701 to 3.747	No	ns
BMP2-F (62.5 ng/well) vs. BMP2-FT (62.5 ng/well)	0.5975	-2.626 to 3.821	No	ns
BMP2-FT (500 ng/well) vs. BMP2-FT (250 ng/well)	-0.01860	-3.242 to 3.205	No	ns
BMP2-FT (500 ng/well) vs. BMP2-FT (125 ng/well)	0.2512	-2.972 to 3.475	No	ns
BMP2-FT (500 ng/well) vs. BMP2-FT (62.5 ng/well)	0.3256	-2.898 to 3.549	No	ns
BMP2-FT (250 ng/well) vs. BMP2-FT (125 ng/well)	0.2698	-2.954 to 3.493	No	ns
BMP2-FT (250 ng/well) vs. BMP2-FT (62.5 ng/well)	0.3442	-2.879 to 3.568	No	ns
BMP2-FT (125 ng/well) vs. BMP2-FT (62.5 ng/well)	0.07442	-3.149 to 3.298	No	ns
10				
BMP2-F (500ng/well) vs. BMP2-F (250ng/well)	2.997	-0.2271 to 6.220	No	ns
BMP2-F (500ng/well) vs. BMP2-F (125 ng/well)	2.555	-0.6685 to 5.779	No	ns
BMP2-F (500ng/well) vs. BMP2-F (62.5 ng/well)	3.350	0.1259 to 6.573	Yes	*
BMP2-F (500ng/well) vs. BMP2-FT (500 ng/well)	2.830	-0.3936 to 6.054	No	ns
BMP2-F (500ng/well) vs. BMP2-FT (250 ng/well)	3.284	0.06075 to 6.508	Yes	*

BMP2-F (500ng/well) vs. BMP2-FT (125 ng/well)	3.008	-0.2158 to 6.232	No	ns
BMP2-F (500ng/well) vs. BMP2-FT (62.5 ng/well)	2.682	-0.5417 to 5.906	No	ns
BMP2-F (250ng/well) vs. BMP2-F (125 ng/well)	-0.4413	-3.665 to 2.782	No	ns
BMP2-F (250ng/well) vs. BMP2-F (62.5 ng/well)	0.3531	-2.871 to 3.577	No	ns
BMP2-F (250ng/well) vs. BMP2-FT (500 ng/well)	-0.1664	-3.390 to 3.057	No	ns
BMP2-F (250ng/well) vs. BMP2-FT (250 ng/well)	0.2879	-2.936 to 3.512	No	ns
BMP2-F (250ng/well) vs. BMP2-FT (125 ng/well)	0.01136	-3.212 to 3.235	No	ns
BMP2-F (250ng/well) vs. BMP2-FT (62.5 ng/well)	-0.3146	-3.538 to 2.909	No	ns
BMP2-F (125 ng/well) vs. BMP2-F (62.5 ng/well)	0.7944	-2.429 to 4.018	No	ns
BMP2-F (125 ng/well) vs. BMP2-FT (500 ng/well)	0.2749	-2.949 to 3.499	No	ns
BMP2-F (125 ng/well) vs. BMP2-FT (250 ng/well)	0.7292	-2.494 to 3.953	No	ns
BMP2-F (125 ng/well) vs. BMP2-FT (125 ng/well)	0.4527	-2.771 to 3.676	No	ns
BMP2-F (125 ng/well) vs. BMP2-FT (62.5 ng/well)	0.1268	-3.097 to 3.350	No	ns
BMP2-F (62.5 ng/well) vs. BMP2-FT (500 ng/well)	-0.5195	-3.743 to 2.704	No	ns
BMP2-F (62.5 ng/well) vs. BMP2-FT (250 ng/well)	-0.06518	-3.289 to 3.158	No	ns
BMP2-F (62.5 ng/well) vs. BMP2-FT (125 ng/well)	-0.3417	-3.565 to 2.882	No	ns
BMP2-F (62.5 ng/well) vs. BMP2-FT (62.5 ng/well)	-0.6676	-3.891 to 2.556	No	ns
BMP2-FT (500 ng/well) vs. BMP2-FT (250 ng/well)	0.4543	-2.769 to 3.678	No	ns
BMP2-FT (500 ng/well) vs. BMP2-FT (125 ng/well)	0.1778	-3.046 to 3.401	No	ns
BMP2-FT (500 ng/well) vs. BMP2-FT (62.5 ng/well)	-0.1481	-3.372 to 3.076	No	ns
BMP2-FT (250 ng/well) vs. BMP2-FT (125 ng/well)	-0.2765	-3.500 to 2.947	No	ns
BMP2-FT (250 ng/well) vs. BMP2-FT (62.5 ng/well)	-0.6025	-3.826 to 2.621	No	ns
BMP2-FT (125 ng/well) vs. BMP2-FT (62.5 ng/well)	-0.3259	-3.550 to 2.898	No	ns

Test details	**Mean 1**	**Mean 2**	**Mean Diff.**	**SE of diff.**	**N 1**	**N 2**	**q**	**D F**
5								

BMP2-F (500ng/well) vs. BMP2-F (250ng/well)	6.427	4.787	1.640	1.017	3	3	2.279	48
BMP2-F (500ng/well) vs. BMP2-F (125 ng/well)	6.427	2.882	3.545	1.017	3	3	4.927	48
BMP2-F (500ng/well) vs. BMP2-F (62.5 ng/well)	6.427	1.981	4.446	1.017	3	3	6.179	48
BMP2-F (500ng/well) vs. BMP2-FT (500 ng/well)	6.427	2.453	3.974	1.017	3	3	5.523	48
BMP2-F (500ng/well) vs. BMP2-FT (250 ng/well)	6.427	3.084	3.342	1.017	3	3	4.646	48
BMP2-F (500ng/well) vs. BMP2-FT (125 ng/well)	6.427	2.189	4.237	1.017	3	3	5.889	48
BMP2-F (500ng/well) vs. BMP2-FT (62.5 ng/well)	6.427	1.989	4.437	1.017	3	3	6.167	48
BMP2-F (250ng/well) vs. BMP2-F (125 ng/well)	4.787	2.882	1.905	1.017	3	3	2.648	48
BMP2-F (250ng/well) vs. BMP2-F (62.5 ng/well)	4.787	1.981	2.806	1.017	3	3	3.900	48
BMP2-F (250ng/well) vs. BMP2-FT (500 ng/well)	4.787	2.453	2.334	1.017	3	3	3.244	48
BMP2-F (250ng/well) vs. BMP2-FT (250 ng/well)	4.787	3.084	1.703	1.017	3	3	2.366	48
BMP2-F (250ng/well) vs. BMP2-FT (125 ng/well)	4.787	2.189	2.597	1.017	3	3	3.610	48
BMP2-F (250ng/well) vs. BMP2-FT (62.5 ng/well)	4.787	1.989	2.797	1.017	3	3	3.888	48
BMP2-F (125 ng/well) vs. BMP2-F (62.5 ng/well)	2.882	1.981	0.9005	1.017	3	3	1.252	48
BMP2-F (125 ng/well) vs. BMP2-FT (500 ng/well)	2.882	2.453	0.4289	1.017	3	3	0.5961	48
BMP2-F (125 ng/well) vs. BMP2-FT (250 ng/well)	2.882	3.084	-0.2027	1.017	3	3	0.2817	48
BMP2-F (125 ng/well) vs. BMP2-FT (125 ng/well)	2.882	2.189	0.6920	1.017	3	3	0.9619	48
BMP2-F (125 ng/well) vs. BMP2-FT (62.5 ng/well)	2.882	1.989	0.8920	1.017	3	3	1.240	48
BMP2-F (62.5 ng/well) vs. BMP2-FT (500 ng/well)	1.981	2.453	-0.4716	1.017	3	3	0.6555	48
BMP2-F (62.5 ng/well) vs. BMP2-FT (250 ng/well)	1.981	3.084	-1.103	1.017	3	3	1.533	48
BMP2-F (62.5 ng/well) vs. BMP2-FT (125 ng/well)	1.981	2.189	-0.2084	1.017	3	3	0.2897	48
BMP2-F (62.5 ng/well) vs. BMP2-FT (62.5 ng/well)	1.981	1.989	-0.008430	1.017	3	3	0.01172	48
BMP2-FT (500 ng/well) vs. BMP2-FT (250 ng/well)	2.453	3.084	-0.6316	1.017	3	3	0.8778	48
BMP2-FT (500 ng/well) vs. BMP2-FT (125 ng/well)	2.453	2.189	0.2632	1.017	3	3	0.3658	48

BMP2-FT (500 ng/well) vs. BMP2-FT (62.5 ng/well)	2.453	1.989	0.4632	1.017	3	3	0.6438	48
BMP2-FT (250 ng/well) vs. BMP2-FT (125 ng/well)	3.084	2.189	0.8947	1.017	3	3	1.244	48
BMP2-FT (250 ng/well) vs. BMP2-FT (62.5 ng/well)	3.084	1.989	1.095	1.017	3	3	1.522	48
BMP2-FT (125 ng/well) vs. BMP2-FT (62.5 ng/well)	2.189	1.989	0.2000	1.017	3	3	0.2780	48
7								
BMP2-F (500ng/well) vs. BMP2-F (250ng/well)	7.321	7.183	0.1381	1.017	3	3	0.1920	48
BMP2-F (500ng/well) vs. BMP2-F (125 ng/well)	7.321	2.811	4.511	1.017	3	3	6.269	48
BMP2-F (500ng/well) vs. BMP2-F (62.5 ng/well)	7.321	2.505	4.817	1.017	3	3	6.695	48
BMP2-F (500ng/well) vs. BMP2-FT (500 ng/well)	7.321	2.233	5.089	1.017	3	3	7.073	48
BMP2-F (500ng/well) vs. BMP2-FT (250 ng/well)	7.321	2.251	5.070	1.017	3	3	7.047	48
BMP2-F (500ng/well) vs. BMP2-FT (125 ng/well)	7.321	1.981	5.340	1.017	3	3	7.422	48
BMP2-F (500ng/well) vs. BMP2-FT (62.5 ng/well)	7.321	1.907	5.414	1.017	3	3	7.526	48
BMP2-F (250ng/well) vs. BMP2-F (125 ng/well)	7.183	2.811	4.372	1.017	3	3	6.077	48
BMP2-F (250ng/well) vs. BMP2-F (62.5 ng/well)	7.183	2.505	4.679	1.017	3	3	6.503	48
BMP2-F (250ng/well) vs. BMP2-FT (500 ng/well)	7.183	2.233	4.951	1.017	3	3	6.881	48
BMP2-F (250ng/well) vs. BMP2-FT (250 ng/well)	7.183	2.251	4.932	1.017	3	3	6.855	48
BMP2-F (250ng/well) vs. BMP2-FT (125 ng/well)	7.183	1.981	5.202	1.017	3	3	7.230	48
BMP2-F (250ng/well) vs. BMP2-FT (62.5 ng/well)	7.183	1.907	5.276	1.017	3	3	7.334	48
BMP2-F (125 ng/well) vs. BMP2-F (62.5 ng/well)	2.811	2.505	0.3063	1.017	3	3	0.4257	48
BMP2-F (125 ng/well) vs. BMP2-FT (500 ng/well)	2.811	2.233	0.5783	1.017	3	3	0.8037	48
BMP2-F (125 ng/well) vs. BMP2-FT (250 ng/well)	2.811	2.251	0.5596	1.017	3	3	0.7779	48
BMP2-F (125 ng/well) vs. BMP2-FT (125 ng/well)	2.811	1.981	0.8294	1.017	3	3	1.153	48
BMP2-F (125 ng/well) vs. BMP2-FT (62.5 ng/well)	2.811	1.907	0.9038	1.017	3	3	1.256	48
BMP2-F (62.5 ng/well) vs. BMP2-FT (500 ng/well)	2.505	2.233	0.2719	1.017	3	3	0.3780	48
BMP2-F (62.5 ng/well) vs. BMP2-FT (250 ng/well)	2.505	2.251	0.2533	1.017	3	3	0.3521	48

BMP2-F (62.5 ng/well) vs. BMP2-FT (125 ng/well)	2.505	1.981	0.5231	1.017	3	3	0.7271	48
BMP2-F (62.5 ng/well) vs. BMP2-FT (62.5 ng/well)	2.505	1.907	0.5975	1.017	3	3	0.8305	48
BMP2-FT (500 ng/well) vs. BMP2-FT (250 ng/well)	2.233	2.251	-0.01860	1.017	3	3	0.02586	48
BMP2-FT (500 ng/well) vs. BMP2-FT (125 ng/well)	2.233	1.981	0.2512	1.017	3	3	0.3491	48
BMP2-FT (500 ng/well) vs. BMP2-FT (62.5 ng/well)	2.233	1.907	0.3256	1.017	3	3	0.4525	48
BMP2-FT (250 ng/well) vs. BMP2-FT (125 ng/well)	2.251	1.981	0.2698	1.017	3	3	0.3750	48
BMP2-FT (250 ng/well) vs. BMP2-FT (62.5 ng/well)	2.251	1.907	0.3442	1.017	3	3	0.4784	48
BMP2-FT (125 ng/well) vs. BMP2-FT (62.5 ng/well)	1.981	1.907	0.07442	1.017	3	3	0.1034	48
10								
BMP2-F (500ng/well) vs. BMP2-F (250ng/well)	5.600	2.604	2.997	1.017	3	3	4.165	48
BMP2-F (500ng/well) vs. BMP2-F (125 ng/well)	5.600	3.045	2.555	1.017	3	3	3.551	48
BMP2-F (500ng/well) vs. BMP2-F (62.5 ng/well)	5.600	2.251	3.350	1.017	3	3	4.656	48
BMP2-F (500ng/well) vs. BMP2-FT (500 ng/well)	5.600	2.770	2.830	1.017	3	3	3.934	48
BMP2-F (500ng/well) vs. BMP2-FT (250 ng/well)	5.600	2.316	3.284	1.017	3	3	4.565	48
BMP2-F (500ng/well) vs. BMP2-FT (125 ng/well)	5.600	2.593	3.008	1.017	3	3	4.181	48
BMP2-F (500ng/well) vs. BMP2-FT (62.5 ng/well)	5.600	2.919	2.682	1.017	3	3	3.728	48
BMP2-F (250ng/well) vs. BMP2-F (125 ng/well)	2.604	3.045	-0.4413	1.017	3	3	0.6134	48
BMP2-F (250ng/well) vs. BMP2-F (62.5 ng/well)	2.604	2.251	0.3531	1.017	3	3	0.4908	48
BMP2-F (250ng/well) vs. BMP2-FT (500 ng/well)	2.604	2.770	-0.1664	1.017	3	3	0.2313	48
BMP2-F (250ng/well) vs. BMP2-FT (250 ng/well)	2.604	2.316	0.2879	1.017	3	3	0.4002	48
BMP2-F (250ng/well) vs. BMP2-FT (125 ng/well)	2.604	2.593	0.01136	1.017	3	3	0.01578	48
BMP2-F (250ng/well) vs. BMP2-FT (62.5 ng/well)	2.604	2.919	-0.3146	1.017	3	3	0.4372	48
BMP2-F (125 ng/well) vs. BMP2-F (62.5 ng/well)	3.045	2.251	0.7944	1.017	3	3	1.104	48
BMP2-F (125 ng/well) vs. BMP2-FT (500 ng/well)	3.045	2.770	0.2749	1.017	3	3	0.3821	48
BMP2-F (125 ng/well) vs. BMP2-FT (250 ng/well)	3.045	2.316	0.7292	1.017	3	3	1.014	48

BMP2-F (125 ng/well) vs. BMP2-FT (125 ng/well)	3.045	2.593	0.4527	1.017	3	3	0.6292	48
BMP2-F (125 ng/well) vs. BMP2-FT (62.5 ng/well)	3.045	2.919	0.1268	1.017	3	3	0.1762	48
BMP2-F (62.5 ng/well) vs. BMP2-FT (500 ng/well)	2.251	2.770	-0.5195	1.017	3	3	0.7221	48
BMP2-F (62.5 ng/well) vs. BMP2-FT (250 ng/well)	2.251	2.316	-0.06518	1.017	3	3	0.09059	48
BMP2-F (62.5 ng/well) vs. BMP2-FT (125 ng/well)	2.251	2.593	-0.3417	1.017	3	3	0.4750	48
BMP2-F (62.5 ng/well) vs. BMP2-FT (62.5 ng/well)	2.251	2.919	-0.6676	1.017	3	3	0.9280	48
BMP2-FT (500 ng/well) vs. BMP2-FT (250 ng/well)	2.770	2.316	0.4543	1.017	3	3	0.6315	48
BMP2-FT (500 ng/well) vs. BMP2-FT (125 ng/well)	2.770	2.593	0.1778	1.017	3	3	0.2471	48
BMP2-FT (500 ng/well) vs. BMP2-FT (62.5 ng/well)	2.770	2.919	-0.1481	1.017	3	3	0.2059	48
BMP2-FT (250 ng/well) vs. BMP2-FT (125 ng/well)	2.316	2.593	-0.2765	1.017	3	3	0.3844	48
BMP2-FT (250 ng/well) vs. BMP2-FT (62.5 ng/well)	2.316	2.919	-0.6025	1.017	3	3	0.8374	48
BMP2-FT (125 ng/well) vs. BMP2-FT (62.5 ng/well)	2.593	2.919	-0.3259	1.017	3	3	0.4530	48

7.3.6.2. Alizarine red staining

Alizarine red staining
Ordinary Two-way ANOVA
Alpha: 0.05

Source of Variation	% Of total variation	P value	P value summary	Significant?
Interaction	16.01	0.0002	***	Yes
cmRNA conc.	25.22	< 0.0001	****	Yes
coating type	46.15	< 0.0001	****	Yes

ANOVA table	SS	DF	MS	F (DFn, DFd)	P value
Interaction	3.977	3	1.326	F (3, 24) = 10.15	P = 0.0002
cmRNA conc.	6.264	3	2.088	F (3, 24) = 15.98	P < 0.0001
coating type	11.46	1	11.46	F (1, 24) = 87.75	P < 0.0001
Residual	3.135	24	0.1306		

Multiple comparisons within coating type fibrin or fibrinogen, comparing the different cmRNA concentrations rows (simple effects within columns)
Number of families 2
Number of comparisons per family 6

Tukey's multiple comparisons test	Mean Diff.	95% CI of diff.	Significant?	Summary
BMP2-F				
500 vs. 250	1.164	0.4589 to 1.869	Yes	***
500 vs. 125	1.342	0.6374 to 2.047	Yes	***

500 vs. 62.5	2.179	1.474 to 2.884	Yes	****
250 vs. 125	0.1785	-0.5265 to 0.8835	No	ns
250 vs. 62.5	1.015	0.3102 to 1.720	Yes	**
125 vs. 62.5	0.8367	0.1318 to 1.542	Yes	*
BMP2-FT				
500 vs. 250	0.2959	-0.4091 to 1.001	No	ns
500 vs. 125	-0.1301	-0.8351 to 0.5749	No	ns
500 vs. 62.5	0.3080	-0.3970 to 1.013	No	ns
250 vs. 125	-0.4260	-1.131 to 0.2790	No	ns
250 vs. 62.5	0.01209	-0.6929 to 0.7171	No	ns
125 vs. 62.5	0.4381	-0.2669 to 1.143	No	ns

Test details	Mean 1	Mean 2	Mean Diff.	SE of diff.	N1	N2	q	DF
BMP2-F								
500 vs. 250	2.958	1.795	1.164	0.2556	4	4	6.441	24
500 vs. 125	2.958	1.616	1.342	0.2556	4	4	7.428	24
500 vs. 62.5	2.958	0.7794	2.179	0.2556	4	4	12.06	24
250 vs. 125	1.795	1.616	0.1785	0.2556	4	4	0.9877	24
250 vs. 62.5	1.795	0.7794	1.015	0.2556	4	4	5.618	24
125 vs. 62.5	1.616	0.7794	0.8367	0.2556	4	4	4.630	24
BMP2-FT								
500 vs. 250	0.7086	0.4127	0.2959	0.2556	4	4	1.637	24
500 vs. 125	0.7086	0.8387	-0.1301	0.2556	4	4	0.7201	24
500 vs. 62.5	0.7086	0.4006	0.3080	0.2556	4	4	1.704	24
250 vs. 125	0.4127	0.8387	-0.4260	0.2556	4	4	2.357	24
250 vs. 62.5	0.4127	0.4006	0.01209	0.2556	4	4	0.06690	24
125 vs. 62.5	0.8387	0.4006	0.4381	0.2556	4	4	2.424	24

Ordinary Two-way ANOVA
Alpha: 0.05

Source of Variation	% Of total variation	P value	P value summary	Significant?
Interaction	16.01	0.0002	***	Yes
cmRNA conc.	25.22	< 0.0001	****	Yes
coating type	46.15	< 0.0001	****	Yes

ANOVA table	SS	DF	MS	F (DFn, DFd)	P value
Interaction	3.977	3	1.326	F (3, 24) = 10.15	P = 0.0002
cmRNA conc.	6.264	3	2.088	F (3, 24) = 15.98	P < 0.0001
coating type	11.46	1	11.46	F (1, 24) = 87.75	P < 0.0001
Residual	3.135	24	0.1306		

Multiple comparisons comparing fibrin vs fibrinogen coatings within each cmRNA concentration.
Number of families: 1
Number of comparisons per family: 4

Sidak's multiple comparisons test	Mean Diff.	95% CI of diff.	Significant?	Summary
BMP2-F - BMP2-FT				
500	2.250	1.562 to 2.938	Yes	****
250	1.382	0.6940 to 2.070	Yes	****

125	0.7774	0.08946 to 1.465	Yes	*
62.5	0.3787	-0.3092 to 1.067	No	ns

Test details	Mean 1	Mean 2	Mean Diff.	SE of diff.	N1	N2	t	DF
BMP2-F - BMP2-FT								
500	2.958	0.7086	2.250	0.2556	4	4	8.804	24
250	1.795	0.4127	1.382	0.2556	4	4	5.407	24
125	1.616	0.8387	0.7774	0.2556	4	4	3.042	24
62.5	0.7794	0.4006	0.3787	0.2556	4	4	1.482	24

Abbreviations

Abbreviation	Description
Ti	Titanium metal, or Titanium grade IV foil
BMP2	Bone morphogenetic protein 2
RT	Room temperature
mRNA	Messenger RNA
cmRNA	Chemically modified messenger RNA
MetLuc	Metridia Luciferase
WFI	Water for injection
cmRNA	Chemically modified messenger RNA
F	Fibrinogen
T	Thrombin
FT	Fibrin

ALP	Alkaline phosphatase
AR	Alizarine red
ELISA	Enzyme-linked immunosorbent assay
BMP2	Bone morphogenetic protein 2
PDLLA	Ploy D, L-lactic acid
F/FT	Fibrinogen or Fibrin coating of Ti discs
MetLuc	Metridia Luciferase reporter protein
RLU	Relative light unit
RFL	Relative fluorescence unit